REPUBLIQUE ALGERIENNE DEMOCRATIQUE ET POPULAIRE

MINISTERE DE L'ENSEIGNEMENT SUPERIEUR ET DE LA RECHERCHE SCIENTIFIQUE

المدرسة الوطنية المتعددة التقنيات
Ecole Nationale Polytechnique

**École Nationale Polytechnique**

**Département Génie des Procédés et de l'Environnement**

**Groupe SAIDAL**

صيدال
SAIDAL

# End-of-study project dissertation

*For obtaining the State Engineer's degree in*

*Process and Environmental Engineering*

# Development of bioadsorbents from fennel seeds and thapsia roots for the treatment of dyes in wastewater

*Produced by*:

**Mr. BERRADJA Oussama**

Presented and defended publicly on (08/07/2023)

Composition of the Jury:

| | | | |
|---|---|---|---|
| Chairman | Mr Abdelkader NAMANE | Professor | ENP |
| Supervisor | Mr Mohamed HENTABLI | Engineer | SAIDAL |
| Co-supervisor | Mr Yacine KERCHICH | Professor | ENP |
| Examiner | Mr Abdelmalek CHERGUI | Professor | ENP |
| Guest | Mr Elias BENAMIRA | MCB | ENP |

**- ENP 2023 -**

REPUBLIQUE ALGERIENNE DEMOCRATIQUE ET POPULAIRE

MINISTERE DE L'ENSEIGNEMENT SUPERIEUR ET DE LA RECHERCHE SCIENTIFIQUE

المدرسة الوطنية المتعددة التقنيات
Ecole Nationale Polytechnique

**École Nationale Polytechnique**

**Département Génie des Procédés et de l'Environnement**

**Groupe SAIDAL**

صيدال
SAIDAL

# End-of-study project dissertation

*For obtaining the State Engineer's degree in*

*Process and Environmental Engineering*

# Development of bioadsorbents from fennel seeds and thapsia roots for the treatment of dyes in wastewater

*Produced by*:

**Mr. BERRADJA Oussama**

Presented and defended publicly on (08/07/2023)

Composition of the Jury:

| | | | |
|---|---|---|---|
| Chairman | Mr Abdelkader NAMANE | Professor | ENP |
| Supervisor | Mr Mohamed HENTABLI | Engineer | SAIDAL |
| Co-supervisor | Mr Yacine KERCHICH | Professor | ENP |
| Examiner | Mr Abdelmalek CHERGUI | Professor | ENP |
| Guest | Mr Elias BENAMIRA | MCB | ENP |

**- ENP 2023 -**

REPUBLIQUE ALGERIENNE DEMOCRATIQUE ET POPULAIRE

MINISTERE DE L'ENSEIGNEMENT SUPERIEUR ET DE LA RECHERCHE SCIENTIFIQUE

المدرسة الوطنية المتعددة التقنيات
Ecole Nationale Polytechnique

**École Nationale Polytechnique**

**Département Génie des Procédés et de l'Environnement**

**Groupe SAIDAL**

صيدال
SAIDAL

# Mémoire de projet de fin d'études

*En vue de l'obtention du Diplôme d'ingénieur d'état en*

*Génie des Procédés et de l'environnement.*

# Développement de bioadsorbants à partir de graines de fenouil et de racines de thapsia pour le traitement des colorants

*Réalisé par*:

**Mr. BERRADJA Oussama**

Présenté et soutenu publiquement le (08/07/2023)

Composition du Jury:

| | | | |
|---|---|---|---|
| Président | Mr Abdelkader NAMANE | Professeur | ENP |
| Encadreur | Mr Mohamed HENTABLI | Ingénieur | SAIDAL |
| Co-encadreur | Mr Yacine KERCHICH | Professeur | ENP |
| Examinateur | Mr Abdelmalek CHERGUI | Examinateur | ENP |
| Invité | Mr Elias BENAMIRA | MCB | ENP |

**الملخص:**

الهدف من هذه الدراسة هوالهدف من هذا العمل هو استغلال اثنين من المواد الماصة الحيوية، وهما بذور الشمر وجذور الثابسيا، لامتصاص الملوثات الصيدلانية مثل الكلورتتراسيكلين HCl (CTC-HCl) والميثيلين الأزرق .(MB) وجرى تنشيط بيولوجي لبذور الشمر، وكشفت مقارنة بين البذور المنشطة والبذور غير المنشطة عن نتائج محسنة من حيث الكمية الممتزة عند التوازن. تم تطبيق التصاميم التجريبية لتحسين ظروف الامتزاز، وتم تنفيذ نمذجة isotherm الامتزاز باستخدام 32 نموذجًا تم تحسينها بواسطة خوارزمية .Dragonfly وتعطي النتائج قدرة امتزاز قصوى تبلغ 296.43 ملغم/غرام و179.39 ملغم/غرام للألياف الحيوية الناتجة عن المعالجة البيولوجية لبذور الشمر (FBIO) وبذور الشمر (FEN)على التوالي.

**الكلمات الرئيسية:** الامتزازات الحيوية، بذور الشمر، جذور الثابسيا الناعمة، الامتزاز، النمذجة، التحسين، خوارزمية Dragonfly.

***Résumé:***

Le but de ce travail est de valoriser deux bioadsorbants, à savoir les graines de fenouil et les racines de thapsie, pour l'adsorption de polluants pharmaceutiques tels que la chlortétracycline HCl (CTC-HCl) et le bleu de méthylène (MB). Une activation biologique des graines de fenouil a été réalisée, et une comparaison entre les graines activées et non activées révèle des résultats améliorés en termes de quantité adsorbée à l'équilibre. Des plans d'expérience ont été appliqués pour optimiser les conditions optimales d'adsorption, et une modélisation des isothermes d'adsorption a été réalisée en utilisant 32 modèles optimisé par l'algorithme Dragonfly. Les résultats donnent une capacité d'adsorption maximale de 296,43 mg/g et de 179,39 mg/g pour les fibres biologiques résultant du traitement biologique des graines de fenouil (FBIO) et des graines de fenouil (FEN) respectivement.

**Mots-clés:** bioadsorbants, graines de fenouil, racines de thapsie, adsorption, modélisation, optimization, algorithme Dragonfly.

***Abstract:***

The aim of this work is to exploit two bio-adsorbents, namely fennel seeds and sweet thapsia roots, for the adsorption of pharmaceutical pollutants such as chlortetracycline HCl (CTC-HCl) and methylene blue (MB). Biological activation of fennel seeds was carried out, and a comparison between activated and non-activated seeds revealed improved results in terms of the quantity adsorbed at equilibrium. Experimental designs were applied to optimise the adsorption conditions, and adsorption isotherm modelling was carried out using 32 models optimised by the Dragonfly algorithm. The results give a maximum adsorption capacity of 296.43 mg/g and 179.39 mg/g for the bio-fibres resulting from the biological treatment of fennel seeds (FBIO) and fennel seeds (FEN) respectively.

**Keywords:** bio-adsorbents, fennel seeds, smooth thapsia roots, adsorption, modelling, optimization, Dragonfly algorithm.

# *Acknowledgements*

*First of all, I would like to thank Allah for having given me the strength, the will, and the patience to carry out this modest work.*

*This work was carried out at the Quality Control Laboratory (QCL) at Saidal Group in Medea. I would like to thank Miss Bekhti, Director of this Laboratory, for her interest in this work, as well as Mr. Ben Toumiya and Miss Sadouke, who were a big help to me by providing me with necessary equipment in the laboratory.*

*My sincere thanks also go to the whole team at Saidal in Médéa for Their warm reception and dignity, which helped me work peacefully.*

*I thank my supervisor, Dr. Mohamed Hentabli, for all the information, his great help, and his great patience with me through all the work.*

*Also, I thank my Co-supervisor, Pr. Yacine Kerchiche, for having accepted to supervise me, for helping me, and for having directed me through all the work.*

*I would like to express My sincere thanks to the jurors who took the trouble to evaluate this modest work. I would like to thank Mr Abdelkader NAMANE, Professor at the National Polytechnic School (ENP) who did me the honor of chairing the defense jury and for the interest he showed in our work.*

*I would also like to thank the members of the jury, Mr Abdelmalek CHERGUI, Professor at the National Polytechnic School (ENP), for agreeing to examine this work.*

*Finally, I couldn't end this list without saying a special thank you to those who have supported me behind the scenes: my parents, my brothers, and my friends, without whom this work would never have seen the light of day.*

# *Dedications*

*To my dearest parents May God keep them*

*To my two brothers Sohaib and Mohammed for their support*

*To all my family that took care of me*

*To all my friends that always supported me*

*To all those who are close to my heart and whose names I have not mentioned*

*I dedicate this modest work*

# Table of Contents

# List of tables

# List of figures

# List of abbreviations

**WWTP:** Wastewater treatment plants

$\boldsymbol{Q_e}$**:** adsorbed capacity/adsorbed quantity in equilibrium (mg/g)

$\boldsymbol{C_0}$**:** the initial concentration of the adsorbate (mg/L)

$\boldsymbol{C_e}$**:** the final equilibrium concentration of the adsorbate (mg/L)

$\boldsymbol{V}$*:* solution volume (L)

$\boldsymbol{m}$*:* mass of the adsorbent (g)

$\%\boldsymbol{R}$ or $\boldsymbol{R}$**:** adsorption yield, elimination rate, removal efficacity or efficiency

$\boldsymbol{Q_{max}}$*:* maximum adsorption capacity (mg/g)

$\boldsymbol{K_H}$*:* Henry adsorption constant (L/g)

$\boldsymbol{K_L}$**:** Langmuir isotherm constant (L/mg)

$\boldsymbol{K_T}$**:** adsorption potential constant of Temkin

$\boldsymbol{K_F}$**:** adsorption potential constant of Freundlich

$\boldsymbol{n_F}$**:** affinity (strength) constant of Freundlich

$\boldsymbol{K_{BS}}$**:** adsorption potential constant of Brouers-Sotolongo

$\alpha_{\boldsymbol{BS}}$**:** exponent of Brouers-Sotolongo

$\boldsymbol{K_{VS}}$**:** adsorption potential constant of Vieth-Sladek

$\boldsymbol{\beta_{VS}}$**:** exponent of Vieth-Sladek

$\boldsymbol{C_{BET}}$ *:* adsorption constant of BET

$\boldsymbol{C_{sat}}$ *:* Concentration of saturation of the surface adsorbent

$\boldsymbol{R}$**:** gas constant (8.31 Jmol-1 k-1)

$\boldsymbol{T}$**:** absolute temperature (K)

$\boldsymbol{b_0}$ ***or*** $\boldsymbol{K_B}$*:* the equilibrium constant of Baudu

$\boldsymbol{x}$ and $\boldsymbol{y}$ : Baudu parameters

$\boldsymbol{K_1}$**,** $\boldsymbol{K_2}$**:** Fritz–Schlunder adsorption constants

$\boldsymbol{n_1}$**,** $\boldsymbol{n_2}$ **:** Fritz–Schlunder exponents

***PFO :*** Pseudo first order

***PSO :*** Pseudo second order

***IDM :*** Intraparticle Diffusion Model

$Q_t$**:** amount of solute per unit mass of adsorbent at time **t** (mg/g)

$t$ **:** time (min)

$k_1$ **:** PFO rate coefficient ($min^{-1}$)

$k_2$ **:** PSO rate coefficient ($min^{-1}$)

$k_{int}$ **:** the intraparticle diffusion rate constant ($mg.g^{-1}.s^{-1/2}$) ;

$c$ **:** an intercept, represents the boundary layer thickness (mg/g).

$B_T$ **:** la constante de Temkin (J.mol-1)

***IR :*** Infra-red

***FTIR :*** Fourier-transform infrared spectroscopy

***DA :*** Dragonfly Algorithm

***RMSE :*** Root mean square error

$R^2$ **:**The coefficient of determination

$AdjR^2$ **:** Adjusted coefficient of determination

***ANOVA :*** Analysis of Variance

$\lambda_{max}$ : Longueur d'onde du colorant (nm)

***MB :*** Methylene Blue

***CTC-HCl :*** Chlortetracycline hydroxide

***FEN :*** Bioadsorbent based on Fennel seeds

***FBIO :*** Biological fibers based on Fennel seeds

***TH :*** Bioadsorbent based on Thapsia roots

$df$ : degree of freedom

***pHpcz :*** pH at zero charge

# *General introduction*

# General introduction

Water has always been the core of life on earth; many living things depend on it. It is a fundamental resource for all forms of life and specifically for mankind, and its scarcity has become a critical environmental issue during the last few years. Humans are an integral part of the earth's ecosystem, and their influence on ecosystems is unmeasurable. The consistency of human needs, in health specifically, made them create and synthesize all sorts of complex molecules, such as medicines for medical or veterinary use, plant protection products, plasticizers, etc. However, the increased production and utilization of chemicals have raised concerns regarding their presence in the environment [1]–[3].

Human activities in modern society heavily depend on chemicals and the chemical industry, which play a vital role in various aspects of our lives and mainly introduce and generate the natural presence of other contaminants [2].

Water pollution is a serious problem today, in spite of human efforts to control it. Many of these waters are suffering the effects of indirect or diffuse discharges of pollutants associated with stormwater runoff from adjacent lands. It can be caused mainly by bacterial or chemical pollutants [4]. The fight against chemical pollutants, both mineral and organic, has given rise to many questions in recent years: Can this pollution be controlled?

The treatment of industrial effluents has become a major concern in the environmental sciences due to the varied nature of the toxic substances they contain and the various stages of their degradation. Many Wastewater treatment Plants were created to reduce and control water pollution. The treatment involves physical, chemical, and biological processes such as coagulation, filtration, ion exchange, and aerobic and anaerobic treatment, but it wasn't enough to be totally treated [5], [6].

Advanced water treatment processes are used to remove contaminants from water sources that traditional treatment methods cannot remove. They involve advanced oxidation processes (Djakaou, n.d.; Gertsen & Sønderby, 2009; Zaviska et al., 2009), membrane technologies (Baruth et al., 2005; Crini & Lichtfouse, 2019; Sonune & Ghate, 2004), adsorption (Baruth et al., 2005; Singh et al., 2021; Sonune & Ghate, 2004), nanomachine technology, electrolysis, microbial reduction, and activated sludge, which offer different levels of pollution. However, most of these advanced processes require a significant financial input, which limits their use and puts the "cost" factor ahead of the issue of pollution control [7].

Faced with this problem, The activated carbon adsorption technique was introduced as an interesting alternative, leading to numerous studies into the process of adsorption of organic and pharmaceutical compounds present in aqueous solutions onto activated carbons [8].

Activated carbon was chosen as an adsorbent because of its high adsorption capacity, but its relatively high cost limits its use. This has encouraged the emergence of research into treatment processes using less expensive and widely available biomaterials, which refer to a

large number of products of biological or plant origin capable of fixing organic or inorganic pollutants without prior transformation[9].

The main objective of this study was to develop composite biomaterials based on Fennel seeds and Thapsia roots with different treatments for the elimination of organic compounds likely to pollute water in batch systems in order to model their kinetics and equilibrium and the factors influencing the adsorption in order to optimize the elimination.

This thesis is divided into three parts:

- Firstly, a bibliographical study is presented in three different chapters:
  - ✓ The first chapter presents a literature review, focusing first on water pollution and pharmaceutical pollutants;
  - ✓ The second chapter presents a general description of the adsorption phenomenon and covers the essential data and mathematical models for it;
  - ✓ The third chapter presents all the theoretical concepts of modelling and optimization, which cover the main aspects of the experimental design methodology, the evaluation metrics, and a general description of the Dragonfly Algorithm (DA) used in nonlinear regression.
- The second part presents the preparation and characterization protocols for the biosorbents studied, as well as the experimental procedures used in Methylene Blue and Chlortetracycline Hydroxide adsorption tests, with a study of all possible influencing factors. Followed by a presentation and discussion of the various experimental results obtained relating to the characterization of the biosorbents and the application of the above-mentioned model adsorbates in adsorption tests in batch systems.
- The third part presents modelling all the influencing factors on Chlortetracycline hydroxide adsorption using Box-Behnken design to find the optimum operation conditions and modelling of the above-mentioned adsorbates adsorption kinetics and equilibriums using the DA algorithm to help us in the nonlinear regression.

Finally, the conclusions of the study and the prospects offered by the results obtained are presented.

# *Chapter I:*

# *Water pollution*

# Chapter I: Water pollution

## I.1. Introduction:

Water is a fundamental resource for generally all forms of life and specifically human life, and its scarcity has become an increasingly critical environmental issue. Despite scientific and technological advancements, obtaining an adequate supply of clean water remains challenging due to factors like population growth and industrial demands. Water pollution has become a global concern that poses significant threats to the environment and human health. As societies continue to develop and industrialize, the discharge of various pollutants into water bodies has reached dangerous levels, especially in pharmaceutical industries [1].

This chapter aims to provide an overview of water pollution, including some generalities, the classification of pollutants based on some criteria, and the specific issue and effects of pharmaceutical pollutants. Additionally, we will explore various applied pollution treatment methods that are being employed to mitigate the detrimental effects of water pollution.

## I.2. Generalities:

The modern society heavily depends on chemicals and the chemical industry, which play a vital role in various aspects of our lives. Pharmaceutical, petrochemical, industrial, agricultural and food chemicals all contribute to shaping our modern lifestyles. However, the increased production and utilization of chemicals have raised concerns regarding their presence in the environment [1], [10].

The release of these "foreign" chemical compounds into our environment stems from various sources, including pesticides, personal care products, cleaning materials, pharmaceuticals, and more. The presence of trace amounts of pharmaceuticals in water, designed to have potent physiological effects, is an emerging water issue. The intensification of land and water use for industry and agriculture has necessitated wastewater reclamation, but it also increases the risk of water contamination. Pharmaceuticals, due to their polar structure, can infiltrate groundwater and appear in trace concentrations in drinking water [1], [3], [10].

To reconcile industrial activities with environmental preservation, many countries implement stringent environmental legislation and prioritize Green Technology and Green chemistry, which promotes the use of environmentally friendly processes and the reduction of hazardous substances, plays a significant role in achieving sustainable development [1].

To address concerns related to chemicals in the environment, the precautionary principle is often employed. This principle advocates for setting targets of "no contamination" rather than simply reducing pollution. For example, The North Sea countries have agreed to conditionally reduce emissions and losses of hazardous substances, with the aim of decreasing concentrations in the marine environment to baseline values for natural substances and close

to null for synthetics [10], and The Federal Water Pollution Control Act, known as Clean Water Act ,is the cornerstone of water quality legislation in the United States [4].

- **Impacts:**

Water pollution arises from various human activities, including the discharge of sewage, industrial waste, and improper waste management. Natural processes can also contribute to water pollution, but human activities are the primary cause. Wastewater, a combination of liquid waste from different sources, contains oxygen-demanding wastes, pathogens, organic materials, nutrients, inorganic chemicals, minerals, and sediments. If left untreated, it leads to serious pollution when released into waterways [6]. It can have devastating consequences for aquatic organisms, wildlife, and human health. The introduction of pollutants into rivers and streams causes destruction and disrupts the natural balance. Industrial and commercial waste, agricultural practices, and transportation contribute to the increasing variety and quantity of pollutants in water bodies. The growing population, rapid industrialization, urbanization, and modern agricultural practices further compound the issue[3], [6].

It has significant impacts, and according to B. Crathorne et Al. 2001 [10], these impacts can be categorized as follows:

- Aesthetic effects: Visual nuisances such as litter, discoloration, and unpleasant odors.
- Temperature effects: Elevation of water temperatures, which negatively impacts aquatic ecosystems.
- Deoxygenation: Reduction of oxygen levels in water, leading to harm to aquatic and human life.
- Toxicity: Exhibition of acute or chronic toxicity, causing harm to aquatic or human life.
- Sublethal toxicity: Certain pollutants, such as those causing endocrine disruption or biodiversity changes, can have subtle yet harmful effects.
- Acidity/alkalinity disturbances: Disruption of the pH balance of water bodies.
- Eutrophication: Excessive nutrient levels can trigger the overgrowth of certain organisms, disrupting the overall balance of ecosystems.

Freshwater contamination is a pressing concern as the global water supply is shrinking while pollution continues to increase. Factors such as population growth, industrialization, urbanization and modern agricultural activities contribute to water pollution. Millions of tons of sewage, industrial waste and agricultural waste are dumped

into water bodies every day, causing harmful changes and threatening freshwater resources [3].

Water pollution was the cause of 1·4 million premature deaths in 2019, leading to 829,000 annual deaths from diarrhea, including 300,000 children under five and other diseases like cancer, skin diseases, gastrointestinal illness, and Lack of water and sanitation also increases diseases such as cholera, trachoma, schistosomiasis and parasitic diseases. The decline in the number of deaths was attributed to traditional pollution is most evident in Africa, where improvements in water supply, sanitation, antibiotics, treatments and cleaner fuels have created measurable breakthroughs in mortality statistics [11], [12].

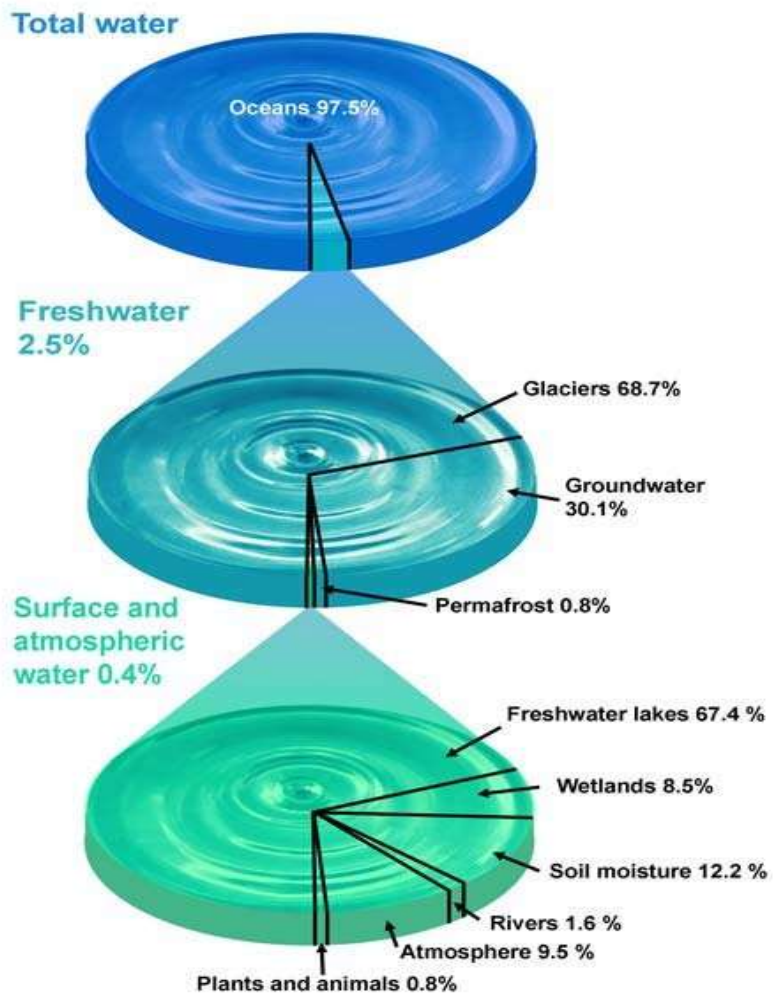


*Figure 1: Estimated deaths worldwide by major risk factor [3]*

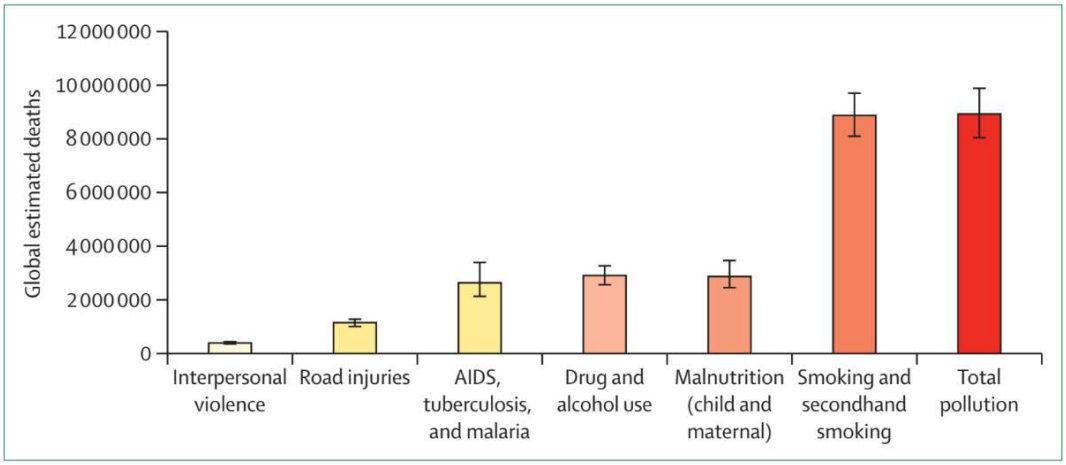


*Figure 2: Global estimated deaths by major risk factor [11]*

## I.3. Classification of pollution and pollutants:

### I.3.1. Based on the source:

Water pollution is often attributed to many causes, namely stormwater runoff, domestic discharges, industrial discharges, and the use of water control structures. According to J. Peirce et al. 1997, water pollutants are categorized into:

- Point-source pollution is one identifiable local source that is relatively easy to identify, quantify, and control, mainly from industrial plants and domestic wastewater treatment plants. The types of pollutants in a sewage system depend entirely on what is thrown into it [3], [13].
- Non-point source pollution is characterized by several discharge points and cannot be traced to a single point. It's difficult to monitor and control pollution from diffuse sources since all pollutants enter waterways during the dry season through pipes or canals (rainwater discharges, agricultural runoff, construction sites, etc.). Agricultural activities are considered as a major source of non-point pollution[3], [13].

### I.3.2. Based on the mode of occurrence:

They have been classified into physical, chemical and biological pollutants[3] with each class having the nature of the occurrence that effect the environment, according to Table 1:

*Table 1: Classification of pollutants [3]*

| *Occurrence* | *Nature* | *Example* |
|---|---|---|
| *Physical* | Temperature turbidity | Waste heat from industry, micropollutants |
| | Color | Dyes and pigments |
| | Suspended and floatingmatter | Soil particles, rubber and leather, woods…etc. |
| *Chemical* | Inorganic | N, P, Cl, F, etc. |
| | | Plastics, detergent plastics |
| | Organic | Pesticides, fertilizers |
| *Biological* | Pathogenic | Microorganisms, bacteria and worms |
| | Nuisance organisms | Algae |

## I.3.3. Based on the nature of activity:

all human activity causes some disturbance to the environment which pollutes the surrounding waters. Activities such as such as eating (bodily waste, food, etc.), gardening (fertilizing, etc.) or others leave behind byproducts that can enter the water cycle [3]. According to H. Qadri [3], we can classify the majority sources of water pollution to three categories:

- Industrial wastes: are the primary origin of all water pollutants. The production sector is responsible for many extremely reactive and harmful pollutants, such as a range of organic substances and heavy metals. Although there are other industries with lower potential for environmental impact, they are still regarded as significant sources of pollution. For instance, power generation industries are largely responsible for the emission of heat and radioactivity.
- Agricultural wastes: growing crops and raising livestock are major contributors to sediment contamination, including cultivation and other activities that remove vegetation and destroy soil. Sediments from agricultural runoff affect water quality. This reduces the volume of freshwater bodies and also reduces the penetration of light into the water, disturbing the underwater flora. As a result, the fish and other creatures that feed on flora are disturbed, affecting the entire food chain.

- Domestic wastes: they are household wastes, including sewage and septic tank leakage, fertilizers used on lawns and gardens and synthetic detergents that often contain phosphates, that cause natural water pollution, harm aquatic organisms and reduce water quality. Irresponsible littering in water bodies can lead to accumulation of household items such as cans, bottles and plastics. Untreated or improperly treated sewage can introduce infectious diseases such as typhus, cholera, dysentery and skin diseases into the water supply. Different types of pollution have different effects on freshwater bodies, affecting their physical, chemical and biological aspects.

## I.4. Pharmaceutical pollutants:

Pharmaceutical pollutants are considered any wastes or discharges after the usage of chemical substances in labor or during or after a manufacturing process in the pharmaceutical industry. Active pharmaceutical substances (APS), also known as pharmaceutical active compounds (PhAC), such as antibiotics, are created and utilized globally, and for most of their resistance genes, they have been discovered in microorganisms isolated from human societies. The PhAC and its byproducts are introduced into the environment via the discharge of human waste and sewage. Insufficient wastewater treatment in low- and middle-income countries where pharmaceutical industries exist contributes to the release of these compounds into the environment or wastewater systems. Expensive and labor-intensive techniques, such as nanotechnologies, membrane technologies, advanced oxidation processes, or adsorption, are required for eliminating PhACs from wastewater. Water resources such as surface water, groundwater, and lake water are contaminated with PhACs due to overworked sewage treatment facilities coupled with insufficient advanced treatment methods. Despite being a widespread issue, the study of water contamination caused by PhACs has predominantly centered on developed nations, including Japan, Europe, and the United States [14].

The industry responsible for producing medicine for both human and animal consumption involves the production, extraction, processing, purification, and packaging of chemical and biological substances in solid and liquid forms.

Wastewaters within the pharmaceutical manufacturing sector commonly stem from the production and preparation stages of pharmaceutical synthesis and formulation. The majority of the Application Programming Interfaces (APIs). Chemical synthesis is employed to produce products that are distributed globally, incorporating organic, inorganic, and biological reactions. The amount of wastewater produced in a multiproduct pharmaceutical industry is usually higher than necessary due to the reactors and separators being oversized or operated inefficiently, as they are not specifically designed for capacity. The level of production has been enhanced. In the pharmaceutical industry, numerous subprocesses take place making it challenging to categorize all forms of product waste. An attempt has been made to create a more comprehensive categorization system that takes into account factors such as the type of

materials used, the resulting products, and the distinct features of plants. Smartly paraphrased: The arrangement [5].

This process adopts a similarity-based approach towards chemical operations and treatments, along with specific product categories. Pharmaceutical industries can be categorized into five major subgroups based on their manufacturing procedures [5]:

1) fermentation plants;
2) synthesized organic chemicals plants;
3) fermentation/synthesized organic chemicals plants;
4) natural/biological product extractions (antibiotics, vitamins, etc.);
5) drug mixing, formulation, and preparation plants (capsules, and solutions, etc.).

The Table 2 summarizes the different pharmaceutical processes and the categorization based on these processes.

*Table 2: Categorization of various manufacturing process based on the methods utilized for pharmaceuticals mass production [5]*

| chemical synthesis | fermentation | natural product extraction |
|---|---|---|
| antibiotics; antihistamines; cardiovascular agents; centralnervous system (CNS) stimulants; CNS depressants; hormones vitamins | antibiotics; antineoplasticagents; therapeutic nutrients; vitamins; steroids | antineoplastic agents; enzymes and digestive aids; CNS depressants; hematological agents; insulin; vaccines |

One of the possible pharmaceutical pollutants that has attention due to its wide usage in the pharmaceutical industry: the colorants.

- **Colorants:** are chemicals compounds capable of dying objects or surfaces permanently or temporarily. they are mainly composed of chromophore groups, auxochromes and conjugated aromatic structures. They are widely used in the textile industry, tanneries, plastic (pigment) industry, pharmaceutical industry, food industry, pulp and paper industry, cosmetic industry and soap industry. Therefore, the textile industry is still the largest consumer of dyes [15].

*Table 3: Main chromophore and auxochrome groups classified by increasing intensity [16]*

| Groupe chromophores | Groups auxochromes |
|---|---|
| Azo (-N=N-) | Amino (-NH2) |
| Nitroso (-N=O-) | Methylamino (-NHCH3) |
| Carbonyl (>C=O) | Di Methylamino (-N(CH3)2) |
| Vinyl (-C=CH2) or methine (>C=) | Hydroxyl (-OH) |
| Nitro (-NO2) | Alkoxy (-OR) |
| Thiocarbonyl (>C=S) | |

There are two main families of colorants: natural colorants (extracted from mineral or organic materials) and synthesis colorants [15]–[17]:

- Natural colorants used by humans appear to come from minerals (colored earths), plant or animal origin, especially used when managing the weaving.
- Synthetic colorants are gradually replacing natural dyes, and their value lies mainly in chemical and photolytic stability, ease of synthesis, and color variation.

They can be classified according to their chemical composition (azo, anthraquinone, indigoid, xanthene, phthalocyanine, nitro and nitroso dyes, triphenylmethane) or according to the field of application or tinctorial classification (acid or anionic, basic or cationic colorants, vat colorants, mordant colorants, metal complex colorants type 1:1 and type 1:2, naphthol colorants, reactive colorants, sulfur colorants, and plastosoluble colorants) [16], [17].

## I.5. Applied pollution treatment methods:

To assure the consistency of the production, the pharmaceutical industry requires a big amount of high-quality of water which imply big quantity of wastewater during or after the process. Although the treatment of these wastewater in the past decade usually was dealt with tertiary wastewater treatment plants (WWTP) with some specific technologies that are shown in Table 3 [5].

In general, wastewater treatment plants use the main wastewater treatment processes presented in Figure 3, but other technologies such as advanced oxidation processes([1], [18]), membrane technologies([6], [7], [19]) or adsorption ([6], [19], [20]) have also shown their

effectiveness in wastewater treatment and other technologies that can be found in appendice 1.

*Table 4: Wastewater treatment technologies with its cost [5]*

| The technology | Treatment methods | Capacity | Capital cost |
|---|---|---|---|
| Decentralised wastewater treatment (DWWT) | sedimentation, anaerobic digestion, filtration and phyto-remediation | 1000 KLD | 580-1200 |
| Soil biotechnology | sedimentation, filtration, biochemical process | 5 KLD to tens of MLD | 160-250 |
| Biosanitizer/Ecochip | biocatalyst: breaking the toxic/organic contents | 100 mg/KLD | 160 for chip only |
| soil scape filter | filtration through biologically activated medium | 1-250 KLD | 300-500 |
| Ecosanitation zerodischarge toilets | separation of fecal matter and urine | Individual to community level | 650-850 (excluding toilet constructions) |
| Nualgi technology | phyco-remediation (use of micro/macro-algae): fix CO2, removenutrients, and increase DO | 1 kg treats up to MLD | 6 $/MLD |
| Bioremediation | decomposition of organic matter using Persnickety 713 | 1 billion CFU/ml | 3570-500 $/MLD |
| Green bridgetechnology | filtration, sedimentation, biodigestion, and biosorption by microbesand plants | 50-200 KLD/$m^2$ | 4-8 |

With: KLD refers to Kiloliters per day and MLD refers to Megaliters per day;

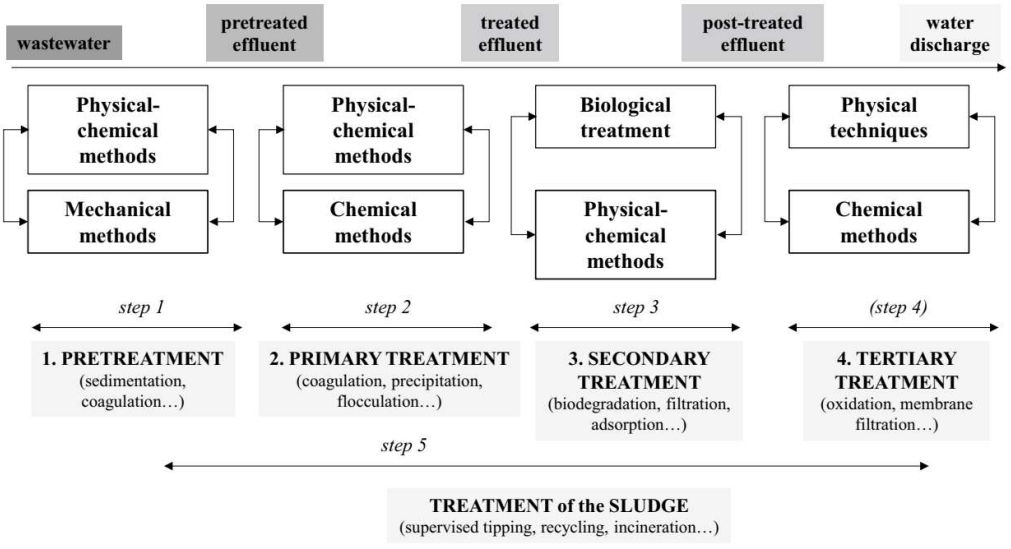


*Figure 3: Main processes for the treatment of industrial wastewater [7]*

## I.6. Conclusion:

Water pollution caused by chemical pollutants, particularly pharmaceutical pollutants, represents a major challenge for the environment and human health. By classifying pollutants and pollution according to their sources, the way they appear, and the nature of their activity, societies have made great progress in understanding their complexity and have been able to combat pollution effectively by applying specialized treatment methods. However, this requires a collective commitment from governments, industries, communities, and individuals to implement regulations, adopt sustainable practices, and invest in advanced treatment technologies.

Adsorption is one of the most commonly used and proven treatment methods.

# *Chapter II:*

# *Adsorption*

# Chapter II: Adsorption

## II.1. Introduction:

Adsorption plays an important role in many scientific and technological applications. From environmental remediation to industrial production, the adsorption process is an important means of purifying, separating, and regenerating substances. It is essential to understand its principles and mechanisms in order to exploit its potential and design efficient systems.

This chapter reviews some of the fundamental aspects of adsorption and examines its properties, mechanisms, equilibria, kinetics, types of adsorbents, and their characteristics, as well as the factors that influence this interesting phenomenon.

## II.2. Definition:

Adsorption is a physico-chemical process and an interfacial and reversal phenomenon in which molecules or atoms of a fluid solvent accumulate and adhere to a solid or liquid surface. It can also be defined as the accumulation of chemical species from the fluid phase on the surface of solids or liquids [21], [22].

During adsorption, the substance is retained on the surface, in contrast to absorption, which involves diffusion into solution, and desorption, which is the reversion (check Figure ). This occurs through various mechanisms limited by the available surface area of the solid material and its nature (ion exchange, complexation, or precipitation at the surface). The solid material that forms the surface is the adsorbent, and the collected species are the adsorbates [21].

The adsorption at the solid-liquid interface can be seen in two different ways: it can be confined below the surface to a monolayer or a multilayer (stacked monolayers). Adsorption is used in industrial applications such as water purification and synthetic resins. In the laboratory, adsorption is often studied using "batch" techniques, in which suspensions are stirred until equilibrium is reached.

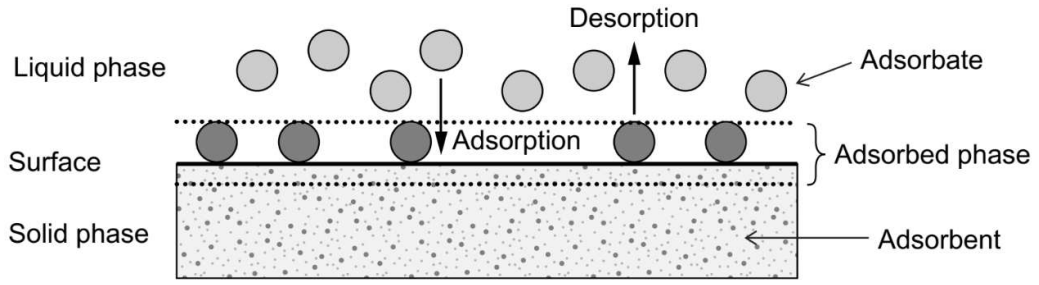


*Figure 4: Schematic representation of adsorption [21]*

## II.3. Adsorbents:

According to the definition **Error! Reference source not found.**, adsorbent refers to a solid material that accumulates molecules of a solute present in either a gas or liquid. They are essential for successful commercial separation processes, whether they involve bulk separation or purification. The key characteristics of an adsorbent material, according to W. J. Thomas and B. Crittenden [23], are:

- High internal volume (easy accessibility to the components being removed from the fluid);
- Highly porous solid;
- High internal surface area;
- Mechanical properties like strength and resistance to attrition
- Good kinetic properties (rapid transfer of adsorbing molecules to the adsorption sites);
- Regeneration of the adsorbent after use;
- Cost-effective materials and production methods for adsorbents.

Adsorbents can have internal surface areas ranging from approximately 100 $m^2/g$ to over 3000 $m^2/g$, but the practical range usually falls between 300 and 1200 $m^2/g$. Most adsorbents consist of porous structures of varying sizes, such as micropores (diameter is lesser than 2 nm), mesopores (diameter in the range 2–50 nm), and macropores (diameter exceeds 50 nm), which contribute to the creation of the internal surface area. Common adsorbent materials are often amorphous and has intricate networks of interconnected pores [23].

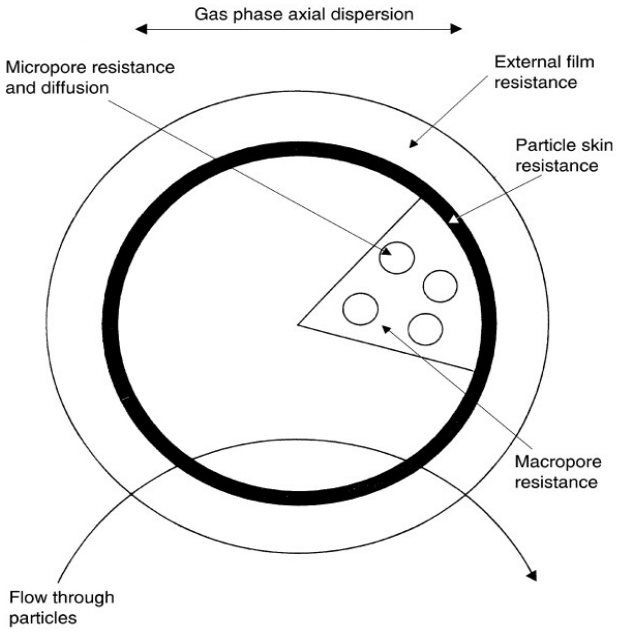


*Figure 5: General structure of adsorbent particle and relative resistance to absorption of fluid molecules [23]*

The most used adsorbents in the separation processes are:

## II.3.1. Activated carbon:

Activated carbon is created from carbon-rich materials like coconuts, wood, coal, peat, etc., through carbonization and subsequent activation using chemicals (dehydrating chemicals) or gases (air, steam, etc.). With internal surface areas of 800-1,000 m2/g, it exhibits excellent adsorption properties, especially for organic substances. It can be regenerated through thermal processes and finds wide applications in recovering organic vapors, decolorizing liquids, and treating water supplies and wastewater [21], [22].

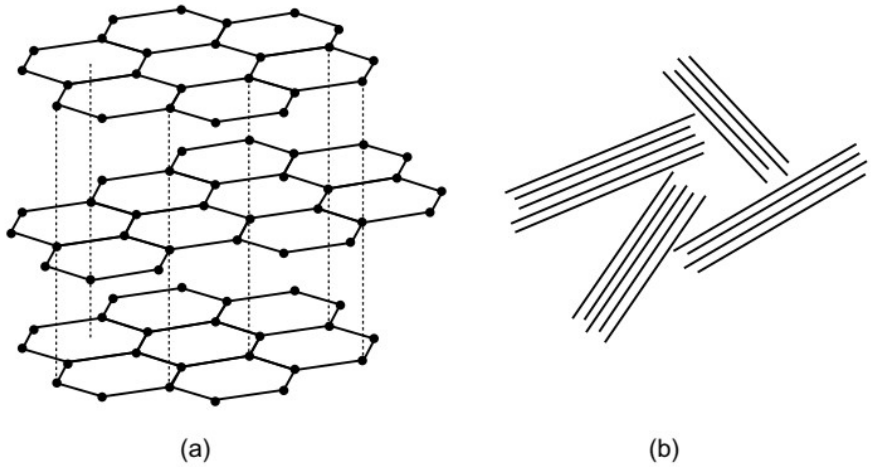


*Figure 6: Structural of activated carbons : (a) graphite structure, (b) graphite microcrystallites [21]*

## II.3.2. Polymeric adsorbents:

Polymeric adsorbents produced by polymerizing styrene or acrylic esters with divinylbenzene as a cross-linking agent (as demonstrated in Figure 7), selectively adsorb nonpolar organic substances from aqueous solutions or polar solvents. Their selective adsorption properties can be attributed to a controlled matrix structure, high surface areas that can reach up to 750–800 $m^2/g$, and a precise, narrow pore-size distribution. Recovery can be achieved by a variety of methods, including steam desorption, solvent elution, pH changing, and chemical extraction. However, they are more expensive than other adsorbents and not ideal for large-scale water treatment. Nevertheless, they are highly beneficial for recycling chemicals from process wastewater and can recover a wide range of solutes, including phenol, benzene, pesticides, antibiotics, and more [21].

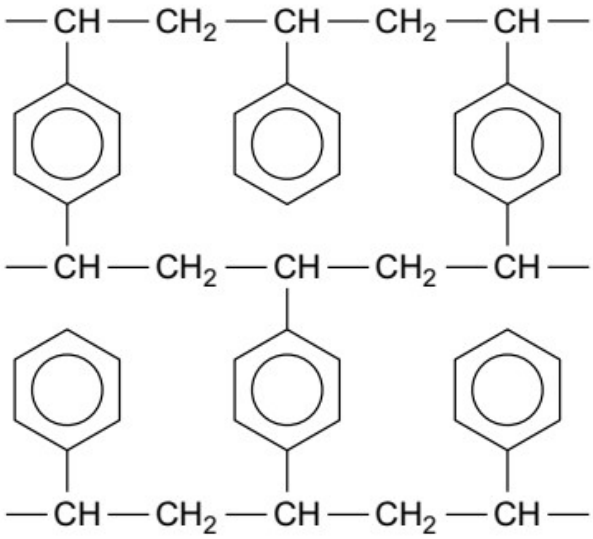

*Figure 7: Styrene-divinylbenzene copolymer structure*

## II.3.3. Zeolites:

Zeolites show a wide range of natural variations. However, synthetic zeolites are generally preferred for practical applications. Synthetic zeolites are porous aluminosilicate crystalline ($(Me^{II}, Me^{I}_2)O\cdot Al_2O_3 \cdot nSiO_2 \cdot p\ H_2O$) formed by mixing an alkaline aqueous of silicate $SiO_4$ and $AlO_4$ aluminate (solution of silicium and aluminum compounds joined together through oxygen atoms) under hydrothermal conditions[21].

Zeolites have a porous structure characterized by windows and caves of specific dimensions. The crystalline form of zeolites differs from other adsorbents because there is no pore size distribution. This uniform lattice structure determines the access to adsorbate molecules. The cages of the crystal cells can seize adsorbates. With their high internal porosity, adsorption usually happens internally and it's controlled by the channel diameter, which is influenced by the crystal composition. Due to this property, zeolites excel at effective separation based on size [21]–[24].

Adsorption and desorption processes on zeolites depend on differences in molecular size, shape and other properties such as polarity.

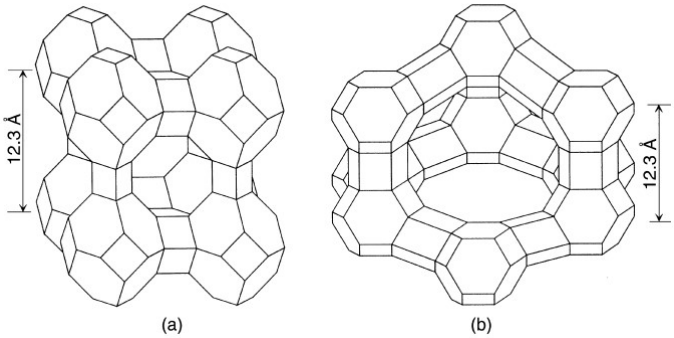


*Figure 8: The structure of two different zeolite (a) and (b) [23]*

And other adsorbents like activated alumina, activated silica, oxidic adsorbents and low-cost adsorbents as presented in Figure 9.

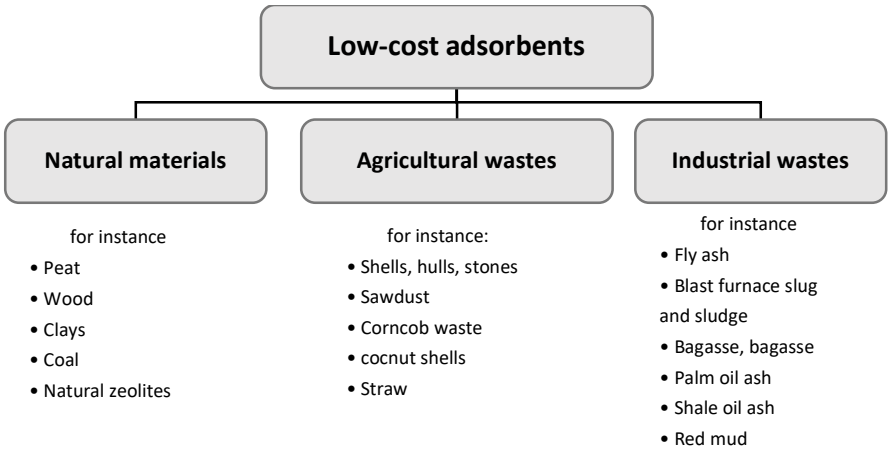


*Figure 9: Examples on low-cost adsorbents*

## II.4. Adsorption mechanism:

It depends on the physical and chemical characteristics of the adsorbents (diameter, density, porosity, pore size and size distribution) and the adsorbates, and the type of interfacial interactions (nature of the bonding) between them. Therefore, we can distinguish two types of absorption:

- **Physisorption:** is a non-specific adsorption in which the adsorbate adheres to the adsorbent surface under the influence of van der Waals or electrostatic forces (dipoles, hydrophobics or hydrogen bond interactions). It can be multilayer adsorption under high relative pressure. It is always exothermic and reaches equilibrium fairly quickly, but if the transport process is rate-determining, equilibrium may be slow. Physiosorbed molecules retain their identity and, after desorption, return to the fluid phase in their original form [25].

- **Chemisorption:** involves chemical bonding to reactive parts of the adsorbent surface, forming a covalent, ionic or electrostatic bond with the adsorbate and the adsorbent, depending on their reactivity. This applies only to monolayer adsorption. Chemisorbed molecules lose their identities and cannot be recovered by desorption. The chemisorption energy is of the same magnitude as the energy change in comparable chemical reactions, and at low temperatures, it may not have enough heat energy to reach thermodynamic equilibrium. The distance between the surface and the adsorbed molecules is smaller than with physisorption and chemisorption [25].

## II.5. Adsorption equilibrium:

Adsorption equilibrium is crucial in understanding adsorption processes, designing adsorbers, and assessing the adsorbability of water pollutants. It depends on interactions between the adsorbate, adsorbent, and the aqueous solution, including factors like temperature, pH, and competing adsorbates [21]. the relationship between the amount of adsorption and fluid concentration at equilibrium may be expressed as:

$$q = f(T, C) \qquad \textit{(Eq I)}$$

Where:

- $q$: amount of adsorption per unit adsorbent mass at temperature $T$;
- $C$: adsorbate concentration.

Furthermore, if T is kept constant, *(Eq I)* becomes:

$$q = f(C) \qquad \textit{(Eq II)}$$

which refers to as the isotherm equation [22].

The pollutant content in the solid phase (Qe) is generally calculated from the difference between Co, the initial concentration of the pollutant in the solution, and Ce, the final equilibrium concentration [26], [27].

$$Q_e = \frac{(C_0 - C_e) \times V}{m} \qquad \textit{(Eq III)}$$

Where:

- $Q_e$: adsorbed quantity in equilibrium (mg/g)
- $C_0$: the initial concentration of the adsorbate (mg/L)
- $C_e$: the final equilibrium concentration of the adsorbate (mg/L)

- V: solution volume (L)
- $m$: mass of the adsorbent (g)

The shape of the adsorption isotherms depends on the nature of the pollutant, the solvent and the solid [26], [28]. It can provide information on the adsorption mechanisms of pollutants on the surface of solids. According to Chi Tien (2019), there are five main types of isotherms [22]:

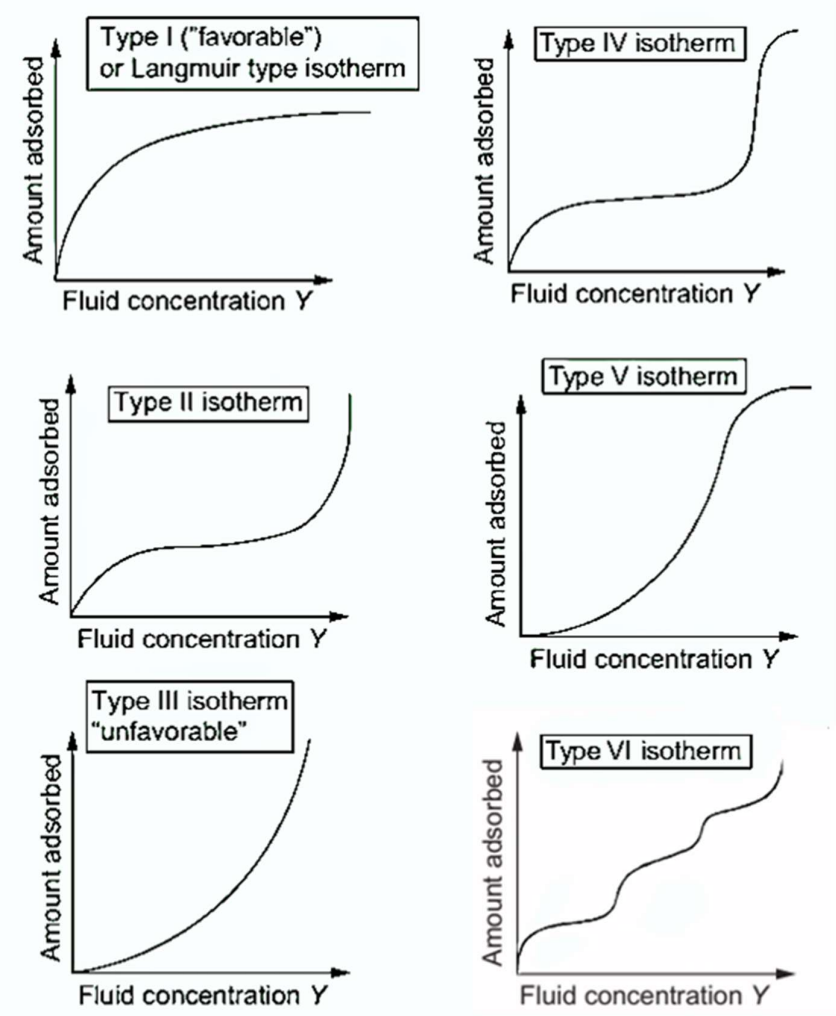


*Figure 10: The types of isotherms*

- **Type I** isotherms represent unimolecular adsorption, are suitable for microporous adsorbents with small pores at low relative pressures, and are usually described by the Langmuir isotherm. A strong interaction (probably chemisorption) may be involved here.
- **Type II:** Adsorbents exhibiting behaviour are characterized by a wide range of pore sizes (macroporous solids) or non-porous solids, so adsorption can range from monolayer to multilayer and ultimately to capillary condensation.

- **Type III:** Adsorbents exhibiting behaviour are characterized by a wide range of pore sizes (macroporous solids) or nonporous solids, so adsorption can range from monolayer to multilayer. The adsorbate/adsorbent interaction is weak compared to the adsorbent/adsorbent (surface/surface) interaction. Adsorption is easier on the first adsorption layer than on the surface.
- **Type IV** isotherms indicated that the adsorption resulted in the formation of two adsorbate surface layers. This is where mesopore filling and capillary condensation in the pores take place. Desorption is possible, which may be parallel to adsorption or have a steeper slope than adsorption.
- **Type V** isotherms: their behaviour is found in the unfavourable adsorption of water vapor by activated carbon. As in type IV, there is mesopore filling and capillary condensation in the pores, but the adsorbate/adsorbent interaction is weaker.
- **Type VI** isotherms are relatively rare and are associated with layer-by-layer adsorption on very homogeneous surfaces. The formation of multilayer depends on the system and the temperature.

Adsorption isotherms can therefore be described by mathematical functions of varying complexity that can be used to estimate the adsorption [22], [28]. These estimation models can be listed as follows:

## II.5.1. Irreversible isotherm and one-parameter isotherm:

The irreversible isotherm equation:

$$Q_e = constant \qquad (Eq\ IV)$$

describes a concentration-independent course typically observed at high concentrations; it is valid at lower concentrations as the isotherm becomes more curved [21].

In the one-parametric, there is only one model which is:

- **Henry isotherm (linear model):** is the most basic model of adsorption isotherm, presenting a linear relationship between the loading of the adsorbent and the concentration, as $K_H$ the isotherm parameter:

$$Q_e = K_H C_e \qquad (Eq\ V)$$

Where:

- $K_H$: Henry adsorption constant (L/g).

This equation is applicable only at very low concentrations. It's suitable for adsorption onto natural adsorbents, where interactions between adsorbate and adsorbent are typically weaker compared to engineered adsorbents like activated carbon. In geosorption, the Henry constant is also known as the distribution coefficient, $K_d$ [21], [27], [28].

## II.5.2. Two-parameter isotherms:

The Langmuir and Freundlich equations are the basic representation of a two-parameter isotherm system:

- **Langmuir isotherm:** one of the first proposed isotherms, assumes that adsorbed and adsorbent interact in an ideal manner on equal surfaces. The equation is [21], [27], [28]:

$$Q_e = Q_{max}\frac{K_L C_e}{1 + K_L C_e} \qquad \textit{(Eq VI)}$$

And the linearized equation is as follows:

$$\frac{1}{Q_e} = \frac{1}{Q_{max}} + \frac{1}{Q_{max} K_L}\frac{1}{C_e} \qquad \textit{(Eq VII)}$$

Where:

- $Q_{max}$*:* the maximum adsorption capacity (mg/g);
- $K_L$: the Langmuir isotherm constant or affinity constant (L/mg).

At low concentrations, the Langmuir equation reduces to the linear Henry isotherm. whereas at high concentrations, a constant saturation value (maximum loading) results in Qe = Qmax = constant [21].

The description of experimental isotherm data obtained for aqueous solutions is frequently considered unsuitable. It is particularly suitable for the monolayer coverage of the adsorbent surface and the energetic homogeneity of the adsorption sites. And it turned out that sometimes it's applicable even when the assumptions are unfulfilled. Another assumption of this isotherm model is the reversibility of the adsorption desorption process[21], [27].

- **Freundlich isotherm:** is the first isotherm model based on experimental results, proposed by Herber Freundlich. It is suitable for studying adsorption on rough and multisite surfaces, as well as multisolute adsorption. The model form is as follows:

$$Q_e = K_F {C_e}^{n_F} \quad \textit{(Eq VIII)}$$

And the linearized equation is as follows:

$$Ln(Q_e) = Ln(K_F) + n_F Ln(C_e) \quad \textit{(Eq IX)}$$

Where:

- $K_F$: adsorption potential constant of Freundlich;
- $n_F$: affinity (strength) constant of Freundlich (commonly between 0.75 and 0.95);

The $K_F$ parameter represents adsorption strength, and higher values indicate higher adsorbent loading.

The exponent $n_F$ determines the curvature of the isotherm and describes surface heterogeneity, with lower values leading to a more concave shape.

- $n_F = 1$ indicates a homogeneous surface, which means a linear model;
- $n_F < 1$ are considered favorable due to high adsorbent loadings at low concentrations;
- $n_F > 1$ are unfavorable.

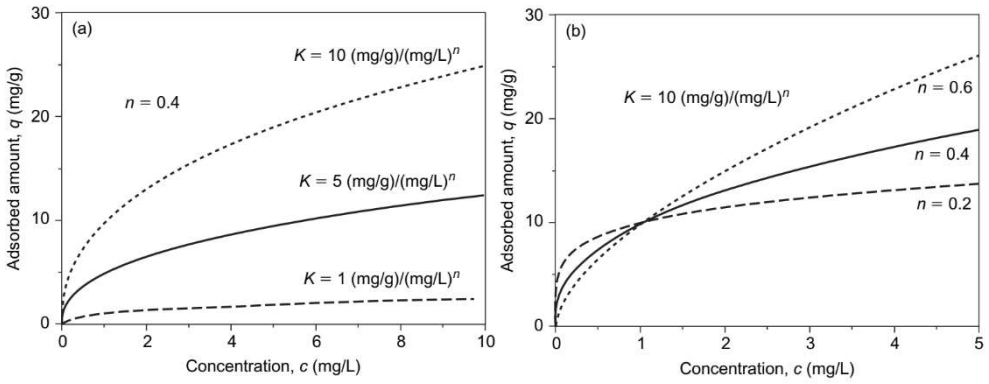


*Figure 11: Influence of the parameters K (a) and n (b) on the isotherm*

$K_F$ and $n_F$ depend on the adsorbent/molecule system studied and the physico-chemical conditions of the medium (T, pH, etc.).

The Freundlich isotherm is commonly used to describe adsorption from aqueous solutions and is a standard equation in water treatment. It can be seen as a combination of Langmuir isotherms representing different adsorption energies.

- **The Dubinin-Radushkevich (D-R) isotherm**: is a model based on the theory of micropore volume filling for intermediate concentrations of adsorbates and is used to describe the adsorption mechanism on heterogeneous surfaces, especially vapors and gases on microporous adsorbents [21], [29]. It has both non-linear and linear forms, represented by equations (Eq X) and (Eq XI) respectively:

$$Q_e = Q_s e^{-K_{DR}\varepsilon^2} \qquad \textit{(Eq X)}$$

$$Ln(Q_e) = Ln(Q_{max}) - K_{DR}\varepsilon^2 \qquad \textit{(Eq XI)}$$

Where:

- $\varepsilon = \mathrm{RTLn}\left(1 + \frac{1}{C_e}\right)$: Polanyi potential;
- $K_{DR}$: Dubinin-Radushkevich constant;
- $R$: gas constant (8.31 Jmol-1 k-1);
- $T$: absolute temperature (K);
- $E = \sqrt{\frac{1}{2K_{DR}}}$: adsorption energy, it's used to predict the adsorption type.

It can be suitable for high solvent activity. However, it exhibits unrealistic asymptotic behaviour and fails to predict Henry's law at low pressure. Unlike the Langmuir and Freundlich models, the DR model assumes that adsorption occurs through pore filling and is considered semi-empirical. A unique aspect of the DR model is its dependence on temperature. It is often used to distinguish between the physisorption and chemisorption of metal ions [29], [30].

## II.5.3. Three-parameter isotherms:

By adding an exponent "n" as an additional parameter, similar to the exponent found in the Freundlich isotherm, three-parameter isotherms can be obtained from the Langmuir isotherm. which creates a variety of models [21], such as:

- **Sips isotherm:** developed by Sips (1948) and formed by combining the Langmuir and Freundlich isotherm models [31], as the following equation:

$$Q_e = Q_{max}\frac{K_S {C_e}^{n_S}}{1 + K_S {C_e}^{n_S}} \qquad \textit{(Eq XII)}$$

And its linearized form is:

$$n_S Ln(C_e) = -Ln\left(\frac{K_S}{Q_e}\right) + Ln(K_S) \quad \textit{(Eq XIII)}$$

Where:

- $K_S$: Sips isotherm constant (L/mg);
- $n_S$: the Sips model exponent.

It aims to predict the heterogeneity of adsorption systems and overcome the limitations associated with high adsorbate concentrations in the Freundlich model[30].

- **Redlich-Peterson isotherm:** Only the denominator has an exponent. The model is combined from Langmuir and Freundlich [30], and its equation is:

$$Q_e = Q_{max}\frac{K_{RP}C_e}{1 + b_{RP}{C_e}^{n_{RP}}} \quad \textit{(Eq XIV)}$$

And its linearized form is:

$$Ln\left(K_{RP}\frac{C_e}{Q_e} - 1\right) = n_{RP}Ln(C_e) + Ln(b_{RP}) \quad \textit{(Eq XV)}$$

Where:

- $K_{RP}$: Redlich-Peterson isotherm constant (L/g);
- $b_{RP}$: Redlich-Peterson isotherm constant (L/mg);
- $n_{RP}$: Redlich-Peterson model exponent $(0 \leq n_{RP} \leq 1)$.

This model is applied when dealing with equilibrium scenarios involving a variety of adsorbent concentrations. It is versatile in its applicability to both homogeneous and heterogeneous systems and exhibits behaviour similar to Henry's region when the degree of dilution reaches infinity [30], [31].

And there are other isotherms with three parameters, such as the Toth isotherm, the Khan isotherm, the Dubinin-Astakhov (D-A) isotherm, etc. [28]

## II.5.4. More than three-parameters isotherms:

The number of parameters in a regression analysis should be less than the number of data pairs. Increasing the parameters requires more experimental effort, but does not necessarily improve the quality of the fit, as experimental error can lead to scatter in the data. Moreover, equations with many parameters complicate numerical

solutions in practical applications. Therefore, isothermal equations with more than three parameters are rarely used. As an example,

- **Baudu isotherm:** is a four-parameters isotherm with the following expression:

$$Q_e = Q_{max} \frac{b_0 {C_e}^{(1+x+y)}}{1 + b_0 {C_e}^{(1+x)}} \qquad \textit{(Eq XVI)}$$

Where:

- $b_0$: the equilibrium constant;
- x and y : Baudu parameters.

This model was formulated to reduce inconsistencies in calculating the Langmuir constant and coefficient using both gradient and tangent methods across different concentrations. it is suitable for concentrations where (1+x+y)<1 and (1+x)<1 [29], [31].

- **Fritz–Schlunder isotherm:** is five-Parametric empirical models are available for a wide variety of equilibrium data (experimental results). The model expression is shown below:

$$Q_e = Q_{max} \frac{K_1 {C_e}^{n_1}}{1 + K_2 {C_e}^{n_2}} \qquad \textit{(Eq XVII)}$$

Where:

- $K_1$, $K_2$, $n_1$ and $n_2$ : Fritz–Schlunder parameters.

And there are a lot of isotherm models that u can find in Annepice 2.

Modelling an isotherm using linear regression analysis requires a deep understanding of adsorption equilibriums [28], [31] and the different types of equilibrium curves [26].

By obtaining an equilibrium curve, we can identify the specific type of isotherm occurring. This information allows us to determine whether the adsorption is monolayer or multilayer, which in turn helps us narrow down our fitting and evaluation of isotherm models based on our data [32]. The corresponding Figure 12 provide visual explanations for these concepts.

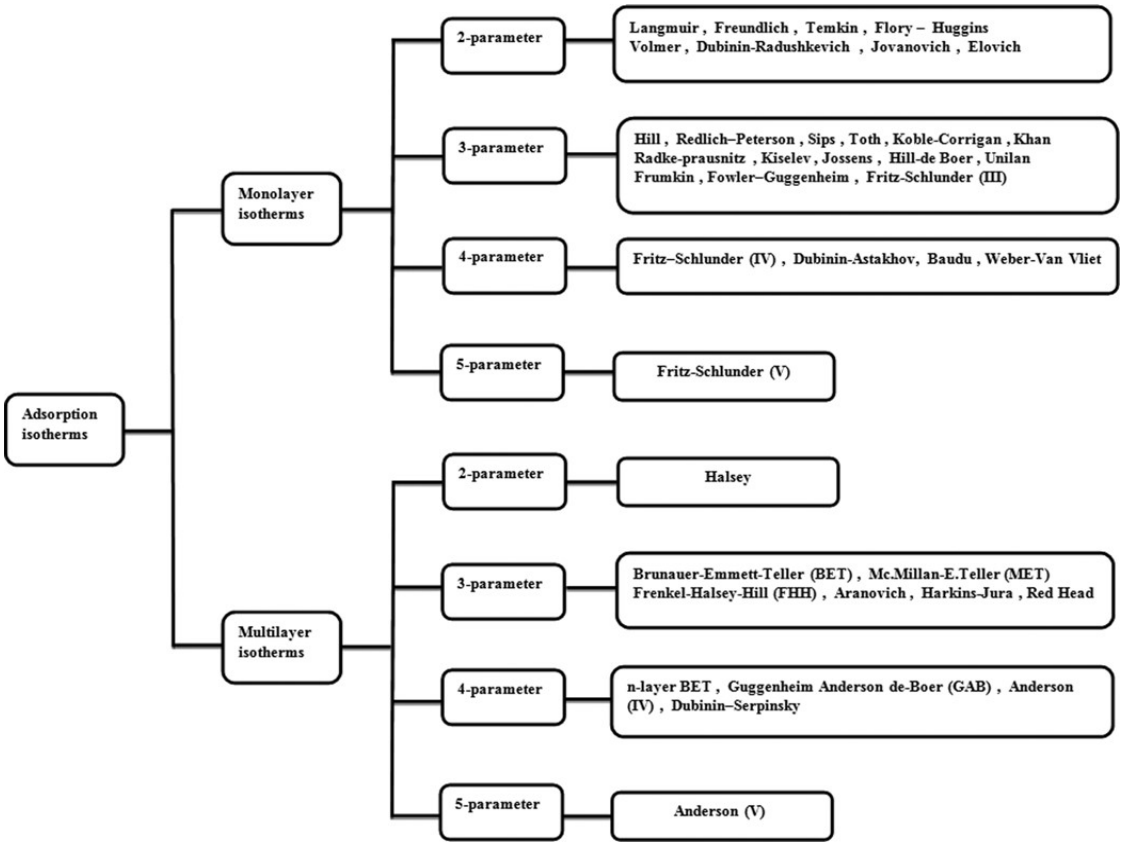


*Figure 12: Models of monolayer and multilayer adsorption isotherms [32]*

## II.6. Adsorption kinetics:

Adsorption kinetics refers to the time progress of the adsorption process, which is often limited by diffusion processes occurring at the external surface of the adsorbent and within its porous particles [33]. The progress of adsorption can be characterized by four consecutive steps:

- Transportation of the adsorbate from the bulk liquid phase to the hydrodynamic boundary layer surrounding the adsorbent particle.
- Diffusion of the adsorbate through the boundary layer to reach the external surface of the adsorbent, known as film diffusion or external diffusion.
- Entry of the adsorbate into the interior of the adsorbent particle through intraparticle diffusion or internal diffusion.
- Chemical interactions as adsorption and desorption occurring between the adsorbate molecules and the adsorption sites.

Adsorption diffusion models are commonly based on three steps: external diffusion, internal diffusion, and mass action adsorption. However, adsorption reaction models, derived from chemical reaction kinetics, consider the overall process of adsorption without explicitly

considering these steps. To encompass both surface reactions and diffusion, a new adsorption kinetic model combining these aspects has been developed [33], [34].

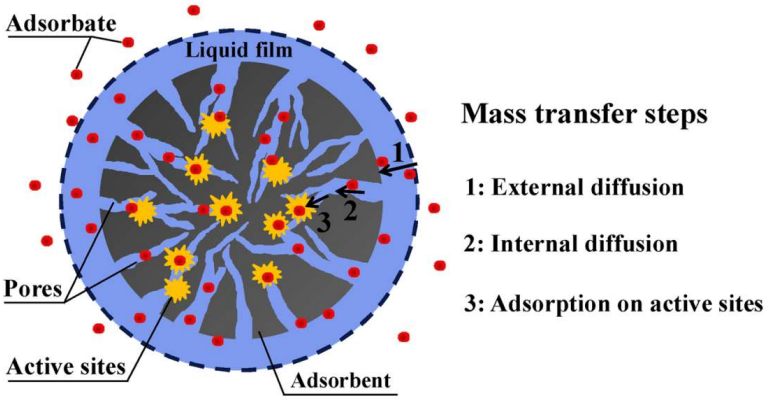


*Figure 13: Mass transfer steps (Adsorption kinetic) [34]*

Despite the existence of many kinetic equations, pseudo-first-order, intraparticle diffusion model, and especially pseudo-second-order equations are still the most popular and renowned kinetic models.

## II.6.1. Pseudo-First-Order Equation (PFO):

Pseudo-First-Order Equation known as the Lagergren equation, which describes the adsorption kinetics using a first-order rate equation. The rate of adsorption is proportional to the difference between the initial concentration and the concentration at any given time [33], [35]. It has the following differential form:

$$\frac{dq}{dt} = k_1(q_e - q_t) \qquad \textit{(Eq XVIII)}$$

And its linearized form (integrating Eq XVIII with boundary conditions: $q_t$=0 at t=0 and $q_t$=$q_t$ at t=t):

$$q_t = q_e(1 - exp(-k_1 t)) \Leftrightarrow ln(q_e - q_t) = lnq_e - k_1 t \qquad \textit{(Eq XIX)}$$

Where:

- $q_t$: the amount of solute per unit mass of adsorbent at time t, $q_t = \frac{V(C_0 - C)}{m}$;
- $q_t$: the equilibrium value of $q_t$;
- t : time;
- $k_1$: PFO rate coefficient.

## II.6.2. Pseudo-Second-Order Equation (PSO):

the simplest and useful model for fitting data, describes the adsorption kinetics using a second-order rate equation. The rate of adsorption is proportional to the product of the remaining adsorption capacity and the square of the concentration at any given time [33], [35]. It has the following differential form:

$$\frac{dq}{dt} = k_2(q_e - q_t)^2 \qquad \textit{(Eq XX)}$$

And its linearized form (integrating Eq XX with boundary conditions: $q_t$=0 at t=0 and $q_t$=$q_t$ at t=t):

$$q_t = \frac{k_2 {q_e}^2 t}{1 + k_2 q_e t} \Leftrightarrow \frac{t}{q_t} = \frac{1}{k_2 {q_e}^2} + \left(\frac{1}{q_e}\right) t \qquad \textit{(Eq XXI)}$$

Where:

- $k_2$: PFO rate coefficient.

The following figure shows the physical meanings of the PFO and PSO models:

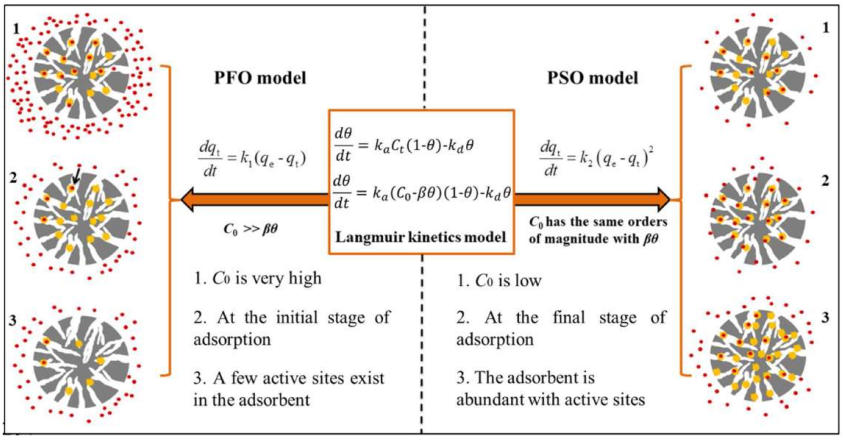


*Figure 14: Physical meaning of PFO and PSO [34]*

## II.6.3. Intraparticle Diffusion Model (IDM):

It states that adsorbate diffusion in the adsorbent is assumed to be the slowest step, while that in the liquid film is instantaneous [34]. The three most widely used IDM models are the Boyd intraparticle diffusion model[33], the Weber and Morris model[36], and the phenomenological internal mass transfer model [34], [36]. For example:

- **Weber-Morris model:** According to Weber-Morris, the phenomenon of adsorption often results in solute uptake having a nearly proportional relationship with $t^{1/2}$ rather than contact time (t), which describes the

phenomenon of intraparticle diffusion. The W&M model is formulated as it's shown below:

$$q_t = k_{int} t^{1/2} + c \qquad \textit{(Eq XXII)}$$

Where:

- $k_{int}$: the intraparticle diffusion rate constant ($mg.g^{-1}.s^{-1/2}$) ;
- $c$: an intercept, represents the boundary layer thickness (mg/g).

## II.7. Factors affecting the adsorption:

The molecular mechanism of adsorption depends on factors such as the chemical structure of the adsorbate. Although it is difficult to establish a direct relationship between the adsorption, adsorbent, and adsorbate properties, understanding these factors is crucial in designing effective adsorption system.

According to R. Gourdon (1997) in his final report [27] and to the results and the remarks on the articles of A.A. Inyinbor et al (2016) [37], Md. Ahmaruzzaman (2008) [38], Ziwen Du et al (2014) [39] and E.I. Ugwu et al (2020) [40], the factors can be identified as follows:

### II.3.1. Adsorbent properties:

They have a large effect on the adsorption:

- **Structure of the adsorbent:** properties such as particle size, pore size, surface area, surface homogeneity, and surface chemistry affect adsorption capacity and rate. Smaller particles, larger pore sizes, and highly porous structures generally improve adsorption capacity, while surface chemistry, including functional groups, influences adsorption behaviour.
- **Specific surface area**: is the main factor in adsorption. By increasing the surface area, more species are adsorbed. Therefore, to achieve significant adsorption, an adsorbent with a large surface area is preferred.
- **Adsorbent concentration:** Increasing the amount will generally increase the adsorption efficiency but decrease the adsorption density. A higher dose provides more available adsorption sites, increasing removal efficiency. However, particle interactions and aggregation can reduce the total surface area and increase the diffusion path length, thereby affecting adsorption.

### II.3.2. Solvent/Adsorbate properties:

The properties of the adsorbed molecules, such as the presence and location of substituents, affect their polarity, solubility, and acid-base properties.

- **Polarity:** Polar solutes have a greater affinity for polar solvents or adsorbents, while nonpolar molecules prefer a nonpolar environment. Presence of other ions in solution: If the adsorbate is a metal ion, the presence of other metal ions may compete for adsorption sites on the adsorbent.
- **Solution pH:** In general, solution pH affects adsorption differently depending on the nature of the adsorbate and the pH of the adsorbent. Changes in Ph affect the polarity of the reactive moieties of the surface area, resulting in weakening electrostatic, ionic, and hydrogen bonding interactions between adsorbate and adsorbent.
- **Molecular size and shape:** larger molecules may have difficulty accessing adsorption sites in the pores of the material.
- **Solubility:** less soluble substances generally get adsorbed more easily due to fewer interactions with ions in water.
- **Adsorbate concentration:** In general, at constant temperature, the amount of adsorption increases with increasing concentration.

### II.3.3. Operating/Process conditions:

- **Temperature:** Effect, especially in the process of physical adsorption Lower temperatures generally result in better adsorption because physical adsorption is exothermic. At equilibrium, the amount of adsorbed species increases with decreasing temperature. However, as the temperature increases, adsorption decreases because it is an exothermic process.
- **Contact time:** Equilibrium between adsorbent and solute must be achieved for adsorption to be complete. Therefore, equilibrium interactions require a certain amount of time to ensure adsorption. The time required to reach equilibrium is called the contact time.

## II.8. Conclusion:

Adsorption is an effective and well-established technique for treating various industrial effluents. Through continuous research, the adsorption process can be further improved and optimized, unlocking greater potential for solving environmental and industrial problems. Its efficiency makes it an invaluable tool for creating a cleaner, safer, and more sustainable future.

All factors that can affect adsorption must be taken into consideration, as well as the nature of the pollutants (adsorbates) and the physiochemical characteristics of the adsorbents, in order to achieve the desired results.

# *Chapter III:*

# *Theorical concepts in optimization and modelling*

# Chapter III: Theorical concepts in optimization and modelling

## III.1. Introduction:

Knowledge of the theoretical basis and concepts of the modelling and optimization process is essential in order to develop and apply effective and efficient mathematical models and techniques to solve real-world problems.

This chapter reviews some of the theoretical concepts of modelling and optimization, providing a solid foundation for subsequent analysis and practical applications. It focuses on four key areas: the response surface method (RSM) and design of experiments (DOE), which will help us to model the factors that affect the adsorption process in order to find the optimal operation conditions to maximize the adsorption; the dragonfly algorithm, which will help in the optimization of choosing the starting point; and finally, model validity checking.

## III.2. Response surface methodology (RSM):

Response surface methodology (RSM) is a mathematical technique used for analyzing relationships between variables and responses. It was initially developed by Box and Wilson in 1951 and has since become a widely adopted approach for experimental design. It involves fitting mathematical models to experimental data to understand and optimize the underlying processes [41], [42].

RSM follows a six-step process:

1) Selection of independent factors and possible responses;
2) screening experiments (choosing experimental designs such as full factorial designs or fractional factorial designs) that can help identify the most influential variables;
3) Selecting appropriate ranges for these variables (which increases the chances of identifying optimal conditions);
4) Selection of an experimental design strategy (central composite design (CCD), Box-Behnken design (BB), etc.);
5) Fitting mathematical surfaces to experimental data to capture the relationship between the predictor variables and the response;
6) Determine the optimal conditions.

By systematically varying parameters, RSM improves process performance and reduces variability. It is widely used in engineering and is supported by software tools such as Design Expert, Minitab, Statistica, JMP, and Matlab. RSM provides a systematic approach to process

optimization and efficiency improvement, reducing costs and minimizing experiment time [41], [42].

## III.3. Design of experiments (DOE):

Design of experiments (DOE) is a systematic statistical method and a fundamental component of RSM for planning, conducting, analyzing, and interpreting experiments to understand the relationships between input variables (factors) and specific output variables (responses) of interest. It enables optimization, prediction, and interpretation of the process. This approach leads to enhanced process performance, a reduced number of variables by focusing on the most significant factors, and decreased operation costs and experimental time. These features make it applicable in various industries and sciences and useful in making decisions to improve the efficiency, quality, and performance of processes and products, which is common across all disciplines [41], [43], [44].

The purpose of DOE is to optimize and improve a process, product, or system by effectively studying the effects of various factors and their interactions. This involves carefully selecting variables, defining their levels or settings, and designing experiments so that valid conclusions can be drawn from a limited number of observations

DOE enables optimization, prediction, and interpretation of the process. This approach leads to enhanced process performance, a reduced number of variables by focusing on the most significant factors, and decreased operation costs and experimental time. These features make it applicable in various industries and sciences and useful in making decisions to improve the efficiency, quality, and performance of processes and products, which is common across all disciplines [43].

A response value is obtained from every experimental point, and this value is represented by a polynomial function with unknown coefficients that nee d to be determined. Upon completion of the experimental layout, a system is presented with a set of n formulas involving p variables for which values need to be determined [44].

According to Goupy (2013), this system can be written simply in matrix notation:

$$y = aX + e \qquad \textit{(Eq XXIII)}$$

Where:

- $y$ : vector of responses;
- $X$ : calculation matrix, or model matrix, which relies on both the selected experimental data and the assumed model;
- $a$ : coefficient vector;
- $e$: deviation (errors) vector.

In this system, there are n equations and p + n unknowns. To solve it, we use a regression method based on the least-squares criterion. Estimates of the coefficients are denoted by $\check{a}$, and the result is:

$$a = (X'X)^{-1}X'y \qquad \textit{(Eq XXIV)}$$

Where: X' is the transposed matrix of X.

Two matrices are constantly involved in experimental design theory:

- The information matrix $(X'X)$
- The dispersion matrix $(X'X)^{-1}$

The concepts and properties of the most classical experimental designs are needed to solve that system. Understanding the experimental design method is based on two essential notions:

## III.2.1. Concept of experimental space:

Experimental space represents the space where experiments are conducted and visualized. It's a two-dimensional space that will facilitate graphical representations, which make it easy to extend the concepts introduced to multidimensional spaces [44].

It includes:

- **Factors:** are any variables that are definitely controllable and can affect the observed response. It can be an assumption or a specific cause of a phenomenon. The values assigned to the experimental factors are called levels. To study the effect of a given factor, its variation is usually constrained between two limits. Lower limit (-1) and upper limit, which is called the factor's range of variation, or simply the factor's domain. They are represented by axes, and points in the space represent specific experiments [44], [45].

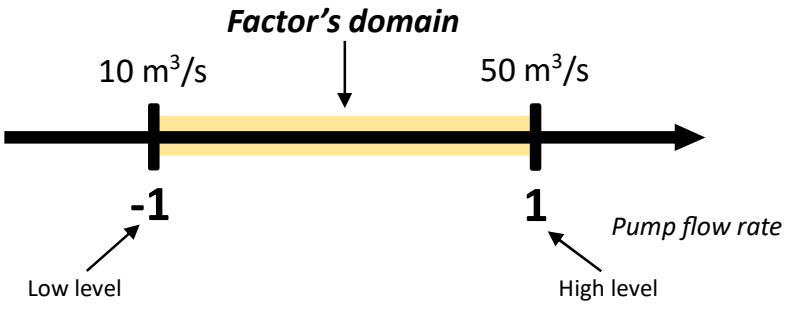


*Figure 15: The pump's flow variation range*

- These values can have two important modifications: the offset of the measurement start and the change in the unit of measurement. These two

modifications introduce new variables called reduced center variables (encoded variables). The advantage of coding units is that the design of experiments can be represented in the same way regardless of the field of study and factors [44].

$$X = \frac{x - x_0}{Step} \quad \textit{(Eq XXV)}$$

Where:

- $Step = \frac{x_{+1} - x_{-1}}{2}$
- X: the centered (coded) variable
- $x_0 = \frac{x_{-1} + x_{+1}}{Step}$: the central value between high and low levels
- $x_{-1}$and $x_{+1}$: variables at low and high levels respectively.

- **Responses:** are quantity that is measured to determine the effect of factors on the system. it can be quantitative or qualitative. it's a variable of interest depends on factors, and their levels are represented on the axes [45].

The definitions given above apply to continuous variables. But there are other types of variables. There are discrete variables, orderable quantities such as distances. Here, the notion of experimental space still exists, but this space has different properties.

## III.2.2. Concept of response surface:

The response surface is composed of all the points within the study domain, with each point representing a response. The difficulty is to decide on the quantity and positioning of experimental data points that can ensure the maximum precision of the response surface, but at the same time, reduce the number of conducted experiments to a minimum. To graphically represent the response space in experimental design, an extra dimension is needed in comparison to the experimental space [44].

## III.2.3. Designing an experiment:

It is usually divided into two phases: The first is to examine several important factors that are expected to have a significant impact on the final outcome, which is called the screening phase. This second is to select important factors that are systematically optimized to reach the best solution, which is called optimization phase.

a) **Screening phase:** is performed to identify factors and their interactions that have a significant impact on the final result. This is accomplished by using factorial designs, which test all factors simultaneously. [43], [46].

For k factors at two different levels (-1) for the lower level and (1) for the upper level, $2^k$ experiments with different results must be performed. All experiences can be represented in the form of a general matrix containing all combinations of levels which can show that two types of effects can be derived: main effects of the factors ($x_1, x_2$) and the possible interaction effects of the factors ($in\ form\ x_1x_2\ or\ x_1x_2x_3$) [43]. This means an outcome $y$ can be described as a function based on experimental factors, which is called the transfer function.

It's a mathematical model of the posed problem that can be obtained by a linear regression fit of the data obtained; it can be either linear or quadratic depending on the interaction of the factor with itself.

Full factorial, fractional factorial, and Plackett-Burman designs for each two-level factor (k) are most commonly used in the factor selection step because they are economical and efficient. The factorial fractional design allows the assessment of numerous factors using only a few experiments by fractionating a complete factorial 2k design into a 2kp design, with "p" denoting the number of independent design generators chosen to fractionate the design [43], [46]. The basic model designs can be shown in the annepice 2

All calculations can be carried out using a spreadsheet program, but this requires programming and time. It is therefore preferable to use JMP8, a software package that not only calculates the coefficients, but also performs all the statistical calculations needed to assess the quality of the mathematical model.

b) **Optimization phase:** determining the optimum conditions for a process using optimization designs. Simple linear and interaction models might not provide a comprehensive understanding of the process, especially when curvature and local optima need to be considered. Therefore, quadratic models are often employed, which include linear terms, squared terms, and products of pairs of factors.
Central composite design (CCD) and Box-Behnken design (BBD) are commonly employed to fit quadratic models and determine the optimum points efficiently. CCD, as the $3^n$ full factorial design, incorporates a factorial or fractional factorial design with axial points, while BBD uses midpoints of edges and the center of a cube. These designs aid in exploring the system and achieving optimal results [41], [43], [46].

## III.4. Dragonfly Algorithm (DA):

The Dragonfly Algorithm (DA) is an optimization algorithm inspired by the swarming behaviors of dragonflies. The algorithm mimics the two main swarming behaviors of dragonflies: static swarm and dynamic swarm, which correspond to the exploration and exploitation phases of the optimization process, respectively [47].

In the static swarm, small groups of dragonflies move in a small area to hunt for other insects. This behaviour involves local movements and abrupt changes. On the other hand, in the dynamic swarm, a large number of dragonflies form a single group and move together in one direction for a long distance. The behaviors of these swarming types serve as the main inspiration for the DA [47].

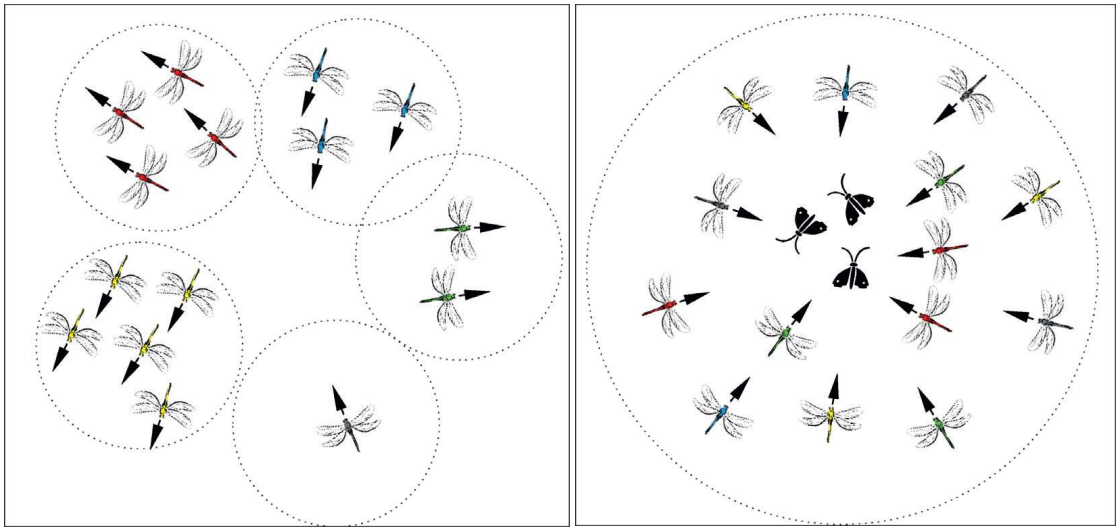

(a) (b)

*Figure 16 :Behaviour of dragonflies: (a) dynamic swarming and (b) static swarming [47]*

To guide the artificial dragonflies in different paths, the algorithm uses six weights: separation weight (s), alignment weight (a), cohesion weight (c), food factor (f), enemy factor (e), and inertia weight (w).

Mathematically, According to Mirjalili (2016) and Rahman & Rashid (2019) each of the aforementioned weight factors are shown in the following equations:

- The separation for as mentioned by Reynolds:

$$S_i = -\sum_{k=1}^{N} X - X_k \qquad \textit{(Eq XXVI)}$$

Where:

- $X$: The current position of the individual dragonfly;
- $X_k$: The position of the k$^{th}$ neighbour;
- $N$: Number of individuals in the dragonfly swarm;
- $S_i$: separation for the individual $i$.

- The alighement:

$$A_i = \frac{1}{N}\sum_{k=1}^{N} V_K \qquad \textit{(Eq XXVII)}$$

Where:

- $V_K$: Velocity of the k[th] neighbour;
- $A_i$: Alignement for the individual $i$.

- The cohesion:

$$C_i = \frac{\sum_{k=1}^{N} X_K}{N} - X \qquad \textit{(Eq XXVIII)}$$

Where:

- $X$: The current position of the individual dragonfly;
- $X_k$: The position of the k[th] neighbour;
- $N$: Number of individuals in the dragonfly swarm;
- $C_i$: Cohesion for the individual $i$.

- Attraction towards a food source:

$$F_i = X^{fs} + X \qquad \textit{(Eq XXIX)}$$

Where:

- $X$: The current position of the individual dragonfly;
- $X^{fs}$: The position of the food source.

- Distraction outwards an enemy:

$$E_i = X^{e} + X \qquad \textit{(Eq XXX)}$$

Where:

- $X$: The current position of the individual dragonfly;
- $X^{e}$: The position of the enemy.

These weights are adjusted during the optimization process to balance exploration and exploitation. High alignment and low cohesion weights are used for exploration, while low alignment and high cohesion weights are used for exploitation [47].

The position updating in the search space is performed using two vectors: the step vector $\Delta X$ and the position vector $X$ [47]–[49]. The step vector represents the direction of movement

and is calculated based on separation, alignment, cohesion, food, and enemy factors, as shown in the following equation:

$$\Delta X_{t+1} = (sS_i + aA_i + cC_i + fF_i + eE_i) + \omega \Delta X_t \quad \textit{(Eq XXXI)}$$

Where:

- $S_i$: separation for the individual $i$;
- $A_i$: Alignement for the individual $i$;
- $C_i$: Cohesion for the individual $i$;
- $F_i$: position of food source for the individual $i$;
- $E_i$: position of the enemy for the individual $i$;
- $\omega$ : inertia weight;
- $t$ : iteration.

The position vector is then updated based on the step vector:

$$X_{t+1} = X_t + \Delta X_{t+1} \quad \textit{(Eq XXXII)}$$

The DA algorithm also incorporates stochastic behaviour and exploration of the search space by including a random walk (Levy flight) when no neighbouring solutions are available. This randomove increases randomness and enhances the exploration of the artificial dragonfly individuals [47]. The DA algorithm is used in combination with the Support Vector Machine (SVM) technique for optimization. The DA-SVM model starts with a random combination of hyperplane parameters for the SVM algorithm. The DA then generates a new population of hyperplanes, and the optimization process is repeated to find the best root mean square error (RMSE) value[50].

```
Initialize the dragonflies population Xi (i = 1,2,…,n)

Initialize step vectors ΔXi (i = 1,2,…,n)
            while the end condition is not satisfied
        Calculate the objective values of all dragonflies
        Update the food source and enemy
        Update w, s, a, c, f, and e
        Calculate S, A, C, F, and E using equations (XXXIV)–(XXXVIII)
        Update neighbouring radius
        If a dragonfly has at least one neighbouring dragonfly
            Update velocity vector using equation (XXXIX)
            Update position vector using equation (XL)
        Else
            Update the position vector using Lévy flight
        End if
        Check and correct the new positions based on the
        boundaries of variables
End while
```

*Figure 17: Pseudo code of DA [48]*

## III.5. Verification of model validity:

### III.5.1. Evaluation Metrics:

- **Mean Absolute Error (MAE):** Mean Absolute Error (MAE) is the most commonly used metric in regression problems; it measures the absolute difference between actual and predicted values. MAE provides simple and robust analysis, but its effectiveness depends on the data and the presence of outliers [51]–[53]. The mathematical expression is written as:

$$MAE = \frac{1}{n}\sum_{i=1}^{n}\left|Y_{pre_i} - Y_{exp_i}\right| \qquad \textit{(Eq XXXIII)}$$

Where:

- $Y_{pre_i}$: Predicted value of i[th] experiment/observation;
- $Y_{\exp_i}$: Actual or experimental value of i[th] experiment/observation;
- $n$: Total numbers of observations/experiments.

- **Mean square error (MSE):** is a widely used regression metric that measures the average of the squared differences between actual and predicted values. It emphasizes outliers that need to be detected, provides a smooth gradient for optimization, and is great for attributing larger weights to the points. Lower MSE values (closer to zero) indicate better model performance [51]–[53]. MSE penalizes the error more than MAE. The mathematical expression is written as:

$$MSE = \frac{1}{n}\sum_{i=1}^{n}\left(Y_{pre_i} - Y_{exp_i}\right)^2 \qquad \textit{(Eq XXXIV)}$$

- **Mean regression square sum (MSR):** measures the average of the squared differences between the predicted values of a regression model and the mean of the true values[52]. The mathematical expression is written as:

$$MSR = \frac{1}{n}\sum_{i=1}^{n}\left(Y_{pre_i} - \bar{Y}\right)^2 \qquad \textit{(Eq XXXV)}$$

Where:

- $\bar{Y} = \frac{1}{n}\sum_{i=1}^{n} Y_{\exp_i}$: the mean of the true values or the average of actual values.

- **Mean total square sum (MST):** measures the average of the squared differences between the actual values and the mean of the true values [52]. The mathematical expression is written as:

$$MST = \frac{1}{n}\sum_{i=1}^{n}\left(Y_{exp_i} - \bar{Y}\right)^2 \qquad \textit{(Eq XXXVI)}$$

And according to Chicco et al (2021), it can also be written as:

$$MST = MSE + MSR \qquad \textit{(Eq XXXVII)}$$

- **Root mean square error (RMSE):** is measured by the square root of MSE, which represents the average magnitude of errors. A higher RMSE value indicates a larger deviation from the actual value, while the opposite indicates a better prediction. It's valuable for assessing elemental validity[51], [52]. The mathematical expression is written as:

$$RMSE = \sqrt{MSE} = \sqrt{\frac{1}{n}\sum_{i=1}^{n}\left(Y_{pre_i} - Y_{exp_i}\right)^2} \qquad \textit{(Eq XXXVIII)}$$

- **The coefficient of determination ($R^2$):** is expressed as the fraction of the variance of the dependent variable that can be predicted from the independent variables. If an $R^2$ was:
  - $0.50 > R^2 > 0.66$: discrimination between high and low values
  - $0.66 > R^2 > 0.80$: approximate quantitative predictions.
  - $0.81 > R^2 > 0.90$: good prediction
  - $R2 > 0.90$: excellent prediction.

  The mathematical expression can be written as:

$$R^2 = 1 - \frac{\sum_{i=1}^{n}\left(Y_{pre_i} - Y_{exp_i}\right)^2}{\sum_{i=1}^{n}\left(Y_{exp_i} - \bar{Y}\right)^2} \qquad \textit{(Eq XXXIX)}$$

It can also be expressed as:

$$R^2 = 1 - \frac{MSE}{MST} = \frac{MSR}{MST} \qquad \textit{(Eq XL)}$$

R2 is monotonically related to MSE (MST is fixed), this means that the order of the regression model based on R2 is the same as the model based on MSE or RMSE [53], [54].

- **Adjusted $R^2$:** Adjusted R-squared is a modified version of R-squared that replaces the biased estimators with their unbiased counterparts while considering the biases and the number of independent variables in the model. The unbiased estimators, derived from MSE and MST, are used to calculate the adjusted R-squared, which is also known in the statistical literature as the Ezekiel estimator. The formula for the custom Ezekiel R-squared calculator is as follows:

$$Adjusted - R^2 = 1 - \frac{N-1}{N-P-1}(1-R^2) \qquad \textit{(Eq XLI)}$$

Where:

- N: Number of observations or experiments;
- $P$: Number of predictors or predicted values.

Adjusted R-squared provides a more accurate measurement of fit and helps prevent over-fitting [54].

- **Mean absolute percentage error (MAPE)** is a regression model performance metric that emphasizes relative error. It is recommended when sensitivity to relative variations is more crucial than absolute variations. However, MAPE has limitations. It only works with strictly positive data and is biased towards low forecasts, making it unsuitable for predictive models with expected large errors [52], [53]. The mathematical expression is written as:

$$MAPE = \frac{1}{n}\sum_{i=1}^{n}\left|\frac{Y_{exp_i} - Y_{pre_i}}{Y_{exp_i}}\right| \qquad \textit{(Eq XLII)}$$

## III.5.2. Statistical analysis of coefficients:

The student's test, also known as t-test, is a statistical method that evaluates the effects of factors and their interactions, which are interpreted by the coefficients of the postulated model, by calculating $t_i$ for each one of them and then comparing it with $t_{crit}$ to decide whether they are significant or not [55]. The t-test evaluates the following hypothesizes:

- $H_0$: $a_i = 0$, $a_i$ is not significant.
- $H_1$: $a_i \neq 0$, $a_i$ is significant

$t_i$ will be the ratio of the coefficient $a_i$ to its variance$S_i$:

$$t_i = \frac{a_i}{S_i} \qquad \textit{(Eq XLIII)}$$

Where $S_i$ is calculated as:

$$S_i = \sqrt{\frac{S^2}{n}} \qquad \textit{(Eq XLIV)}$$

Where:

$$S^2 = \sum_{i=1}^{n} \left(Y_{pre_i} - Y_{exp_i}\right)^2 \qquad \textit{(Eq XLV)}$$

To determine the significance of the t-statistic, it is compared to a critical value from a t-distribution table. The critical value depends on the chosen significance level $\alpha$ and the degrees of freedom $df = n - p$, where $n$ is number of observations and $p$ is number of coefficients [55], [56]. It can be read directly from the Student table (Appendice 4).

$$t_{crit} = v(\alpha, df) \qquad \textit{(Eq XLVI)}$$

According to Leon (1998), if:

- $|t_i| > t_{crit}$: $H_1$ is accepted, the effect is significant.
- $|t_i| \leq t_{crit}$: $H_0$ is accepted, the effect is not significant.

## III.5.3. Model validation test:

- **Analysis of Variance (ANOVA):** is a statistical method used to determine whether there is any significant difference between the means of two or more groups. It's used to evaluate the overall quality of a regression model. It calculates an F-statistic, which is the ratio of the between-group variation to the within-group variation [56], [57].

  According to Leon (1998), to perform the ANOVA test, two hypotheses are supposed:

  - $H_0$ : All parameters have a value equal to 0.
  - $H_1$ : All parameters have the value obtained after estimation.

Two degrees of freedom, $df_1 = p - 1$ (of regressen) and $df_2 = n - p$, and the chosen significance level $\alpha$ used to determine the critical value of the F-test using Fisher's Table (Appendice 5) [56].

$$F_{crit} = v(\alpha, df_1, df_2) \qquad \textit{(Eq XLVII)}$$

If

- $F_{cal} > F_{crit}$ : $H_1$ is accepted, the regression model is considered valid.
- $F_{cal} \leq F_{crit}$ : $H_0$ is accepted, the model used is inadequate and considered invalid [56].

$F_{cal}$ can be calculated using the following table, which summarizes all the information needed:

*Table 5: Calculation of Fisher F-statistic, ANOVA [56]*

| VARIATION SOURCE | DEGREE OF FREEDOM | VARIANCES | MEAN SQUARE | FISHER F-STATISTIC |
|---|---|---|---|---|
| **REGRESSION** | $p-1$ | $RSS = \sum_{i=1}^{n} \left(Y_{pre_i} - \bar{Y}\right)^2$ | $MRS = \frac{RSS}{p-1}$ | $F_{cal} = \frac{MRS}{MES}$ |
| **RESIDUAL** | $n-1$ | $ESS = \sum_{i=1}^{n} \left(Y_{pre_i} - Y_{\exp_i}\right)^2$ | $MES = \frac{ESS}{n-1}$ | |
| **TOTAL** | $n-p$ | $TSS = \sum_{i=1}^{n} \left(Y_{\exp_i} - \bar{Y}\right)^2$ | $MTS = \frac{TSS}{n-p}$ | |

- **Chi-square test ($\chi^2$):** represents a useful statistical method used to determine the association between two categorical variables. It measures the difference between experimental and predicted values based on a specific model. The test helps in assessing whether the experimental data deviates significantly from the expected values, and it is commonly employed for testing the independence of variables in a contingency table, examining the goodness of fit of experimental data to an expected model, and detecting any deviations from expected values [58], [59].
  The formula for calculating the chi-square for the goodness of fit, which is defined by Bevington & Robinson (2003), is:

$$\chi^2{}_{cal} = \frac{\sum_{i=1}^{n}\left(Y_{exp}{}_i - Y_{pre}{}_i\right)^2}{S_{Y_{cal}}{}^2} \qquad \textit{(Eq XLVIII)}$$

Where: $S_{Y_{cal}}{}^2 = \frac{1}{n-1}\sum_{i=1}^{n}\left(Y_{exp}{}_i - \bar{Y}\right)^2$ is the sample variance of observed values $Y_{cal}$.

To conduct this test, two hypotheses are supposed to exist:

- $H_0$ : There is no significant difference between the $Y_{exp}$ and $Y_{pre}$.
- $H_1$ : The is significant difference.

$\chi^2{}_{cal}$ is compared to the critical values from the chi-square distribution $\chi^2{}_{crit}$ with the corresponding degrees of freedom $df = n - 1$ and a chosen significant level $\alpha$. These critical values are available in statistical tables in appendice 6 [58], [59].

According to Bevington & Robinson (2003), if:

- $\chi^2{}_{cal} \geq \chi^2{}_{\text{crit}}$: the null hypothesis $H_0$ is rejected, then the regression model is considered invalid.
- $\chi^2{}_{cal} < \chi^2{}_{\text{cri}}$ : the null hypothesis is accepted $H_0$, then regression model is considered valid.

For each test, the p-value which refers to the probability of null hypothesis can also evaluate the validation of the model under one of the validation tests and under a chosen significant level, if:

- $p - value \leq \alpha$: $H_0$ is rejected.
- $p - value > \alpha$: $H_1$ is rejected.

# *Chapter IV: Experimental Study*

# *Application of adsorption in wastewater treatment in SAIDAL*

# Chapter IV: Experimental Study-Application of adsorption in wastewater treatment in SAIDAL

## IV.1. Introduction:

Low-cost adsorption refers to the use of inexpensive materials as adsorbents for the removal of pollutants from wastewater. Some examples of low-cost adsorbents include by-products from the agricultural, household, and industrial sectors. The use of low-cost adsorbents is a sustainable solution for wastewater treatment and has received much attention in recent years. Developing adsorbents from plant waste and a biomaterial is interesting from an economic point of view. In fact, it is from simple formations that these basic materials can be directly applied [60].

The aim of our study is to exploit and use of agricultural by-products of our country as adsorbents to solve the problem of treating chemical pollution in pharmaceutical industries, like SAIDAL. The experimental study of this work was carried out in a quality control laboratory of the SAIDAL group.

In this chapter, various practical aspects were presented in this study, namely: the methodologies employed for the preparation of the adsorbents from Fennel seeds and Sweet Thapsia that exist in many internal states in Algeria, which is in Medea in our case, with two modifications, a physical method and a biological method using the bacteria "Escherichia coli", the analysis and measurement techniques, as well as the operating procedure followed for the study of the adsorption kinetics of the pollutants Methylene blue (MB) and Chlortetracycline hydrochloride (CTC-HCl).

The experimental procedure consists of characterizing the selected adsorbent and studying the influence of a number of physico-chemical parameters on the adsorption capacity of this material, such as pH and the initial concentration of the pollutant.

# IV.2. Materials:

## IV.2.1. Equipment and instruments:

| Materials | Brand | Application |
|---|---|---|
| Grinder | - | Grinding plants |
| Analytical balance | SARTORIUS and METTLER TOLEDO | Weighing very light masses with great precision |
| UV–Vis Spectrophotometry | Perkin Elmer Lambda 25 | Measuring the absorbance or transmittance of light by a sample in the range of UV-Vis wavelengths region |
| Magnetic stirrer | KMO 2 | Agitating to homogenize a blend. |
| pH meter | METROHM (827 pH lab) | Measuring and adjusting hydrogen potential pH of a sample |
| Conductivity meter | WTW | Measuring the electrical conductivity of a solution |
| Hot plate with magnetic stirrer | Stuart | Heating solutions at the required temperature. |
| Vacuum oven | Memmert | Vacuum drying equipment to speed up the drying process of various materials such as adsorbents. |
| Drying Oven | Salvislab Thermocenter Oven Model DT-96 | Drying, sterilization, and thermal testing |
| Granulometric analysis sieves (20 µm, 100 µm, 200 µm and 310 µm) | - | Determining the particle size distribution of a granular material by separating it into different size fractions using a series of stacked sieves with varying mesh sizes |
| Fourier-transform infrared spectroscopy (FTIR) | - | Analyzing the molecular composition of a sample by measuring the absorption of IR light, Identifying of functional groups (Chemical characterization) |
| Ultrasonic cleaner | SELECTA® | Utilizes high-frequency sound waves to remove contaminants from objects through the creation and implosion of microscopic bubbles in a cleaning solution (destroying and separating the adsorption on the surface) |
| Centrifuge | ALC - Mod. 4225 | Separating components based on density through high-speed rotation, enabling sedimentation |

| | | |
|---|---|---|
| Volumetric flask (10 ml, 200ml and 1000ml) | GLASSCO | Preparing solutions with a specific volume accurately |
| Graduated cylinder (5 ml, 10 ml, 250 ml and 500 ml) | - | Measuring volume and dispensing solutions with great accuracy |
| Volumetric pipet (1ml and 3ml) | - | Measuring and transferring a specific fixed volume of solutions with high precision and accuracy |
| Erlenmeyer flask (250 ml and 500 ml) | DURAN | Used for mixing, heating, and containing solutions |
| Air filter | - | Removing airborne contaminants, ensuring a sterile environment for sensitive experiments. |

### IV.2.2. Products:

- Hydrogen chloride $HCl$
- Sodium hydroxide $NaOH$
- Potassium hydroxide $KOH$
- Sulfuric acid $H_2SO_4$
- Potassium chloride $KCl$
- Bleach $NaClO$

### IV.2.3. Biomaterials:

- **Smooth Thapsia:** in French *"Thapsia"*, in Arabic "درياس" (Drias) and its scientific name is *"Thapsia garganica L."*, is a standing perennial toxic plant species in the Apiaceae or Umbelliferae family resembling a dill. The genus **"Thapsia"** comes from the ancient Greek " **θαψία** (thapsia)" because the plant was discovered on the island of **Thapsos** according to the Greeks, while **Garganica** is related to Mount Gargano in Italy. It's found in hot countries, especially Algeria, Sicily in Italy, and other countries of the Mediterranean region extending into the Atlantic coasts of Portugal and Morocco [61], [62].


*Figure 18: A map shows regions where smooth Thapsia has grown in the last 3 years [63]*

It can grow up to 1.40 meters tall and is found in cultivated fields, path and road sides, disturbed zones, pine wood, and shrubland with rosemary and thyme garigue [61], [62].

*Figure 19: Smooth thapsia*

It is a medicinally important plant, and its micropropagation has been investigated as an option for conservation purposes as wild populations are becoming sparse [64]. It has been used in traditional medicine for over 2,000 years for the treatment of pulmonary diseases, catarrh, fever, pneumonia, and as a counter-irritant for the relief of rheumatism. The root of Thapsia garganica is a strong purgative. Its rhizome is rough, the thickness of a cubit, striking the ground, gray in color, and submerged in water. Its peels contain 20% amylum and 5% soft yellow gum, which is very reddish and consists of caprylic, angelic, and tapic acids and other nitrogen-neutral substances. They are highly ulcerated [61].

The main compound found in the roots of Thapsia garganica is thapsigargin $C_{34}H_{50}O_{12}$ , which is a sesquiterpene lactone. Thapsigargin has powerful irritant properties for the immune system (activation of a number of immune cells). It has also been identified as a complex molecule that has shown

potential for use in modern medicine, particularly in the treatment of malignant tumors, certain cancers, and possibly COVID-19 [65], [66].

Ripe fruits contain the highest amount of thapsigargin (0.7% to 1.5% of the dry weight) followed by leaves (0.1% of dry weight) and roots (0.2%–1.2% of dry weight) [66].

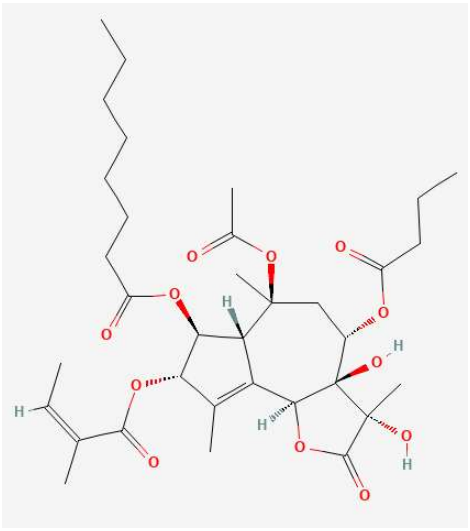

*Figure 20: Chemical Structure of Thapsigargine[65]*

- **Fennel seeds:** come from the plant Fennel, scientifically known as *Foeniculum vulgare Mill.*, an aromatic plant belonging to the Apiaceae family. They are native to the Mediterranean basin but are widely cultivated in temperate and tropical regions worldwide. These versatile seeds have various applications. They are commonly used as a flavoring agent, and their essential oil is utilized in cosmetics and pharmaceutical products. The oil is valued for its balsamic, cardiotonic, digestive, lactogogue, and tonic properties [67], [68].

*Figure 21: Two figures shown the fennel seeds and the fennel plant respectively*

The chemical composition of fennel seeds includes compounds such as fenchone, methyl chavicol, and trans-anethole, 2-pentanone, and

benzaldehyde-4-methoxy. Additionally, they contain moderate concentrations of limonene among the monoterpene hydrocarbons. Cluster analysis has identified distinct chemical subvariants within the (E)-anethole group[67], [69], [70].

Cultivated for its aromatic fruits, fennel is used in culinary preparations and finds application in the cosmetic and pharmaceutical industries. The essential oil derived from fennel seeds consists of phenylpropanoid derivatives, monoterpenoids, and sesquiterpene hydrocarbons. Fennel seeds are rich in polyphenols and flavonoids, which contribute to their antioxidant activity. The essential oil from fennel seeds also exhibits antibacterial properties. Factors such as different accessions and cultivation methods can affect the yields, chemical composition, and antioxidant and antibacterial activities of fennel extracts and essential oils [67], [69], [71]–[73].

### IV.2.4. Pollutants:

Although there are a lot of chemical pollutants, not all pollutants can be adsorbed. In SAIDAIL, 5 pollutants: chlortetracycline Hydrochloride; dexamethasone; diclofenac; methylene blue and cyanocobalamin tested if they would be adsorbed or not by the biosorbents, and chlortetracycline Hydrochloride (CTC-HCl) and methylene blue (MB) were chosen to use them in all experiments because they meet all the following criteria:

- High solubility in water
- Low vapor pressure
- Analysis by UV/visible spectrophotometer
- Cationic structure model
- Widely used in many fields
- It's either toxic or Its degradation produces toxic compounds

- **Methylene blue:** also known as tetramethylthionine chloride $C_{16}H_{18}ClN_3S.xH_2O$ and its nomenclatue is 3,7-bis(dimethylamino)phenothiazin-5-ium, is a cationic dye of the xanthine family. It is a dark green crystalline powder that is soluble in water with deep blue color and slightly soluble in alcohol. It serves as a representative model for medium-sized organic pollutants. It's extensively used in various fields, such as: plastics industry (pigments), food industry (food coloring), cosmetics industry (including hair dyes), pharmaceutical industry (as a coloring and preservative agent), etc [74], [75].

*Table 6: Physical and Chemical properties of Methylene Blue*

| | |
|---|---|
| **Name** | Methylene blue, tetramethylthionine chloride, Basic blue 9, Swiss blue, etc. |
| **Nomenclature** | Est 3,7-bis (diméthylamino) phenazathionium |
| **Family** | Xanthines |
| **Molecular Formula** | $C_{16}H_{18}ClN_3S.nH_2O$ |
| **Molecular Weight (g/mol)** | 319.86 |
| **Topological Polar Surface Area (Å²)** | 43.9 |
| **Solubility in water(g/l) at 25 °C** | 43,6 |
| **pKa** | 3.14 |
| **λ max (mn)** | 659 |
| **Decomposition** | When heated to decomposition it emits very toxic fumes of /nitrogen oxides, sulfur oxides and chloride/. |
| **Stability** | Stable under recommended storage conditions |
| **Solubility at various solvents** | Soluble in ethanol, chloroform; slightly soluble in pyridine; insoluble in ethyl ether |

Methylene blue can have harmful effects on living organisms and aquatic systems. The accumulation of organic matter in water caused by dyes can lead to bacterial growth, putrid odors, and abnormal discoloration. Their consumption by micro-organisms and due to microbial activity release nitrates and phosphates into the environment which promotes uncontrolled aquatic plant growth leading to reduce oxygen levels by inhibiting photosynthesis in deep aquifers aquatic plants in the deeper layers of watercourses and stagnant waters. [76].

Toxicity studies on methylene blue have shown that it is safe when administered in doses of less than 7 mg/kg. However, high doses can cause chest pain, dyspnea, anxiety, tremors, increased blood pressure, and skin discoloration.

Although it is not directly toxic, a significant proportion of its metabolites may be mutagenic, teratogenic, or carcinogenic when broken down into oxidation by-products [76], [77] [75], [78], [79].

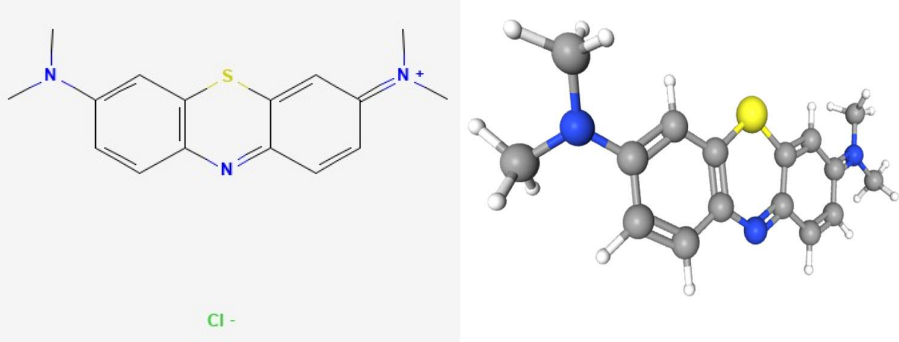


*Figure 22: Interactive Chemical Structure of Methylene Blue*

- **Chlortetracycline hydrochloride (CTC-HCl):** is a hydrochloride salt of an amphoteric chlortetracycline (CTC), from the tetracycline family, with broad-spectrum antibacterial and antiprotozoal activity, produced and derived from Streptomyces aureofaciens (Fam. Streptomycetaceae) and discovered in 1948 by Duggar. It is a yellow, odorless powder composed mainly of crystals in the shape of small hexagons. Stable in the air but is slowly affected by light. It is multifunctional with two chromophores with an α,β-unsaturated ketone in conjugation: aparachlorophenol and an anomalously behaving amide. The tertiary amine is responsible for the basic character, and the phenolic group is acidic. It shares the tetracycline family's ability to form metallic complexes, which makes it useful in the purification and analysis of CTC [80].
  The physical and chemical properties are summarized in the following table.

*Table 7: Physical and Chemical properties of Chlortetracycline hydrochloride [80], [81], [82, p. 64]*

| | |
|---|---|
| **Name** | Chlortetracycline hydrochloride |
| **Nomenclature** | (4S,4aS,6S,12aS)-7-chloro-4-(dimethylamino)-3,6,10,12,12a-pentahydroxy-6-methyl-1,11-dioxo-1,4,4a,5,5a,6,11,12a-octahydrotetracene-2-carboxamide hydrochloride |
| **Family** | Tetracyclines |
| **Molecular Formula** | $C_{22}H_{24}Cl_2N_2O_8$ |
| **Molecular Weight (g/mol)** | 515.35 |
| **Topological Polar Surface Area (Å²)** | 182 |
| **Solubility in water(g/l)** | about 8.6 mg/mL |
| **pKa** | 3.30, 7.44, 9.27 |
| **λ max (mn)** | 376 |
| **Solubility at various solvents** | 1 M NaOH (50 mg/mL), methanol (17.4 mg/mL), 1M NaOH (50 mg/mL) and ethanol (1.7 mg/ml) |

CTC-HCl is the most widely used antibiotic in treating humans, farming animals, and agricultural planting. It acts by inhibiting bacterial protein synthesis by binding to the 30S ribosomal subunit (preventing the addition of amino acids to the peptide chain) [83]. It is highly effective against a wide range of gram-positive and gram-negative bacteria like rickettsial species, certain protozoa, spirochetes, etc. However, certain bacterial strains, such as Staphylococci, have developed resistance to CTC-HCl [80], [81].

The difficulty humans and animals face in metabolizing CTC-HCl leads to its accumulation within their bodies, where it is precisely absorbed, bound to plasma proteins, metabolized in the liver, and excreted in urine and feces in a biologically active form. The chemical stability and resistance of conventional processes make it challenging to eliminate CTC-HCl in wastewater treatment plants. This accumulation and persistence of CTC-HCl residues in the environment can help:

- Inhibiting the growth of freshwater algae;
- having significant toxic effects on phytoplankton species;
- disrupting the activity of anaerobic bacteria, affecting their consumption of acetic acid and butyric acid.

which harm the aquarium system and would leave harmful effects, disrupting the equilibrium of the ecosystem [84]–[87].

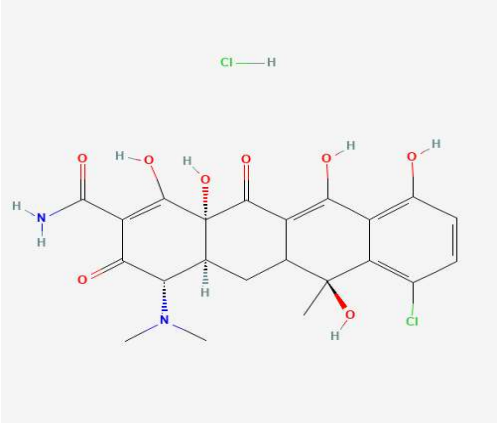

*Figure 23: Chemical structure of Chlortetracycline Hydrochloride [81]*

# IV.3. Methods:

## IV.3.1. Preparation of bioadsorbents:

To prepare the biomaterials (Fennel seeds and Sweet Thapsia roots) to be used in the experiments in this study, the following steps were taken:

1) **Collecting:** obtaining the materials from nature by harvesting or cutting the needed parts. Sweet Thapsia roots and fennel seeds were obtained from the commune of Ksar El-Boukhari, wilaya of Medea.

2) **Washing:** The biomaterials obtained are washed several times with distilled water to eliminate any dust or adhering impurities until clear washing water is obtained.

3) **Peeling and slicing:** After washing them, peeling is carried out to remove the protective layer from the biomaterials, if found, to obtain pure fiber-rich the parts of the plants and to not prevent the absorption during experiments. Then they are cut into small pieces and soaked in distilled water for 24 hours to get rid of the oils and adsorbed substances. All this is done to facilitate the juicing, washing, and grinding processes.

4) **Juicing:** They are placed in a mesh cloth with very small diameter holes, wrapped, and pressed well to get rid of all possible fluids and oils contained inside the plant tissue if possible.

5) **Drying:** the materials are left under the sun for 24 hours, then placed in an oven for 3 to 5 hours between 105°C and 150°C depending on the type of biomaterial.

6) **Grinding:** Grinding was carried out using an electronic mill in order to obtain homogeneous-size materials for laboratory studies, giving small grain sizes.

7) **Sieving:** The particle sizes used for the adsorption tests were mechanically isolated using granulometric analysis sieves with mesh sizes of 315 µm, 100 µm and 20 µm.

Finally, the samples were stored in flasks for subsequent testing away from any external disturbance and protected from possible contamination or accidents and the final results are showing in Figure 24.

*Figure 24: the result of the preparation for biosorbents based on Fennel seeds on the left and Sweet Thapsia on the right*

## IV.3.2. Treatment of bioadsorbents:

In order to improve the adsorption capacity of the obtained bioadsorbents, two experiments have been conducted with the purpose of enhancing their properties. In most cases, the treatments applied have often resulted in an improvement in adsorption capacity and/or kinetics. These treatments have the purpose of disposing of all possible remaining adsorbed substances in the fibers of the obtained bioadsorbents to improve their surface areas.

### a. Rinse method:

A quantity of bioadsorbent is placed in two 400-mL Erlenmeyer flasks filled with distilled water, heated to a temperature of between 50 and 70 °C using a hot plate, stirred using a magnetic stirrer, and then placed in the ultrasound bath for 15 minutes. The aim of these steps is to separate the dirty adsorption on the surface of the bioadsorbent and dissolve and destroy any adsorbed substances using high-temperature ultrasound and sedimentation.

The contents of the flasks are then filtered and sieved using 200 µm, 100 µm, and 20 µm mesh sieves to dispose of the used water. The bioadsorbent obtained was then placed in another two 400-mL Erlenmeyer flasks filled with heated distilled water and placed in the ultrasound bath for another 15 minutes until it settled down. The electrical conductivity of the mixture after it cools down is measured using the conductivity meter to check for the presence of freed substances from the adsorbed substances. After that, the blend is filtrated to get the bioadsorbant. The previous steps are repeated until the conductivity is ≤ 20 µS/cm.


*Figure 25: The difference on turbidity and electric conductivity before and after*

**b. Biological modification:**

In this operational method, the bacterium "*Escherichia coli*" (E. coli) was selected due to its advantageous characteristics, including extensive research, fast growth, high yield, living on a variety of substrates, safety (non-pathogenicity), and facile containment during experimentation [88], [89].

To initiate the process, a specific amount of bioadsorbent (fennel seeds in this case) was added to a bottle containing distilled water and vigorously stirred. Next, a small quantity of E. coli was introduced into the bottle and stirred gently, after which the bottle was placed in an environment with a room temperature of 25 and without light for a period of 3 to 5 days. This allowed the E. coli to cultivate, grow, and consume the substances adsorbed on the fiber surfaces of the biomaterial.

Once the designated time had elapsed, the mixture was emptied through a 100-µm sieve, followed by treatment with bleach and a substantial volume of distilled water to ensure thorough purification and the eradication of all bacteria.

Furthermore, the steps of the rinse method were performed to guarantee the complete removal of any remaining substances.

*Figure 26:The bottle that contain the culture of E. coli in Fennel seeds with air filters and the final results of the treatment*

## IV.3.3. Physico-chemical characterisation of bioadsorbents:

### a. Analysis by Fourier-transform infrared spectroscopy (FTIR):

The analysis by Fourier transform infrared spectroscopy was carried out at the Laboratory of Physical and Chemical Analysis of the Faculty of Technology, Ouzera University Centre, Yahia Fares University in Medea, for a wavelength range of 400–4000 $cm^{-1}$ in order to identify the chemical structure and the nature of the functional groups on the surface of the biosorbents. The KBr pellet technique was used for preparing solid samples for preparation of solid samples for IR analysis by crushing the sample into fine particles and then mixed uniformly with KBr powder then pressed to form a 'KBR pellet'.

### b. Bulk (apparent) density:

According to Ebelegi et al. 2022, The bulk density of each sample is usually determined based of the Archimedes' principle [90], by using the following equation:

$$Bulk\ Density = \frac{M_1 - M_0}{V} \qquad (Eq\ XLIX)$$

Where:

- $M_0$: weight of the empty graduated cylinder;
- $M_1$: weight of the fully packed graduated cylinder with the sample;
- $V$: volume of the graduated cylinder.

By using the taring option in the analytical balances, a 5-mL measuring cylinder is placed on the balance, tare it (set it to zero), and weighted after it is packed with 3-mL of each bioadsorbent and tapped three times. The weight displayed on the balance and the exact volume in the measuring cylinder are noted. Bulk density is calculated by using the following equation:

$$Bulk\ Density = \frac{M'}{V'} \qquad (Eq\ L)$$

Where:

- $M'$: the weight difference displayed on the balance;
- $V'$: the exact volume of bioadsorbent.

**c. Determination of $pH_0$ (or $pH_{pzc}$):**

The pH of point zero charge (PZC) corresponds to the value of pH for which the components of surface charge equal zero for specified conditions. The charges at the surface for the pH of PZC are equally disturbed (negative and positive charges are equal) [91].

According to Al-Maliky et al. (2021), the method consists of preparing 7 bottles containing 100 mg of the biomaterial and a mixture of NaOH 0.1 M, HCl 0.1 M, and distilled water with different concentrations to vary the pH of the medium with agitation for 1 hour in the magnetic stirrer (shown in the table), and the pH was determined as pHi. Then 2 mL of KCL 2M was added to each bottle, which was shaken again for 1 hour. The final pH is measured for each suspension again as pHf. The pH corresponding to equality between the final pH and the initial pH is referred to as the zero charge point [91].

*Table 8: The prepared solutions for pHpzc determination*

| *BOTTLE* | *VOLUME OF 0.1M OF HCl (ML)* | *VOLUME OF 0.1 M OF NAOH (ML)* | *VOLUME OF WATER (ML)* |
|---|---|---|---|
| **1** | 5 | 0 | 15 |
| **2** | 4 | 0 | 16 |
| **3** | 3 | 0 | 17 |
| **4** | 2 | 0 | 18 |
| **5** | 0 | 0 | 20 |
| **6** | 0 | 3 | 17 |
| **7** | 0 | 5 | 15 |

### IV.3.4. The effect of some operating parameters (Batch adsorption):

Adsorption tests were carried out in a batch system for the removal of methylene blue and CTC-HCl from used water using three adsorbents: Fennel seeds and Sweet Thapsia roots from the rinse method (abbreviated as FEN and TH, respectively), and fennel seeds from the biological modification (abbreviated as FBIO).

If a mass *"m"* of adsorbent in (g) is in contact with a volume *"V"* (mL) of a solution with an initial concentration *"$C_0$"* of pollutant (adsorbate) and a concentration *"$C_e$"* at equilibrium, the quantity of pollutant adsorbed *"$Q_e$"* expressed in mg/g is given by the following formula:

$$Q_e = \frac{V(C_0 - C_e)}{m_{ads}} \qquad \textit{(Eq LI)}$$

Where:

- $m_{ads}$ : mass of adsorbent (g);
- $C_0$: initial concentration of adsorbate (pollutant) (mg/mL);
- $C_e$ : equilibrium concentration of adsorbate (pollutant) (mg/mL);
- $V'$: Volume of experimental solution (mL).

The adsorption yield $\%R$ is given by:

$$\%R = \frac{C_0 - C_e}{C_0} \times 100 \qquad \textit{(Eq LII)}$$

The effects on adsorption in the batch system were studied under the following operating conditions: stirring: 300 rpm; temperature: 25°C; quantity of bioadsorbent: 50 mg (for all the effect studies besides the adsorbent dose); volume: 200 mL; time of the experiments: 3 hours (besides the study of the effect of the time contact) and concentration of the stock solution: 0.1 mg/ml (for the effects studies of ph and the adsorbent dose).

The determination of calibration curves of MB and CTC-HCl is explained in details at Appendice 3.

**a. Effect of initial pH:**

The pH of the medium is an important parameter that greatly affects the adsorption capacity of natural adsorbents and biosorbents in particular. It can affect both the surface charge of the adsorbent and the structure of the adsorbate, which makes the optimum pH value vary from one sample to another depending on the adsorbent and the adsorbate used. It is a parameter that must be taken into consideration in any adsorption study.

To do this, the initial pH of the solutions of pollutant MB $C_0$=0.1 mg/mL was adjusted using potassium hydroxide KOH (1M) and sulfuric acid $H_2SO_4$ (1M) solutions for the different pH values studied, ranging from 2 to 12 for the bioadsorbents FEN, TH and FBIO stirred for 3 hours. After stirring, the suspensions were centrifuged for 15 minutes at 6000 rpm in the centrifuge and then analyzed at the required wavelength.

The optimum medium for adsorption of the pollutants was determined by plotting the percentage elimination and the quantity of pollutant adsorbed versus pH curve.

**b. Effect of the adsorbent dose:**

The mass of the adsorbent is one of the most important influencing parameters in the retention and adsorption of pollutants. Adsorption tests were carried out with a 200-ml volume of different initial concentration of the pollutant MB mixed with different masses of bioadsorbents FEN, TH, and FBIO 0.02, 0.05 and 0.1 g, then adding KOH to adjust the pH to 10, stirred for 3 hours. After stirring, the suspensions were centrifuged for 15 minutes at 6000 rpm in the centrifuge and then analyzed at the required wavelength.

**c. Effect of the initial concentration of the pollutant:**

Pollutant concentration is a very important parameter in wastewater treatment in general and in adsorption in particular. To demonstrate the influence of this parameter on the adsorption rate:

- Five samples of 50 mg of FEN and TH bioadsorbent and 20 mg of FBIO bioadsorbent were brought into contact with aqueous solutions of 200 ml volume at different concentrations of CTC-HCl between 0.02 and 0.3 mg/mL, plus a few droplets of 1 M NaOH to adjust the pH to 10.
- Six samples of 50 mg of FEN and TH bioadsorbent and 20 mg of FBIO bioadsorbent were brought into contact with aqueous solutions of 200 ml volume at different concentrations of BM between 0.005 and 0.1 mg/mL, plus a few droplets of 1 M NaOH to adjust the pH to 10.

The operating conditions for these experiments were PH = 10 (adjusted by adding a few droplets of KOH), temperature = 25 (room temperature), time = 3 hours, and stirring speed = 300 rpm.

**d. Effect of contact time:**

Knowledge of adsorption kinetics is of great practical interest for optimal use of adsorbents in industrial operations and for controlling the factors that need to be optimized to manufacture or improve adsorbents. By determining the time corresponding to adsorption equilibrium, adsorption isotherms for each adsorbent could be constructed. Knowing this time is essential for calculating the maximum adsorption capacity and determining the type of adsorption that occurs in monolayers or multilayers.

To do this, the following protocol was followed: A mass of 50 mg of the biosorbents FEN, FBIO, and TH with 200 mL solutions of the pollutant CTC-HCl with an initial concentration of C0 = 0.1 mg/mL was placed in Erlenmeyer flasks for every bioadsorbent-pollutant duo combination. then stirred for 3 to 4 hours. At the end of the time, the suspension was separated by centrifugation for 15 minutes. Supernatants were analyzed by UV-Vis spectroscopy at appropriate wavelengths.

# IV.4. Results and discussion:

## IV.4.1. Physico-chemical characterisation of bioadsorbents:

### a. Analysis by Fourier-transform infrared spectroscopy (FTIR):

The adsorption capacity of bioadsorbents depends on the chemical reactivity of the functional groups on the active side in the surface. Therefore, knowledge of the functional groups on the surface would provide a better understanding of these adsorption capacities.

The results of the FTIR spectro are shown in the figures Figure 27, Figure 28 and Figure 29. The FTIR spectra presented in the Figure 27 and Figure 28 show that the two spectra FEN and FBIO are similar and exhibit the same characteristics with some modifications to the intensity of the bands. Several peaks were observed from the spectra indicating that the Fennel seeds and Sweet Thapsia is composed of various functional groups.

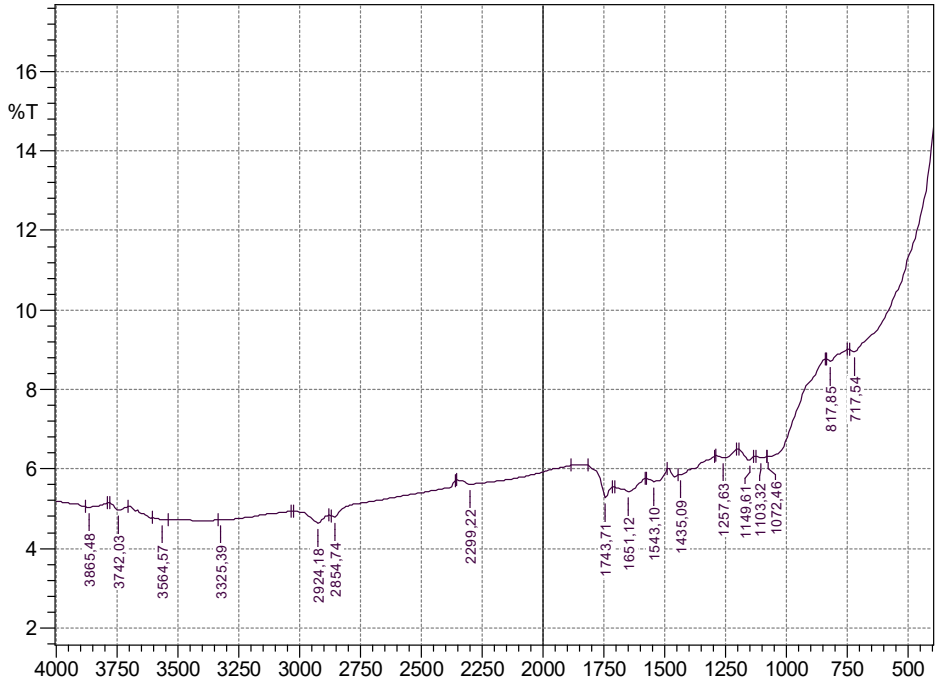


*Figure 27: Infrared spectrum for FEN*

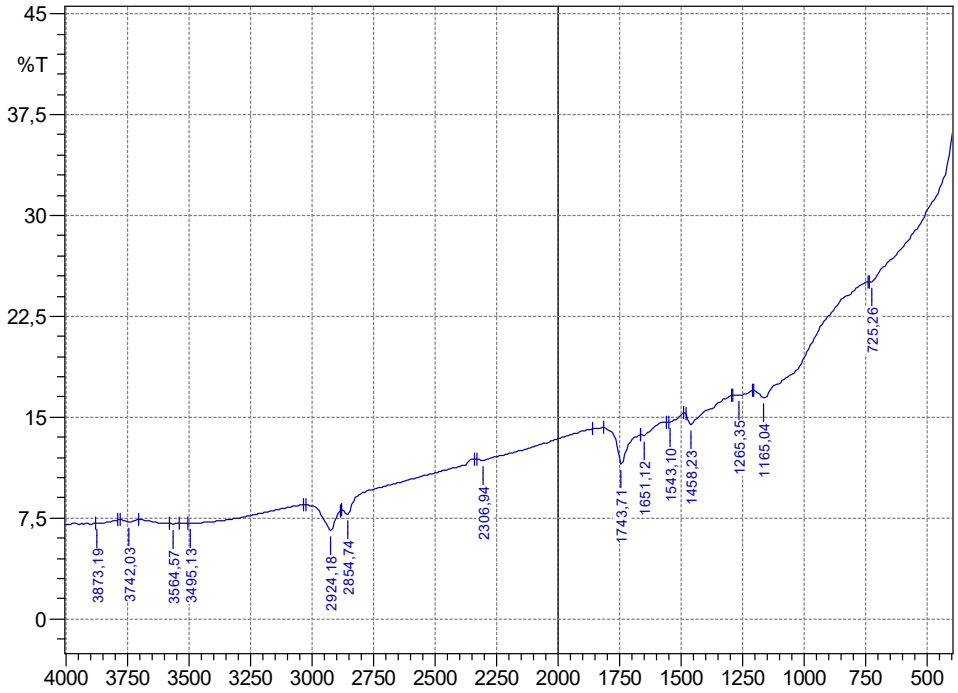


*Figure 28: Infrared spectrum for FBIO*

According to the FTIR spectra of the adsorbents are shown in figures 29 and 30 and to Kawther & Jasim (2019) and Mabungela et al. (2023) in their FTIR study, which indicate that:

- The band on FEN at 3495.13 $cm^{-1}$ and on FBIO at 3325.39 $cm^{-1}$ represented the stretching frequency for the hydroxyl (-OH) group.
- The two small, sharp absorption peaks at 2924.18 and 2854.74 $cm^{-1}$ for FEN and FBIO were linked to the frequencies of C-H (carboxylic) stretch vibration in $CH_3$ and $CH_2$, respectively.
- The peak on FEN and FBIO at 1743.71 $cm^{-1}$ (for an ester) and at 1651.15 $cm^{-1}$ represents the C=O group, although 1651.15 $cm^{-1}$ can also represent a C=C bond.
- The peak was observed for the carboxylic group (-COOH) at 1543.10 $cm^{-1}$ at both.
- The peak at 1435.09 $cm^{-1}$ represents the stretch of the (-CO) group for primary alcohol for FEN, but it shifted to 1458.23 $cm^{-1}$ for FBIO.
- The peaks at 1257.63 $cm^{-1}$ and 1149.61 $cm^{-1}$ represent C-O group and -C-O-C-, respectively, for FEN and at 1265.35 $cm^{-1}$ and 1165 $cm^{-1}$ for FBIO.
- Several unique peaks were observed for FEN at 817.85 $cm^{-1}$ and 717.54 $cm^{-1}$ for FEN, which is assigned for C=C deformation and a C-H deformation for a $CH_2$, and 725.26 $cm^{-1}$ for FBIO, which is assigned for C-H for a $CH_2$.

In general, for both FEN and FBIO, the range of wavelengths is from 1460 $cm^{-1}$ to 1063 $cm^{-1}$ due to C-O group for a primary alcohol.

The possible function groups that could exist in both FEN and FBIO surfaces can be **acids carboxylic, esters, aldehydes, and maybe primary alcohols**. There isn't much difference between them [92], [93].

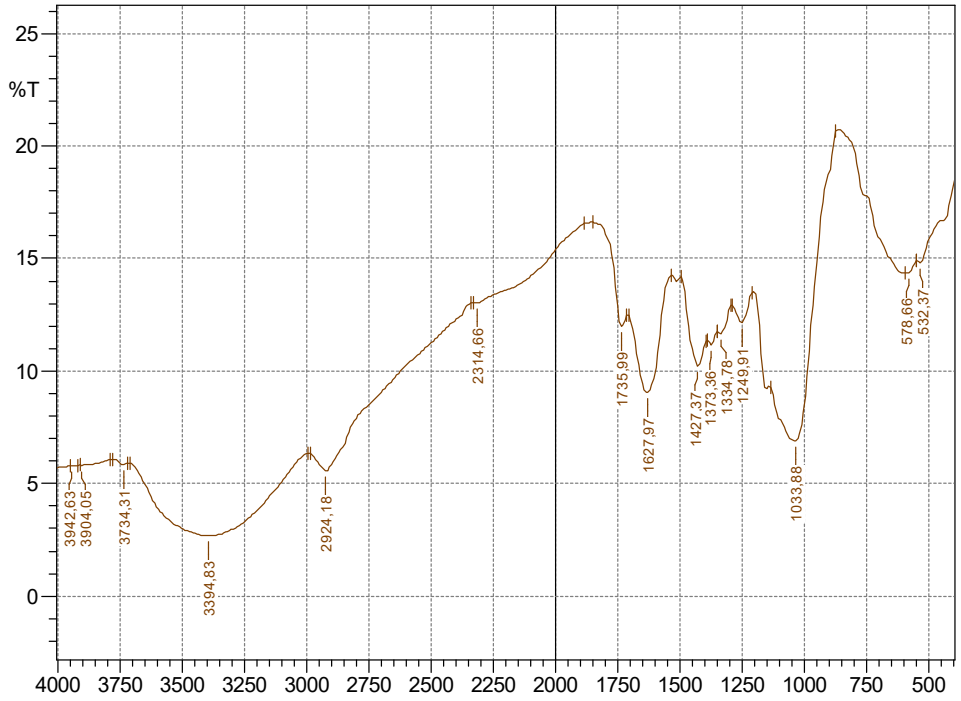


*Figure 29: Infrared spectrum for TH*

According to the FTIR spectra of the adsorbents are shown in Figure 29 and to Machrouhi et al (2019) in their FTIR study, which indicate that:

- The broad band on TH at 3394.83 $cm^{-1}$ represented the stretching frequency for the hydroxyl (-OH) group, or N-H group.
- The small, sharp absorption peaks at 2924.18 $cm^{-1}$ are linked to the frequencies of C-H (carboxylic) stretch vibration in $CH_3$ or $CH_2$.
- The peak was in 1735. 99 $cm^{-1}$ represents C=O groups for an ester (generally for lactones) or an acid carboxylic.
- The peak was in 1627. 97 $cm^{-1}$ represents C=O groups for an amide, although it can also represent a C=C bond.
- The peak at 1427.37 $cm^{-1}$ represents deformation of the O-H group for a primary alcohol.
- The band at 1373.36 $cm^{-1}$ represents C-H groups for methyl ($RCH_2CH_3$), and at 1334.78 $cm^{-1}$ is for a N-O nitro compositions.
- The peaks at 1249.91 cm1 and 1033.88 cm1 represent the C-O bond for an alcohol and the -C-O-C- bond since it's a biomaterial (cellulose).
- There is a hidden peak approximately at 1150 $cm^{-1}$, which represents the C-O bond for esters.

- Peaks in the region of wavenumbers lower than 800 $cm^{-1}$, like the peak at 578.68 $cm^{-1}$, could be attributed to N-containing bioligands, which are C-N bonds.

In general, the possible function groups that the surface can be composed of in TH are **acid carboxylic, ester, primary amide, primary alcohol and maybe an aldehyde**. The Infrared spectroscopy correlation tables were used in this study [95], [96], [97].

**b. Bulk (apparent) density:** The results are shown in the following table:

*Table 9: Bulk density for bioadsorbents FEN, TH and FBIO*

| | VOLUME ($CM^3$) | MASS (G) | MEAN VOLUME | MEAN MASS | BULK DENSITY |
|---|---|---|---|---|---|
| ***Fennel seeds FEN*** | 3.1 | 0.8848 | 3.1333 | 0.8850 | 0.2824 |
| | 3.1 | 0.8849 | | | |
| | 3.2 | 0.8852 | | | |
| ***Biological fibers from fennel seeds FBIO*** | 3.1 | 1.1286 | 3.1000 | 1.1283 | 0.3640 |
| | 3.1 | 1.1278 | | | |
| | 3.1 | 1.1285 | | | |
| ***Sweet Thapsia Roots TH*** | 3.2 | 1.1165 | 3.1667 | 1.1162 | 0.3525 |
| | 3.2 | 1.1168 | | | |
| | 3.1 | 1.1154 | | | |

Table 9 shows the bulk densities obtained for bioadsorbents: FEN (0.2824 $g/cm^3$), FBIO (0.364 $g/cm^3$) and TH (0.3525 $g/cm^3$). The FBIO has the highest bulk density, followed by the TH, and FEN which has the least bulk density.

These results show that all biosorbents used in this study have bulk densities that are lower than those found in previous studies by Chen et al (2012), Ebelegi et al (2022) and Stanford et al (2020) [90], [98]–[100].

Therefore, bulk densities obtained for the bio-sorbents were within the recommended values for bulk density, making them ideal for absorption higher than the minimum requirement of 250 $kg/m^3$ for application in the removal of pollutants from waste water. [90], [101].

**c. Determination of $pH_0$ (or $pH_{pzc}$):**

The adsorption of a solute onto a solid surface is highly dependent on the pH of the solution and the $pH_{PZC}$ of the surface of the adsorbent used. At solute pH values below $pH_{PZC}$ ($pH < pH_{PZC}$), the bioadsorbent surface is positively charged, and at solute pH values above $pH_{PZC}$ ($pH > pH_{PZC}$), the active site of the surface is negatively charged. These pHPZC values indicate whether adsorption is favorable or not (Al-Maliky et al., 2021; Bouchareb, 2023).

Figure 32 indicates that the $pH_{PZC}$ values are approximately 6 for both FEN and FBIO since they have similar functional groups on their surfaces, and 7 for TH, which can be explained by the existence of acidic functional groups on their surfaces. Above these pH values of the biosorbents, the adsorption of cationic substances is favorable, and the opposite for the second case [91].

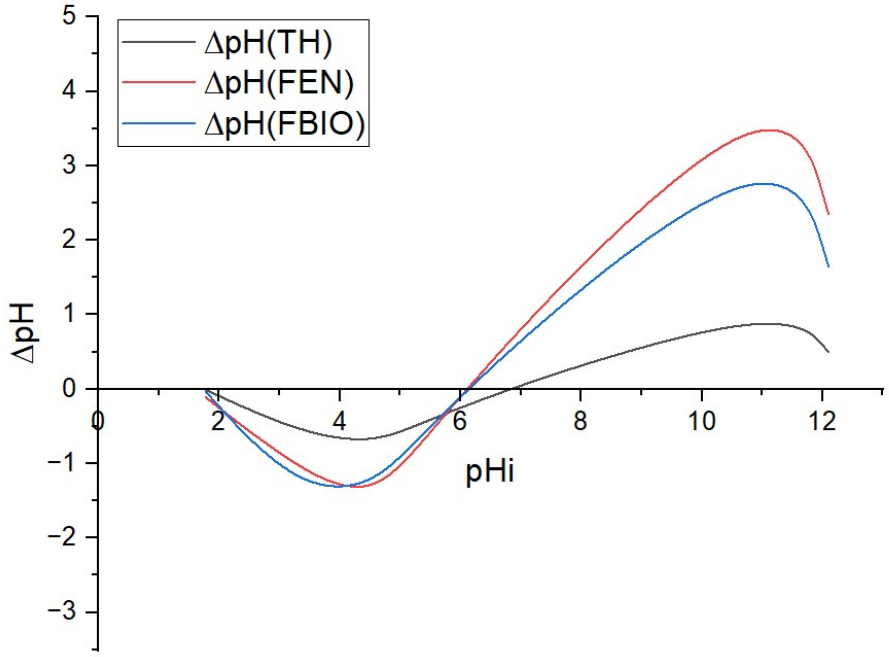


*Figure 30:Determination of the point of zero charge for FEN, FBIO and TH*

## IV.4.2. The effect of some operating parameters (Batch adsorption):

**a. Effect of initial pH:**

The pH effect is dependent on the adsorbent's surface charge. The pH contributes to the adsorbent's surface charge, ionization potential, and distribution of metal ions. Its effect on the biosorption capacity can be interpreted by the competition of the hydronium ions and metal ions for binding sites.

Figure 31 shows that the shape of the six graphs is almost similar for the three biosorbents, where maximum MB elimination is obtained at pH = 10 for FBIO, FEN, and TH, maximum CTC-HCl elimination is observed at pH = 10 for FEN and FBIO, and at pH = 11 for TH, and the minimum is at pH = 2.

The maximum values obtained for the elimination rate and the adsorption capacity are:

*Table 10: Maximum adsorption capacities and elimination rates of biosorption at optimal pH*

| POLLUTANT | BIOADSORBENT | PH(OPT) | QE | R% |
|---|---|---|---|---|
| **MB** | TH | 10 | 272.0596 | 85.58921 |
| | FEN | 10 | 178.0207 | 51.47567 |
| | FBIO | 10 | 206.599 | 25.48507 |
| CTC-HCL | TH | 11 | 26.592 | 8.061634 |
| | FEN | 10 | 213.544 | 64.72301 |
| | FBIO | 10 | 64.192 | 7.921102 |

These results generally show that when the pH of the solution is increased, the quantity of MB and CTC-HCl adsorbed by the bioadsorbents increases. This can be explained by the fact that:

- At low initial pH values, the negatively charged surface of the bioadsorbents is neutralized by the H+ ions, which are observed in large numbers and in turn obstruct the diffusion of the pollutant ions, which reduces the interaction of the MB and CTC-HCl ions (cationic pollutants) with the adsorbent active surface sites (competition between pollutant ions and protons H+) and considerably reduces adsorption. It can also be explained by the repulsive forces between pollutant cations in solution and biosorbent surfaces charged positively at high pH values [40].
- On the other hand, at high pH values, the H+ concentration decreases and the number of negative charges on the surface increases, resulting in good interaction between the dye ions and the surface sites. The net electro-negativity of the biosorbent increases due to the deprotonation of different functional groups present on the biosorbent surface, which means an attraction of positively charged pollutant ions to the negatively charged biosorbent [40], [102].

Similar results were found in the literature by De Gisi et al., 2016; Kim et al., 2006; Maurya & Mittal, 2011 and Ugwu et al., 2020.

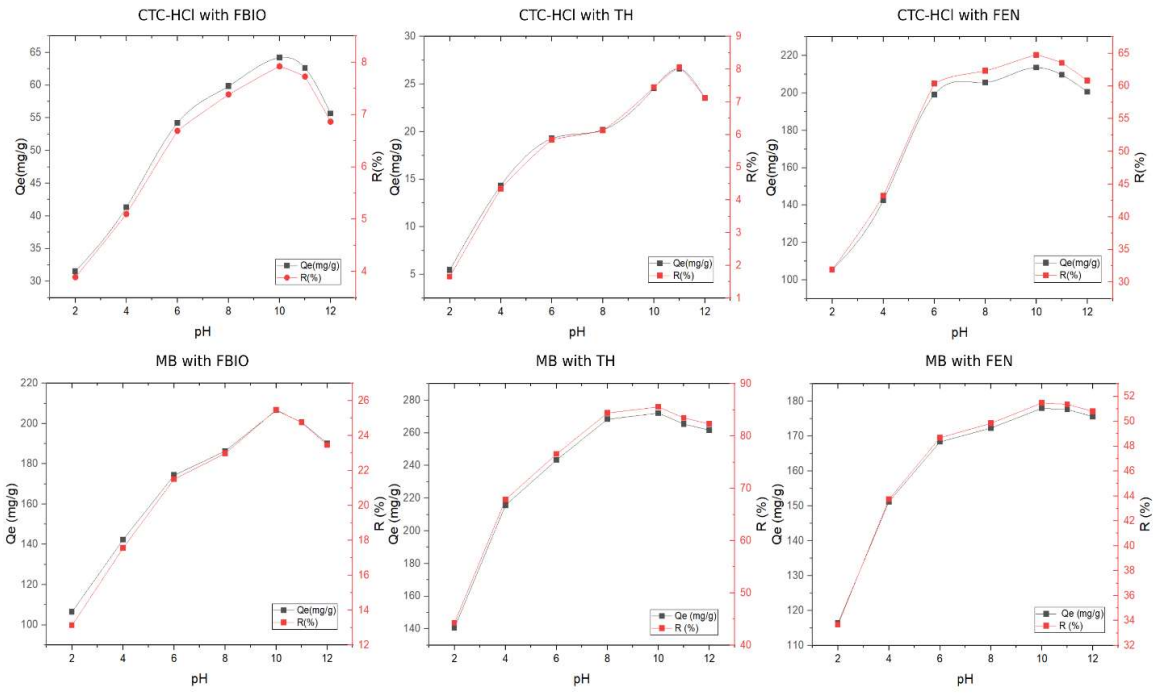


*Figure 31: the influence of pH on adsorption of MB and CTC-HCl by bioadsorbents FEN, FBIO and TH*

**b. Effect of the initial concentration of the pollutant:**

The aim of this investigation is to determine the efficacy of the adsorption system in treating effluents containing pharmaceutical pollutants at different concentrations (from 0.02 mg/mL to 0.3 mg/mL for CTC-HCl and from 0.005 to 0.04 mg/mL for MB) at operation conditions: temperature = 25, stirring speed = 300 rpm, time = 3 h, and pH = 10.

Figure 32 indicates that:

- The adsorption amount Qe of the pollutants MB and CTC-HCl by the biosorbents FEN, FBIO, and TH increases with an increase in the initial concentration of the pollutants until it reaches their maximums:
  - For adsorption of CTC-HCl by FEN: at $C_0$=0.225 mg/mL, $Qe_{max}$= 286.47 mg/g.
  - For adsorption of CTC-HCl by FBIO: at $C_0$=0.237 mg/mL, $Qe_{max}$= 141.40 mg/g.
  - For adsorption of CTC-HCl by TH: at $C_0$=0.082 mg/mL, $Qe_{max}$= 26.86 mg/g.
  - For adsorption of MB by FEN: at $C_0$=0.023 mg/mL, $Qe_{max}$= 66.16 mg/g.
  - For adsorption of MB by FBIO: at $C_0$=0.036 mg/mL, $Qe_{max}$= 213.49 mg/g.
  - For adsorption of MB-HCl by FEN: at $C_0$=0.032 mg/mL, $Qe_{max}$= 98.92 mg/g.

- The removal efficiency increases with an increase in the initial concentration until it reaches a maximum then decreases which is the case for the adsorption of MB and CTC-HCl by FEN ($R\%(CTC\text{-}HCl)_{max}$= 51.78 % at $C_0$=0.082 mg/mL; $R\%(MB)_{max}$= 80.32 % at $C_0$=0.0094 mg/mL) and the adsorption of CTC-HCl by TH ($R\%(CTC\text{-}HCl)_{max}$= 8.58 % at $C_0$=0.082 mg/mL).
- The removal efficiency decreases with increase of the initial concentration that's the case of adsorption of CTC-HCl and MB by FBIO, which means it reached its maximum at an initial concentration lower than $C_0$=0.018 mg/mL for CTC-HCl ($R\%_{max}$= 15.95 %) and $C_0$=0.006 mg/mL for MB ($R\%_{max}$= 78.72 %).
- The removal efficiency increases with an increase in the initial concentration which is the case of the adsorption of MB by TH. That means it didn't reach it

This can be explained by: When the concentrations are low, the ratio of the surface of active sites to pollutants ions in solution is high, meaning all pollutants ions can be retained by the bioadsorbent and completely removed from solution, which implicates that the rate of adsorption increased due to the availability of a larger surface area of the adsorbent until it reached its maximum because of the saturation of the surface of active sites [104]. However, at high concentrations, the fictional force drag-out force due to the concentration gradient is stronger, and the quantity of adsorbent is greater, causing saturation, which left most pollutant ions un-adsorbed, giving a low removal efficacy and a plateau indicating the start of saturation of the adsorption sites.

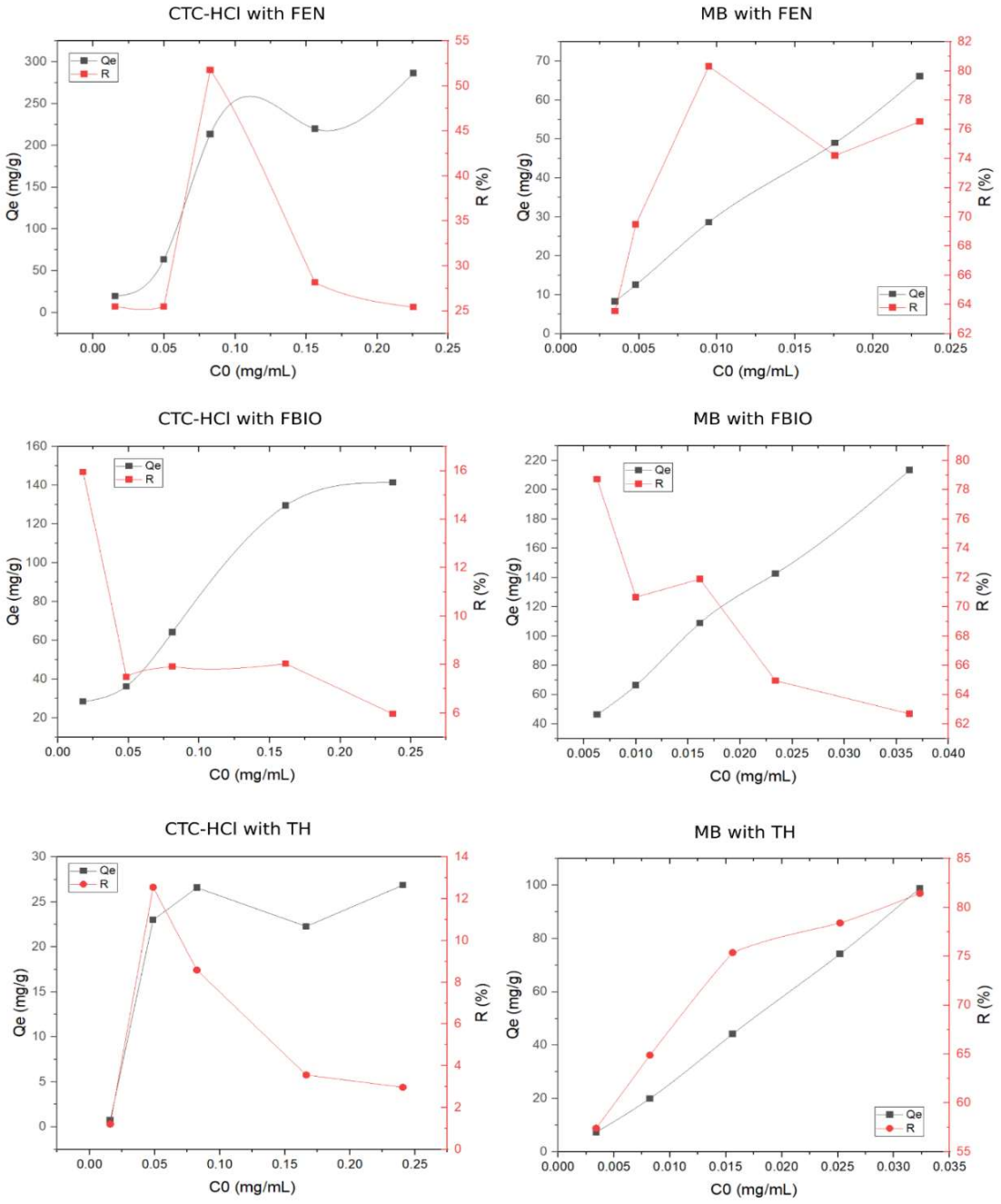


*Figure 32: the influence of the initial concentration on the adsorption capacity and removal efficiency*

**c. Effect of the adsorbent dose:**

The experiments were carried out with a 200-ml volume at a temperature of 25 at different initial concentrations of MB, to which different quantities of FEN, FBIO, and TH were added (0.02g, 0.05 g, and 0.1g).

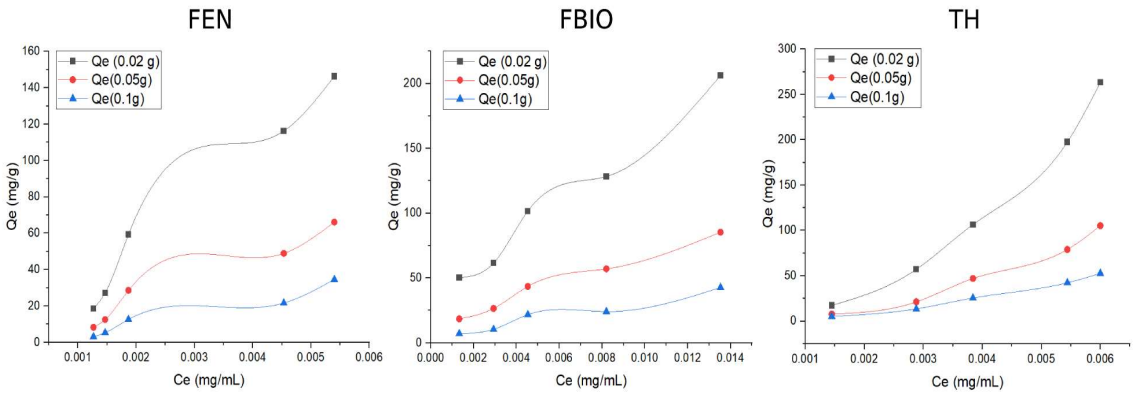


*Figure 33: the influence of the dose of bioadsorbents on the adsorption capacity*

Figure 33 shows that the quantity of MB adsorbed at equilibrium is inversely proportional to the mass of biosorbents. The optimum dose is 0.02 g for FEN, FBIO, and TH.

The results obtained indicate that increasing the dose of adsorbent has a negative influence on the adsorption capacity, which shows a decrease in the quantity of MB adsorbed and in the number of adsorption sites, which increases with the dose of adsorbent towards a state of saturation.

The decrease in adsorption capacity with increasing quantities of FEN, FBIO, and TH is probably due to interactions between the particles (aggregation) resulting from the high quantity of adsorbent. This aggregation would lead to a decrease in the specific surface area of the adsorbent.

On the other hand, increasing the dose of biosorbent had a positive influence on the yield of MB elimination by the adsorbents studied.

**d. Effect of contact time:**

The determination of the time corresponding to adsorption equilibrium enabled adsorption isotherms to be established for each adsorbent. Knowledge of this time is essential for calculating the maximum adsorption capacity and identifying the type of adsorption that should occur in monolayers or multilayers.

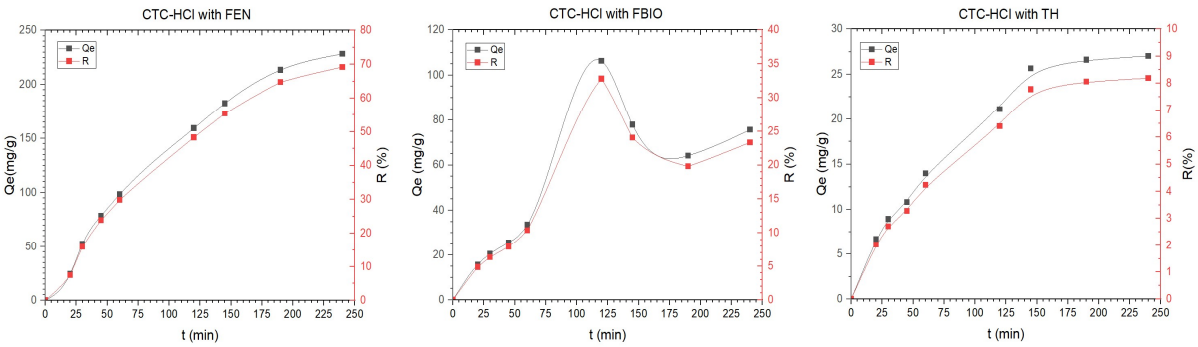


*Figure 34:evolution of the adsorption capacity and removal efficiency of CTC-HCl by FEN, FBIO and TH as a function of contact time*

The results obtained from these experiments, shown in Figure 34, show that:

- The evolution of the adsorption capacity of CTC-HCl by FEN. FBIO and TH as a function of contact time have the same shape as the saturation curves, but adsorption on the three bioadsorbents manifests itself differently.
- The evolution of the adsorption curves for FEN and TH can be broken down into three phases: an initial fast phase, followed by a second phase of moderate speed, to finally reach saturation. This phenomenon can be explained by the existence of an initial stage of adsorption of CTC-HCl on easily accessible sites (explained by the high affinity of the bioadsorbent for CTC-HCl), followed by molecular diffusion of the latter towards less accessible adsorption sites before reaching an equilibrium where all the sites become occupied.
- In the case of FBIO, there is a noticeable increase until it reached a max of 106.28 mg/g at 120 min, then a decrease in the quantity adsorbed and reaching equilibrium over time, indicating a great desorption of CTC-HCl from the solution.
- For the FEN and TH, the time required to reach maximum saturation is much longer—more than 175 min of contact time respectively. Extending this time to more than those max does not lead to a significant improvement in the percentage of elimination of this compound. This justifies taking this contact time into account for the other adsorption experiments.
- FEN is the most profitable when it comes to removing CTC-HCl by 180 min as the optimum time with 64.12% removal efficacy compared to FBIO ($t_{opt}$=120 min and %R=32.79%) and TH ($t_{opt}$ =150 min and %R=6.40%).

## IV.5. Conclusion:

The study was conducted in three main parts: preparation of the bioadsorbents, characterization of the adsorbents, and examination of various parameters influencing the adsorption of MB and CTC-HCl onto the bioadsorbents. These parameters included initial concentration, initial pH, contact time, and bioadsorbent dosage. The bioadsorbents were processed to obtain powders with a particle size of less than 350 nm. The overall results of this study are as follows:

The physicochemical characterization of the bioadsorbents was conducted using FTIR and bulk density measurements. FTIR analysis revealed the presence of different functional groups on the surfaces of all three bioadsorbents, including hydroxyl groups, carboxylic groups, esters, aldehydes, primary alcohols, and additionally amides in the case of TH. Bulk density measurements indicated that FBIO exhibited the highest bulk density (0.364 g/cm3), followed by TH (0.3525 g/cm3) and FEN (0.2824 g/cm3). The determination of the point of zero charge (pHPZC) indicated that FEN and FBIO had pHPZC values of approximately 6, while TH had a pHPZC value of 7.

Moreover, the effects of several operating parameters on the batch adsorption process were investigated. The results demonstrated that:

- The highest adsorption capacities and elimination rates were observed at pH 10 for FEN and FBIO and pH 11 for TH. (TH was the best for MB elimination by Qe=272.06 mg/g, R= 85.59% and FEN for CTC-HCL elimination by Qe=213.54 mg/g, R=64.72%).
- Qe increased with an increase in the initial concentration of the pollutants until reaching a maximum value ($C_{0opt}$: 0.225–0.237 mg/mL for MB and 0.023–0.036 mg/mL for CTC-HCl). However, %R exhibited a maximum at a certain concentration and then decreased.
- Increasing the dosage of the adsorbent had a negative influence on the adsorption capacity but a positive influence on the removal rate due to the availability of active sites.
- FEN demonstrated the highest removal efficacy for CTC-HCl at 180 minutes, with %R = 64.12%, compared to FBIO ($t_{opt}$ = 120 min and %R = 32.79%) and TH ($t_{opt}$ = 120 min and %R = 6.40%). The performance between FEN and FBIO is balanced because the maximum adsorption capacity of FEN at $t_{opt}$ =180 min is similar to the adsorption capacity of FBIO at $t_{opt}$ =120 min, which indicates that the biological treatment made the bioadsorbent faster at getting to equilibrium.

In conclusion, FEN, FBIO, and TH proved to be effective low-cost adsorbents for organic pollutants, but in order to use them to a maximum efficiency, a modelling is needed for the optimisation.

# *Chapter V:*

# *Modelling and optimisation by DOE and Dragonfly Algorithm*

# Chapter V: Modelling and optimisation by DOE and Dragonfly Algorithm

## V.1. Introduction:

Modelling and optimization are essential techniques used in various fields to solve real-world problems. One of the most recent and promising optimization techniques is the Dragonfly Algorithm (DA) and Design of Experiments (DOE), which DA have the ability to optimize and select the most optimal positions that would help in non-linear regression, while the DOE enables the study of the relationship between multiple input variables and key output variables. DOE-based methods, such as response surface methodology (RSM), provide optimum cutting conditions, whereas in soft-computing-based techniques, an objective function is developed to determine a local optimal solution, such as the genetic algorithm in the method [47], [105]. This chapter focuses on applying the vital aspects of modelling and optimization in the context of MB adsorption by FEN, FBIO and TH. The application of the Design of Experiments (DOE) and Dragonfly Algorithm (DA) takes center stage in this exploration to investigate and understand the factors that influence the adsorption process and calculate the optimum and to find the best fit model for the adsorption phenomenon with comparing the performance of linear and nonlinear regression.

## V.2. Modelling and optimisation of factors influencing adsorption and removal efficiency:

In order to optimize the MB removal process by the three bioadsorbents FEN, FBIO and TH, modelling the factors influencing the process was the first point of attention. By focusing on understanding the interactions, effects and optimisation of these factors, the response surface method emerged as the most appropriate approach to use. To this end, the Box-Behnken Design (BBD), a very advantageous type of response surface design, similar to Central Composite Designs (CCDs), was chosen due to its greater efficiency and ability to generate higher order response surfaces while requiring less experimental testing. The factors studied are quantitative.

The three factors and their areas of study are summarized in the table below.

*Figure 35: Factors and range of variations considered*

| *Factors* | *Unite* | *Low level* | *High level* |
|---|---|---|---|
| *pH* | / | 2 | 12 |
| $C_0$ | mg/mL | 0.005 | 0.04 |
| *M* | g | 0.02 | 0.1 |

## V.2.1. Adsorption of MB by FEN:

Table 11 shows the matrix of experiments designed by the Box-Behnken design for the three factors pH, C0, and m and the responses Qe and R, which represent the quantity of MB adsorbed by FEN at equilibrium and the removal efficacy, respectively, for each trial.

*Table 11: Box-Behnken Design for 3 factors*

| | Actual coordinates | | | Coded coordinates | | | | |
|---|---|---|---|---|---|---|---|---|
| Runs | pH | $C_0$ | m | pH | $C_0$ | m | Qe (mg/g) | R (%) |
| 1 | 2 | 0.005 | 0.06 | -1 | -1 | 0 | 5.137 | 44.36948 |
| 2 | 12 | 0.005 | 0.06 | 1 | -1 | 0 | 6.908 | 59.66603 |
| 3 | 2 | 0.04 | 0.06 | -1 | 1 | 0 | 42.658 | 55.6125 |
| 4 | 12 | 0.04 | 0.06 | 1 | 1 | 0 | 54.098 | 70.52663 |
| 5 | 2 | 0.0225 | 0.02 | -1 | 0 | -1 | 56.283 | 53.92859 |
| 6 | 12 | 0.0225 | 0.02 | 1 | 0 | -1 | 79.652 | 76.32002 |
| 7 | 2 | 0.0225 | 0.1 | -1 | 0 | 1 | 12.178 | 58.34287 |
| 8 | 12 | 0.0225 | 0.1 | 1 | 0 | 1 | 17.235 | 82.57015 |
| 9 | 7 | 0.005 | 0.02 | 0 | -1 | -1 | 18.80353 | 54.13685 |
| 10 | 7 | 0.04 | 0.02 | 0 | 1 | -1 | 152.642 | 66.33225 |
| 11 | 7 | 0.005 | 0.1 | 0 | -1 | 1 | 4.023 | 57.91267 |
| 12 | 7 | 0.04 | 0.1 | 0 | 1 | 1 | 30.452 | 66.16625 |
| 13 | 7 | 0.0225 | 0.06 | 0 | 0 | 0 | 29.265 | 84.12238 |
| 14 | 7 | 0.0225 | 0.06 | 0 | 0 | 0 | 29.265 | 84.12238 |
| 15 | 7 | 0.0225 | 0.06 | 0 | 0 | 0 | 29.265 | 84.12238 |

- **Mathematical modelling:**

  The model predicted by BBD design is a quadratic polynomial that describes the variation of the responses (Qe and R) as a function of the three parameters studied ($C_0$, pH, and m) and their possible interactions. After application to Minitab software, the mathematical model is written as follows:

  For the respond Qe, the regression equation in uncoded units is:

$$Q_e = 6.8 + 5.21pH + 3265C_0 - 1101m - 0.244pH^2 + 13189{C_0}^2 + 11360m^2 - 22.9pHm + 27.6pHC_0 - 38361C_0m \quad \textit{(Eq LIII)}$$

  Which had $R^2$ = 95.80% and Adj$R^2$ = 88.24%.

  For the respond R, the regression equation in uncoded units is:

$$R = -1.27 + 7.39pH + 2838C_0 + 538m - 0.3985pH^2 - 54257{C_0}^2 + 3981m^2 - 2.29pHm - 1.1pHC_0 - 1408C_0m \quad \textit{(Eq LIV)}$$

Which had $R^2$ = 98.33% and Adj$R^2$ = 95.33%.

- **Significance of model coefficients (STUDENT t-test):**

A factor is said to be significant at 5% when its observed Student's t value is greater than or equal to the critical Student's t value at a 95% confidence level or its probability (p-value) is inferior to the chosen alpha, which here is 0.05. According to Student's table in appendice 4, at the risk threshold of 0.05 and a degree of freedom of $df = n - p = 15 - 10 = 5$, Student's critical value is equal to 2.571. The results of the coefficient analysis for coded coefficients are shown in the two tables below:

*Table 12:Analysis of model coefficients for the respond Qe*

| *TERM* | *COEF* | *STANDARD ERROR* | *T-VALUE* | *P-VALUE* | *TEST* |
|---|---|---|---|---|---|
| ***CONSTANT*** | 29.27 | 7.56 | 3.872 | 0.012 | Significant |
| ***PH*** | 5.2 | 4.63 | 1.123 | 0.312 | Non-significant |
| ***$C_0$*** | 30.62 | 4.63 | 6.613 | 0.001 | Significant |
| ***M*** | -30.44 | 4.63 | -6.575 | 0.001 | Significant |
| ***$PH^2$*** | -6.1 | 6.82 | -0.894 | 0.412 | Non-significant |
| ***$C_0^2$*** | 4.04 | 6.82 | 0.592 | 0.579 | Non-significant |
| ***$M^2$*** | 18.18 | 6.82 | 2.666 | 0.045 | Significant |
| ***PH*$C_0$*** | 2.42 | 6.55 | 0.369 | 0.727 | Non-significant |
| ***PH*M*** | -4.58 | 6.55 | -0.699 | 0.516 | Non-significant |
| ***$C_0$*M*** | -26.85 | 6.55 | -4.099 | 0.009 | Significant |

*Table 13:Analysis of model coefficients for the respond R*

| *TERM* | *COEF* | *STANDARD ERROR* | *T-VALUE* | *P-VALUE* | *TEST* |
|---|---|---|---|---|---|
| ***CONSTANT*** | 84.12 | 1.64 | 51.38 | 5.28E-08 | Significant |
| ***PH*** | 9.6 | 1 | 9.58 | 0.00021 | Significant |
| ***$C_0$*** | 5.32 | 1 | 5.3 | 0.003192 | Significant |
| ***M*** | 1.78 | 1 | 1.78 | 0.135195 | Non-significant |
| ***$PH^2$*** | -9.96 | 1.48 | -6.75 | 0.001083 | Significant |
| ***$C_0^2$*** | -16.62 | 1.48 | -11.26 | 9.65E-05 | Significant |
| ***$M^2$*** | -6.37 | 1.48 | -4.32 | 0.007571 | Significant |
| ***PH*$C_0$*** | -0.1 | 1.42 | -0.07 | 0.946907 | Non-significant |
| ***PH*M*** | 0.46 | 1.42 | 0.32 | 0.761908 | Non-significant |
| ***$C_0$*M*** | -0.99 | 1.42 | -0.69 | 0.520906 | Non-significant |

After eliminating the insignificant coefficients, the mathematical model became unsatisfactory, so we proceeded to replace in order to rectify the coefficients of determination.

- **Effect of factors:**

For the adsorption capacity Qe, the most influential factor is the initial MB concentration, since its coefficient is the highest, followed by the mass of FEN and the pH factor, which has the lowest coefficient in modulus.

-The initial concentration, the mass of FEN and the pH factors have a positive effect on adsorption capacity, since its coefficient is positive. Thus, an increase in any of them would increase the adsorption capacity on FEN.

-The factors pH of the solution has a double effect but not significant since it has a non-significant positive coefficient that's not high and a negative coefficient that is lower than the positive coefficient for the squared term. Therefore, an increase in the pH of the solution would result in a slight increase until it reaches a maximum then starts decreasing in the adsorption capacity.

- The factors mass of FEN, it's the opposite of the effect of the pH, has a significant negative effect since it has a high negative coefficient. Therefore, an increase in the mass would result in a decrease in the adsorption capacity.

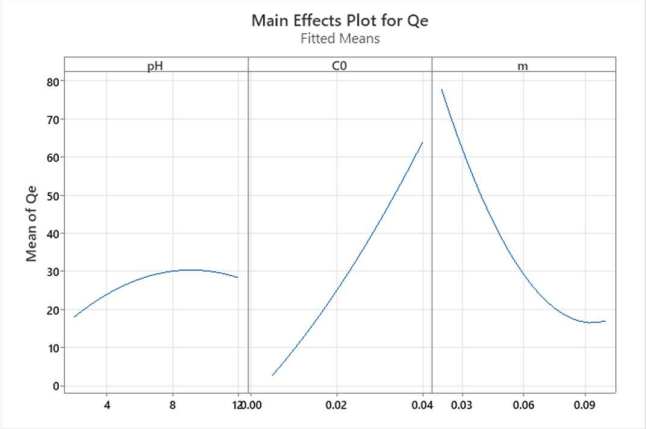


*Figure 36: effects of factors in the adsorption capacity*

For the removal efficacy R, the most influential factor is the initial MB concentration, since its coefficient is the highest, followed by the mass of FEN and the pH factor, which has the lowest coefficient in modulus. They all have positive coefficients, but all negative coefficients are squared, which means they will all cause the removal efficacy to increase until they reach a maximum, which is the maximum value, then decrease, which results in a decrease in removal efficacy.

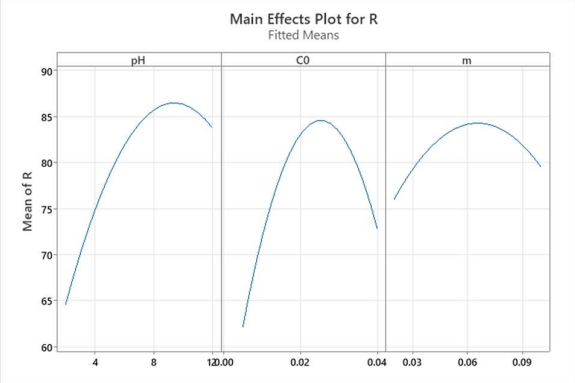


*Figure 37:effects of factors in the removal efficacy*

The interaction profile presented in Figure 38 shows the effect of each factor on the high and low levels of another factor. If the effect lines are not parallel, there is a significant interaction. The stronger the interaction, the greater the difference in the slopes of the lines.

In the Qe, the interaction between ph and mass of FEN and the initial concentration isn't significant at all, while the interaction between the mass and the initial concentration is significant.

In the R, all the Critical interactions are insignificant.

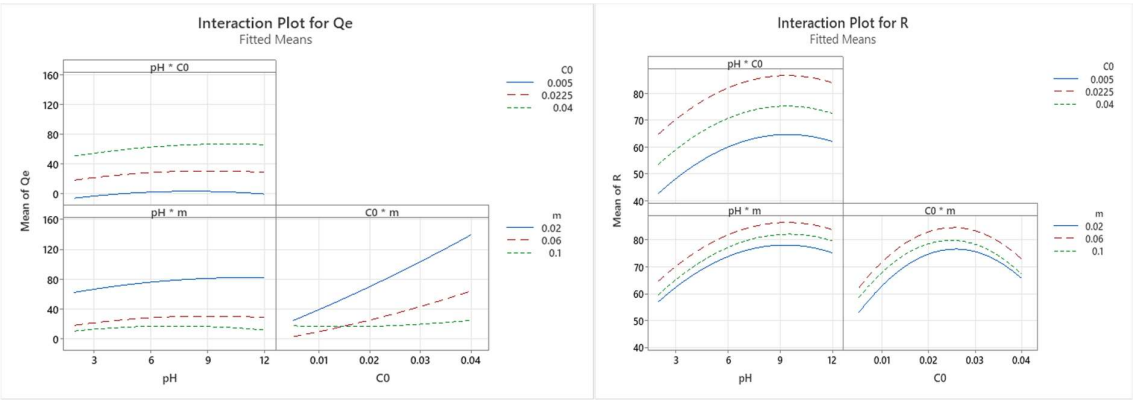


*Figure 38:Effect of Interactions between factors on the adsorption capacity and removal efficacy respectively*

- **Analysis of variance (FISHER's test):**

*Table 14:Analysis of variance for MB adsorption by FEN*

| Source | Degree of freedom | Sum of squares | Mean sum of squares | F-value | P-value |
|---|---|---|---|---|---|
| Model | 9 | 19587.5 | 2176.39 | 12.68 | 0.0007 |
| Error | 5 | 858.4 | 171.68 | | |
| Total | 14 | 20445.9 | | | |

*Table 15:Analysis of variance for MB adsorption by FEN*

| Source | Degree of freedom | Sum of squares | Mean sum of squares | F-value | P-value |
|---|---|---|---|---|---|
| Model | 9 | 2368.6 | 263.18 | 32.73 | 1.63E-05 |
| Error | 5 | 40.22 | 8.04 | | |
| Total | 14 | 2408.81 | | | |

In this test, the hypothesis $H_0$ is rejected because $F_{obs}$, which equals 12.68 for respond Qe and 37.73 for the respond R, is greater than $F_{critical}$= 3.4817, which we got from Fisher's table, $F_{obs}>F_{critical}$ and probability P = 0.0007 & 1.63E-05<0.05), therefore our model is therefore valid.

- **Optimisation and desirability (D):**

According to Figure 39, the maximum adsorbed quantity is 145.4873 ± 15.5 mg/g. This value corresponds to a desirability of 0.9519, for which the optimum operating conditions are as follows:

- An initial MB concentration of 0.04 mg/mL;
- A pH equal to 12;
- A mass of adsorbent equal to 0.02 g

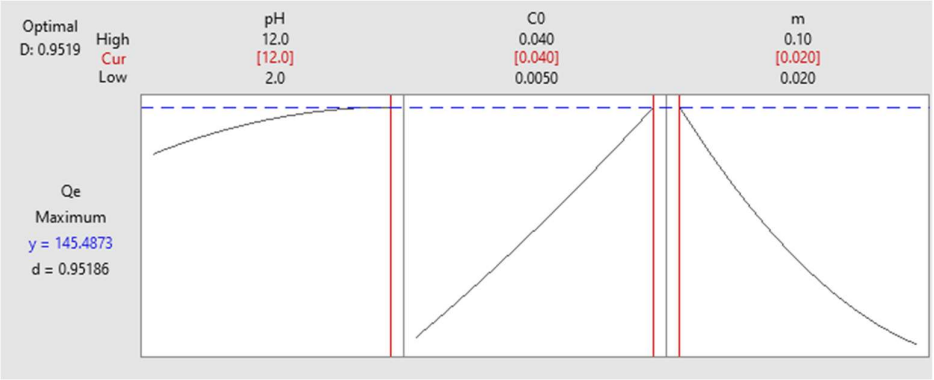


*Figure 39: Prediction profiler and desirability function for Qe*

According to Figure 40, the maximum removal efficacy is 86.9884 ± 1.54 %. This value corresponds to a desirability of 1, for which the optimum operating conditions are as follows:

- An initial MB concentration of 0.025 mg/mL;
- A pH equal to 9.37;
- A mass of adsorbent equal to 0.066 g.

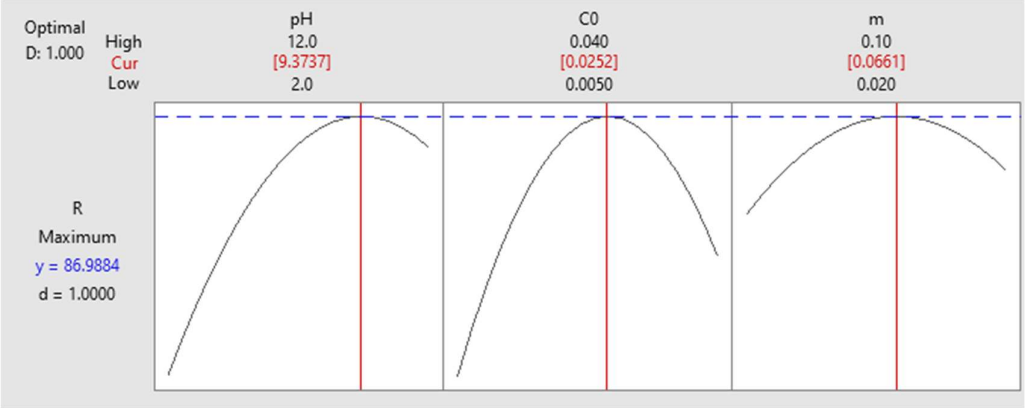


*Figure 40:Prediction profiler and desirability function for R*

According to Figure 41, the optimum operating conditions to maximize Qe and R simultaneously for a, for which Qe = 122.89 ± 9.87 mg/g and R = 74.66 ± 2.14 % corresponding to a desirability of 1, are:

- An initial phenol concentration of 0.034 mg/mL;
- A pH equal to 9.56;
- A mass of adsorbent equal to 0.02 g.

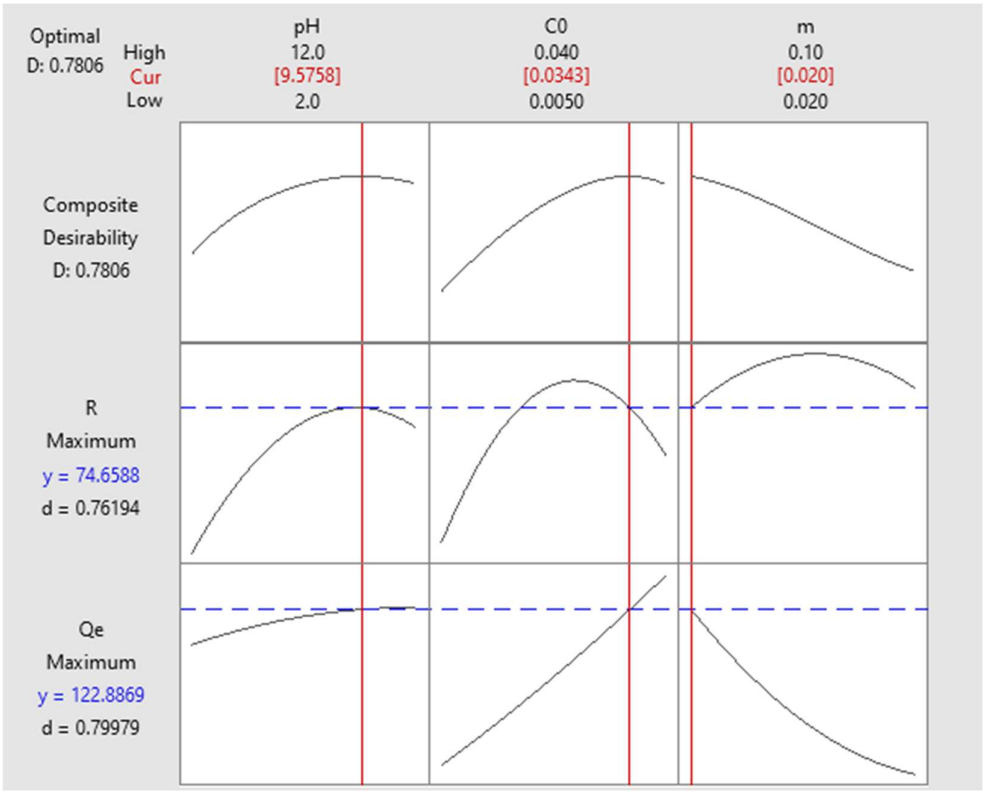


*Figure 41:Prediction profiler and desirability function for both Qe and R*

A spatial representation (3D) of the response was produced using Minitab software to help visualize the results obtained.

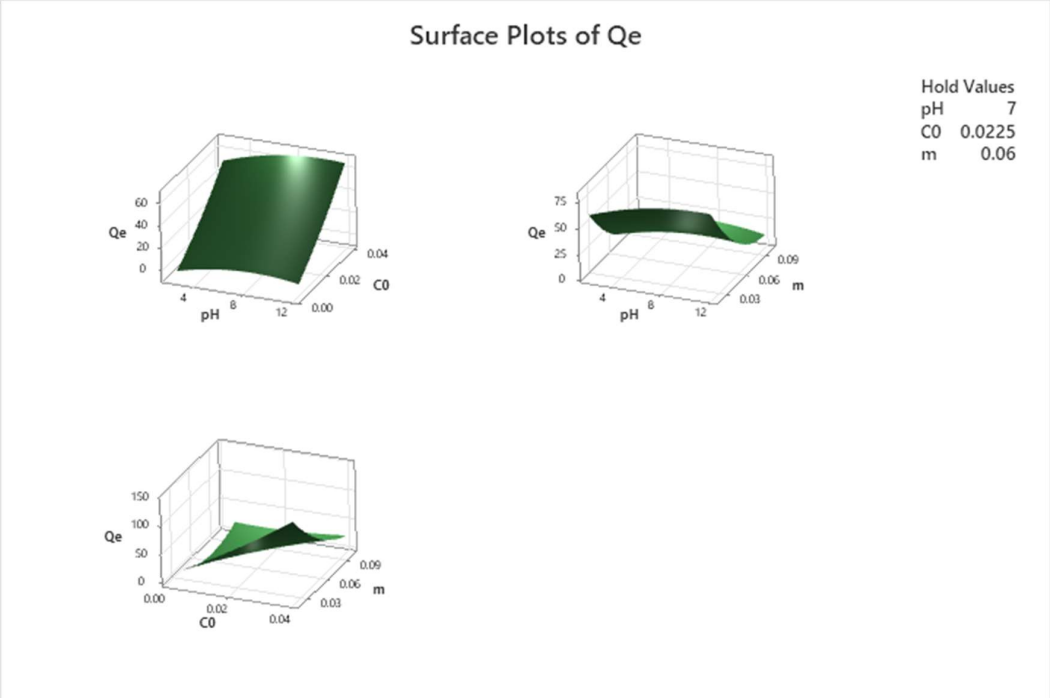


*Figure 42:Spatial representation of the quantity of MB adsorbed by FEN as a function of pH, C and m.*

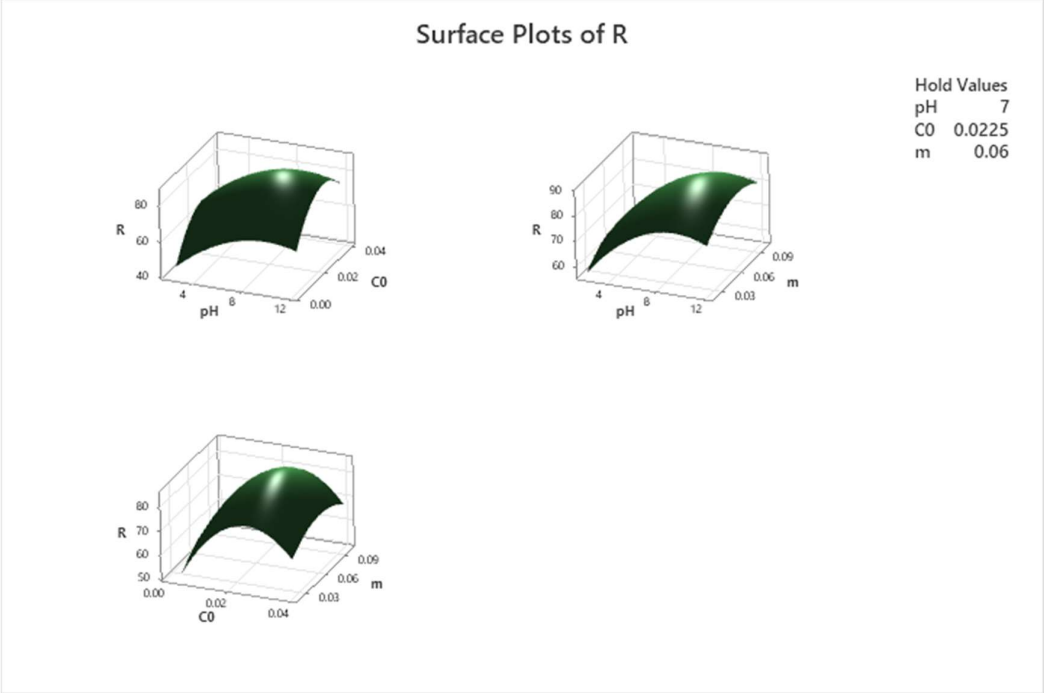


*Figure 43:Spatial representation of the quantity of MB removed by FEN as a function of pH, C and m*

## V.2.2. Adsorption of MB by FBIO:

*Table 16: Box-Behnken Design for 3 factors*

| | Actual coordinates | | | Coded coordinates | | | | |
|---|---|---|---|---|---|---|---|---|
| Runs | pH | $C_0$ | M | pH | $C_0$ | M | Qe (mg/g) | R (%) |
| 1 | 2 | 0.005 | 0.06 | -1 | -1 | 0 | 9.635 | 46.1250 |
| 2 | 12 | 0.005 | 0.06 | 1 | -1 | 0 | 19.650 | 94.0691 |
| 3 | 2 | 0.04 | 0.06 | -1 | 1 | 0 | 65.324 | 54.0364 |
| 4 | 12 | 0.04 | 0.06 | 1 | 1 | 0 | 112.650 | 93.1847 |
| 5 | 2 | 0.0225 | 0.02 | -1 | 0 | -1 | 34.562 | 19.0424 |
| 6 | 12 | 0.0225 | 0.02 | 1 | 0 | -1 | 77.896 | 42.9179 |
| 7 | 2 | 0.0225 | 0.1 | -1 | 0 | 1 | 14.630 | 40.3030 |
| 8 | 12 | 0.0225 | 0.1 | 1 | 0 | 1 | 28.630 | 78.8705 |
| 9 | 7 | 0.005 | 0.02 | 0 | -1 | -1 | 35.234 | 56.2245 |
| 10 | 7 | 0.04 | 0.02 | 0 | 1 | -1 | 312.658 | 86.2108 |
| 11 | 7 | 0.005 | 0.1 | 0 | -1 | 1 | 12.365 | 98.6569 |
| 12 | 7 | 0.04 | 0.1 | 0 | 1 | 1 | 68.256 | 94.1029 |
| 13 | 7 | 0.0225 | 0.06 | 0 | 0 | 0 | 56.986 | 94.1917 |
| 14 | 7 | 0.0225 | 0.06 | 0 | 0 | 0 | 56.986 | 94.1917 |
| 15 | 7 | 0.0225 | 0.06 | 0 | 0 | 0 | 56.986 | 94.1917 |

- **Mathematical modelling:**

  After application to Minitab software, the mathematical model is written as follows:

  For the respond Qe, the regression equation in uncoded units is:

$$Q_e = -61 + 23.2pH + 2813C_0 - 412m - 1.467pH^2 + 102902{C_0}^2 + 11643m^2 - 37pHm - 107pHC_0 - 79119C_0m \quad \textit{(Eq LV)}$$

  Which had S = 42.8135; R-sq = 88.18% and R-sq(adj) = 60.90%.

  For the respond R, the regression equation in uncoded units is:

$$R = -58.1 + 20.24pH - 41C_0 + 1871m - 1.217pH^2 + 26412{C_0}^2 - 11551m^2 + 18.4pHm - 25.1pHC_0 - 1408C_0m \quad \textit{(Eq LVI)}$$

  Which had S = 4.98451; R-sq = 98.73% and R-sq(adj) = 96.43%.

- **Significance of model coefficients (STUDENT t-test):**

  According to Student's table, at the risk threshold of 0.05 and a degree of freedom of $df = n - p = 15 - 10 = 5$, Student's critical value is equal to 2.571. The results of the coefficient analysis for coded coefficients are shown in the two tables below:

*Table 17:Analysis of model coefficients for the respond Qe*

| TERM | COEF | STANDARD ERROR | T-VALUE | P-VALUE | TEST |
|---|---|---|---|---|---|
| **CONSTANT** | 57 | 24.7 | 2.31 | 0.069 | Non-significant |
| **PH** | 14.3 | 15.1 | 0.95 | 0.387 | Non-significant |
| **$C_0$** | 60.3 | 15.1 | 3.98 | 0.011 | Significant |
| **M** | -42.1 | 15.1 | -2.78 | 0.039 | Significant |
| **$PH^2$** | -36.7 | 22.3 | -1.65 | 0.161 | Non-significant |
| **$C_0^2$** | 31.5 | 22.3 | 1.41 | 0.216 | Non-significant |
| **$M^2$** | 18.6 | 22.3 | 0.84 | 0.441 | Non-significant |
| **$PH*C_0$** | 9.3 | 21.4 | 0.44 | 0.681 | Non-significant |
| **PH*M** | -7.3 | 21.4 | -0.34 | 0.746 | Non-significant |
| **$C_0$*M** | -55.4 | 21.4 | -2.59 | 0.049 | Non-significant |

*Table 18:Analysis of model coefficients for the respond R*

| TERM | COEF | STANDARD ERROR | T-VALUE | P-VALUE | TEST |
|---|---|---|---|---|---|
| **CONSTANT** | 94.19 | 2.88 | 32.73 | 0 | Significant |
| **PH** | 18.69 | 1.76 | 10.61 | 0 | Significant |
| **$C_0$** | 4.06 | 1.76 | 2.3 | 0.07 | Non-significant |
| **M** | 13.44 | 1.76 | 7.63 | 0.001 | Significant |
| **$PH^2$** | -30.43 | 2.59 | -11.73 | 0 | Significant |
| **$C_0^2$** | 8.09 | 2.59 | 3.12 | 0.026 | Significant |
| **$M^2$** | -18.48 | 2.59 | -7.12 | 0.001 | Significant |
| **$PH*C_0$** | -2.2 | 2.49 | -0.88 | 0.418 | Non-significant |
| **PH*M** | 3.67 | 2.49 | 1.47 | 0.201 | Non-significant |
| **$C_0$*M** | -8.64 | 2.49 | -3.46 | 0.018 | Significant |

After eliminating the insignificant coefficients, the mathematical model became unsatisfactory, so we proceeded to replace in order to rectify the coefficients of determination.

- **Effect of factors:**

  For the adsorption capacity Qe, the most influential factor is the initial MB concentration, since its coefficient is the highest, followed by the mass of FEN and the pH factor, which has the lowest coefficient in modulus.

  **-**The factors pH of the solution has a double effect but not significant since it has a Critical positive coefficient that's not high and a negative coefficient that is lower than the positive coefficient for the squared term. Therefore, an increase in the pH of the solution would result in a slight increase until it reaches a maximum then starts decreasing in the adsorption capacity.

-The factors mass of FEN, has a significant negative effect since it has a high negative coefficient. Therefore, an increase in the mass would result in a decrease in the adsorption capacity.

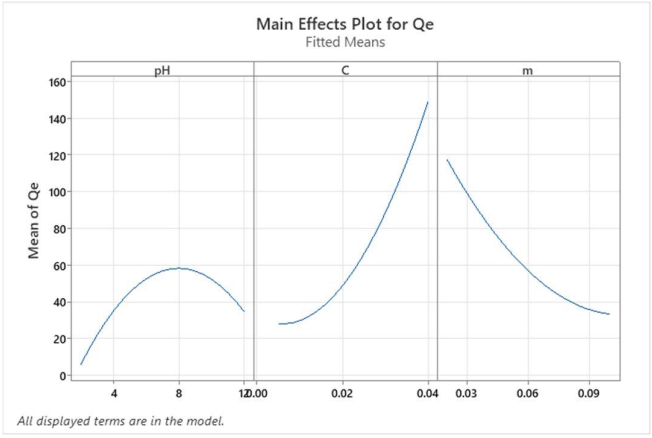


*Figure 44: effects of factors in the adsorption capacity*

For the removal efficacy R, the most influential factor is the mass of FBIO, since its coefficient is the highest, followed by the initial MB concentration and the pH factor, which has the lowest coefficient in modulus.

-The mass of FEN and the pH factors have a double effect, since its coefficient is positive but the coefficients of its square terms are negative and bigger. Thus, an increase in any of them would increase the adsorption capacity on FEN until it reaches maximum then it decreases.

- The initial concentration has a double effect, but the opposite of the previous 2 factors, it has a low negative coefficient but a very high positive coefficient for its square term which meant the more it increases, the removal decreases slowly until it reaches a minimum than it starts increasing

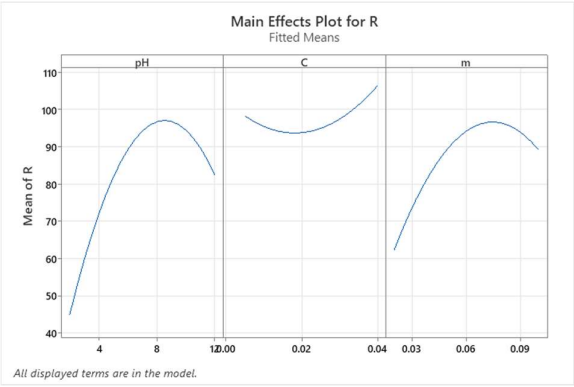


*Figure 45:effects of factors in the removal efficacy*

The interaction profile presented in Figure 46 shows the effect of each factor on the high and low levels of another factor. If the effect lines are not parallel, there is a significant interaction. The stronger the interaction, the greater the difference in the slopes of the lines.

In the Qe, the interaction between pH and mass of FEN and the initial concentration isn't significant at all, while the interaction between the mass and the initial concentration is significant.

In the R, all the interaction between $C_0$ and m are insignificant and the rest 2 interactions are insignificant.

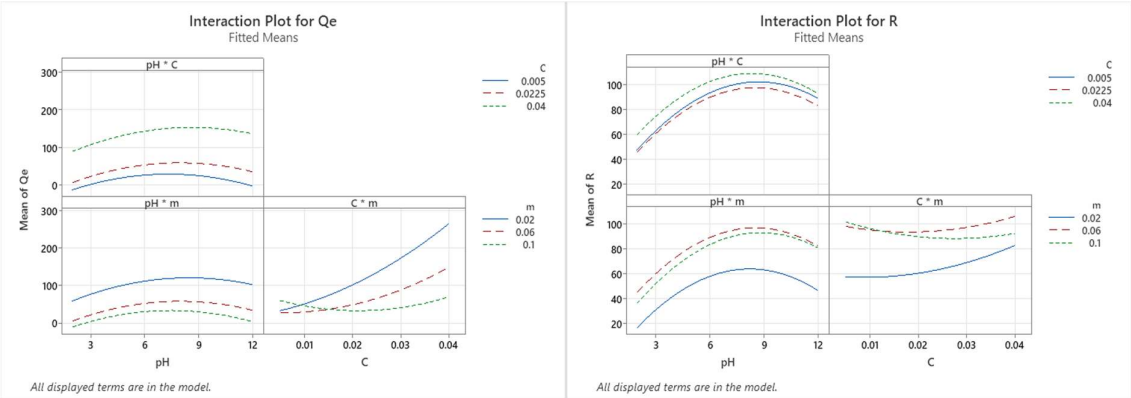


*Figure 46:Effect of Interactions between factors on the adsorption capacity and removal efficacy respectively*

- **Analysis of variance (FISHER's test):**

*Table 19:Analysis of variance for MB adsorption by FBIO*

| Source | Degree of freedom | Sum of squares | Mean sum of squares | F-value | P-value |
|---|---|---|---|---|---|
| Model | 9 | 68364.5 | 7596 | 4.144 | 0.03 |
| Error | 5 | 9165 | 1833 | | |
| Total | 14 | 77528.9 | | | |

*Table 20:Analysis of variance for MB adsorption by FEN*

| Source | Degree of freedom | Sum of squares | Mean sum of squares | F-value | P-value |
|---|---|---|---|---|---|
| Model | 9 | 9630.7 | 1070.08 | 43.06 | 5.11E-06 |
| Error | 5 | 124.23 | 24.85 | | |
| Total | 14 | 9754.93 | | | |

In this test, the hypothesis $H_0$ is rejected because $F_{obs}$, which equals 4.14 for respond Qe and 43.06 for the respond R, is greater than $F_{critical}$= 3.4817, which we got from Fisher's table ($F_{obs}>F_{critical}$ and probability (P = 0.03 & 5.11E-06<0.05), therefore our model is therefore valid.

- **Optimisation and desirability (D):**

  According to Figure 47, the maximum adsorbed quantity is 271.3678 ± 38.9 mg/g. This value corresponds to a desirability of 0.86.37, for which the optimum operating conditions are as follows:

  - An initial MB concentration of 0.04 mg/mL;
  - A pH equal to 9.11;
  - A mass of adsorbent equal to 0.02 g.

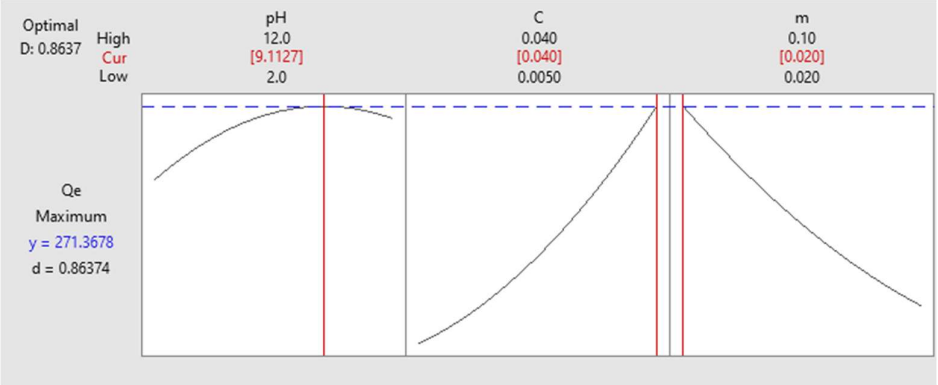


*Figure 47: Prediction profiler and desirability function for Qe*

According to Figure 48, the maximum removal efficacy is 109.2192 ± 3.55 %. This value corresponds to a desirability of 1, for which the optimum operating conditions are as follows:

- An initial MB concentration of 0.005 mg/mL;
- A pH equal to 8.87;
- A mass of adsorbent equal to 0.085 g

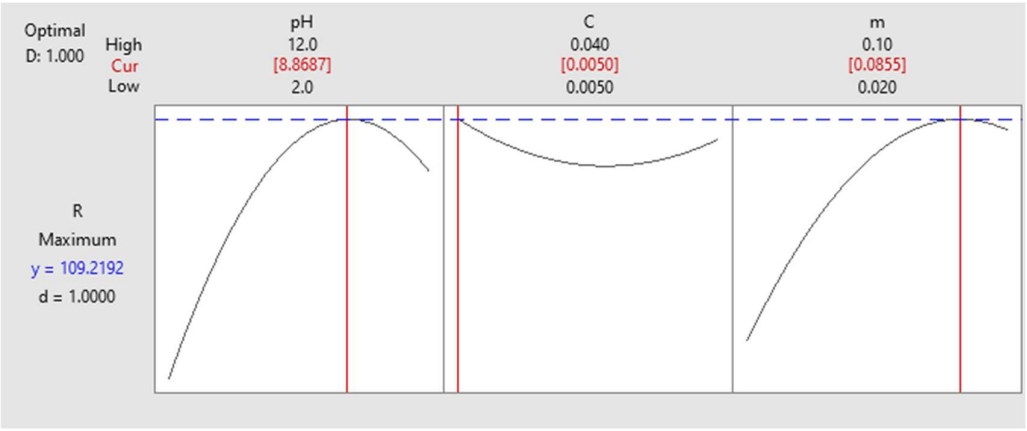


*Figure 48:Prediction profiler and desirability function for R*

According to Figure 49, the optimum operating conditions to maximize Qe and R simultaneously for a, for which Qe = 254.25 ± 34.4 mg/g and R = 89.20 ± 4.01 % corresponding to a desirability of 0.8434, are:

- An initial phenol concentration of 0.034 mg/mL;

- A pH equal to 8.36;
- A mass of adsorbent equal to 0.025g.

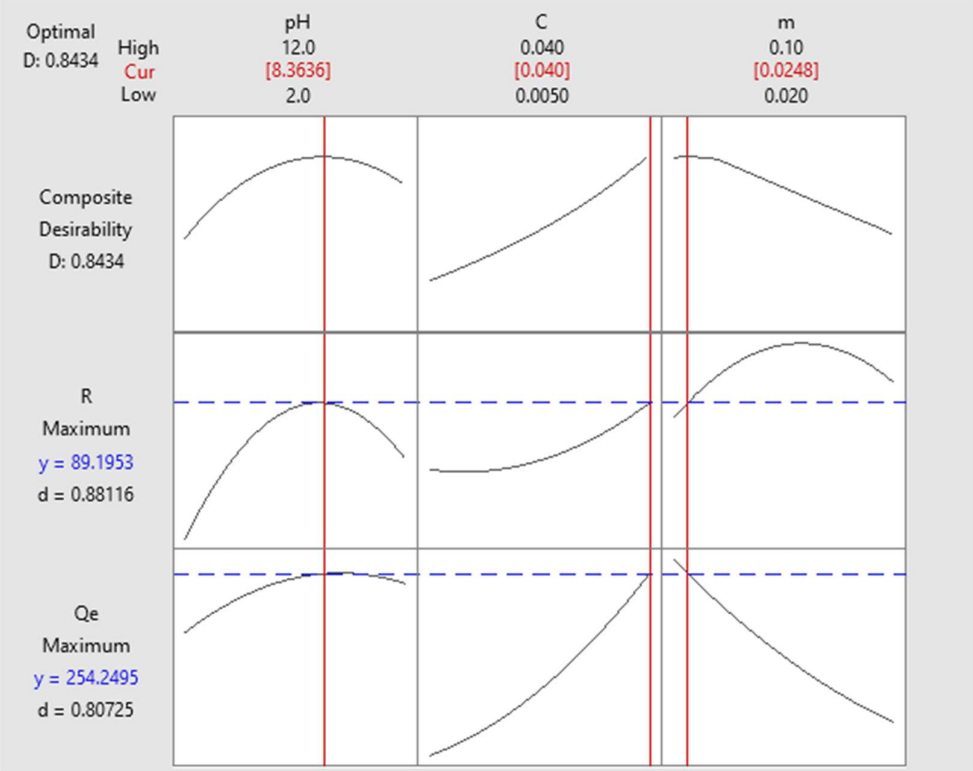


*Figure 49:Prediction profiler and desirability function for both Qe and R*

A spatial representation (3D) of the response was produced using Minitab software to help visualize the results obtained.

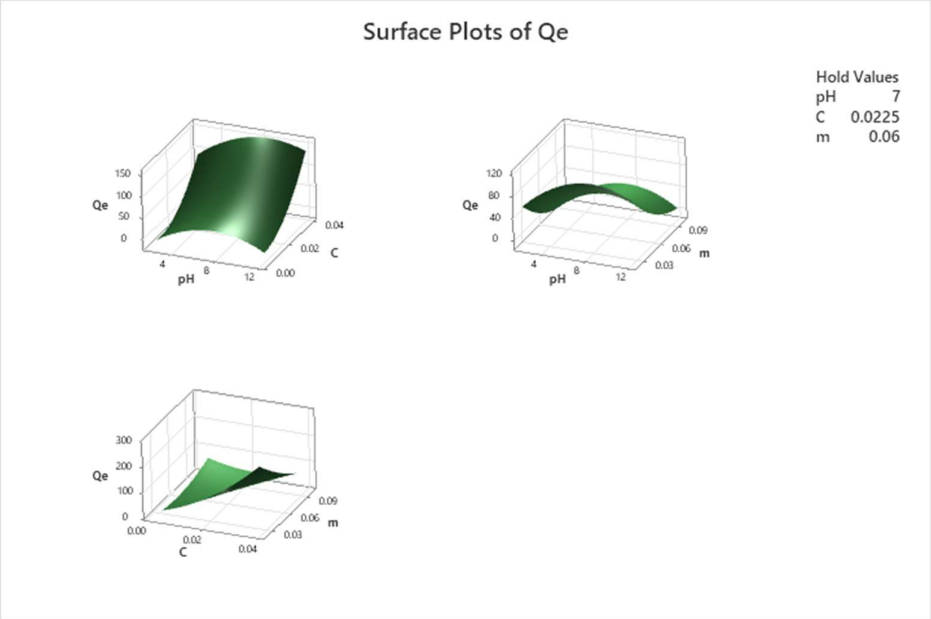


*Figure 50:Spatial representation of the quantity of MB adsorbed BY FBIO as a function of pH, C and m.*

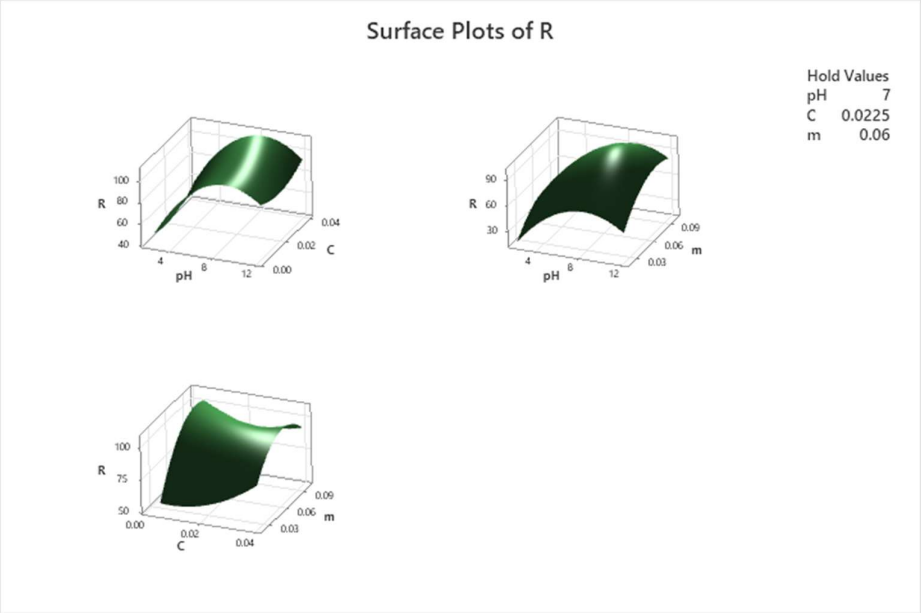


*Figure 51:Spatial representation of the quantity of MB removed BY FBIO as a function of pH, C and m*

## V.2.3. Adsorption of MB by TH:

*Table 21: Box-Behnken Design for 3 factors*

| | Actual coordinates | | | Coded coordinates | | | | |
|---|---|---|---|---|---|---|---|---|
| Runs | pH | $C_0$ | M | pH | $C_0$ | m | Qe (mg/g) | R (%) |
| 1 | 2 | 0.005 | 0.06 | -1 | -1 | 0 | 4.028 | 35.5412 |
| 2 | 12 | 0.005 | 0.06 | 1 | -1 | 0 | 8.000 | 70.5882 |
| 3 | 2 | 0.04 | 0.06 | -1 | 1 | 0 | 37.652 | 34.9348 |
| 4 | 12 | 0.04 | 0.06 | 1 | 1 | 0 | 91.265 | 84.6789 |
| 5 | 2 | 0.0225 | 0.02 | -1 | 0 | -1 | 69.356 | 39.5191 |
| 6 | 12 | 0.0225 | 0.02 | 1 | 0 | -1 | 141.658 | 80.7168 |
| 7 | 2 | 0.0225 | 0.1 | -1 | 0 | 1 | 18.365 | 52.3219 |
| 8 | 12 | 0.0225 | 0.1 | 1 | 0 | 1 | 32.560 | 92.7635 |
| 9 | 7 | 0.005 | 0.02 | 0 | -1 | -1 | 16.356 | 48.1059 |
| 10 | 7 | 0.04 | 0.02 | 0 | 1 | -1 | 271.634 | 84.0105 |
| 11 | 7 | 0.005 | 0.1 | 0 | -1 | 1 | 4.237 | 62.3015 |
| 12 | 7 | 0.04 | 0.1 | 0 | 1 | 1 | 54.230 | 83.8608 |
| 13 | 7 | 0.0225 | 0.06 | 0 | 0 | 0 | 51.469 | 87.9812 |
| 14 | 7 | 0.0225 | 0.06 | 0 | 0 | 0 | 51.469 | 87.9812 |
| 15 | 7 | 0.0225 | 0.06 | 0 | 0 | 0 | 51.469 | 87.9812 |

- **Mathematical modelling:**

  After application to Minitab software, the mathematical model is written as follows:

  For the respond Qe, the regression equation in uncoded units is:

$$Q_e = -34.7 + 15.2pH + 6062C_0 - 1512m - 0.747pH^2 + 7994{C_0}^2 + 20436m^2 - 72.6pHm + 142pHC_0 - 73316C_0m \quad \textit{(Eq LVII)}$$

Which had S = 42.8135; R-sq = 92.28% and R-sq(adj) = 78.38%.

For the respond R, the regression equation in uncoded units is:

$$R = -27.6 + 13.01pH + 2600C_0 + 563m - 0.696pH^2 - 46214{C_0}^2 - 2662m^2 - 0.9pHm + 42pHC_0 - 5123C_0m \quad \textit{(Eq LVIII)}$$

Which had S = 4.98451; R-sq = 95.97% and R-sq(adj) = 88.70%.

- **Significance of model coefficients (STUDENT t-test):**

According to Student's table, at the risk threshold of 0.05 and a degree of freedom of $df = n - p = 15 - 10 = 5$, Student's critical value is equal to 2.571. The results of the coefficient analysis for coded coefficients are shown in the two tables below:

*Table 22:Analysis of model coefficients for the respond Qe*

| *TERM* | *COEF* | *STANDARD ERROR* | *T-VALUE* | *P-VALUE* | *TEST* |
|---|---|---|---|---|---|
| ***CONSTANT*** | 51.5 | 18.5 | 2.78 | 0.039 | Significant |
| ***PH*** | 18 | 11.3 | 1.59 | 0.173 | Non-significant |
| ***$C_0$*** | 52.8 | 11.3 | 4.65 | 0.006 | Significant |
| ***M*** | -48.7 | 11.3 | -4.29 | 0.008 | Significant |
| ***$PH^2$*** | -18.7 | 16.7 | -1.12 | 0.314 | Non-significant |
| ***$C_0^2$*** | 2.4 | 16.7 | 0.15 | 0.889 | Non-significant |
| ***$M^2$*** | 32.7 | 16.7 | 1.96 | 0.107 | Non-significant |
| ***PH*$C_0$*** | 12.4 | 16 | 0.77 | 0.474 | Non-significant |
| ***PH*M*** | -14.5 | 16 | -0.91 | 0.407 | Non-significant |
| ***$C_0$*M*** | -51.3 | 16 | -3.2 | 0.024 | Significant |

*Table 23:Analysis of model coefficients for the respond R*

| *TERM* | *COEF* | *STANDARD ERROR* | *T-VALUE* | *P-VALUE* | *TEST* |
|---|---|---|---|---|---|
| ***CONSTANT*** | 87.98 | 4.14 | 21.23 | 4E-06 | Significant |
| ***PH*** | 20.8 | 2.54 | 8.2 | 0.0004 | Significant |
| ***$C_0$*** | 8.87 | 2.54 | 3.49 | 0.0175 | Significant |
| ***M*** | 4.86 | 2.54 | 1.92 | 0.1129 | Non-significant |
| ***$PH^2$*** | -17.39 | 3.74 | -4.66 | 0.0055 | Significant |
| ***$C_0^2$*** | -14.15 | 3.74 | -3.79 | 0.0128 | Significant |
| ***$M^2$*** | -4.26 | 3.74 | -1.14 | 0.3059 | Non-significant |
| ***PH*$C_0$*** | 3.67 | 3.59 | 1.02 | 0.3545 | Non-significant |
| ***PH*M*** | -0.19 | 3.59 | -0.05 | 0.9621 | Non-significant |
| ***$C_0$*M*** | -3.59 | 3.59 | -1 | 0.3632 | Non-significant |

After eliminating the insignificant coefficients, the mathematical model became unsatisfactory, so we proceeded to replace in order to rectify the coefficients of determination.

- **Effect of factors:**

For the adsorption capacity Qe, the most influential factor is the initial MB concentration, since its coefficient is the highest, followed by the mass of FEN and the pH factor, which has the lowest coefficient in modulus.

**-**The factors pH of the solution has a double effect (mainly positive) since it has a Critical positive coefficient that's not high and a negative coefficient that is lower than the positive coefficient for the squared term. Therefore, an increase in the pH of the solution would result in a slight increase until it reaches a maximum then starts decreasing in the adsorption capacity.

**-**The factors mass of FEN, has a significant negative effect since it has a high negative coefficient. Therefore, an increase in the mass would result in a decrease in the adsorption capacity.

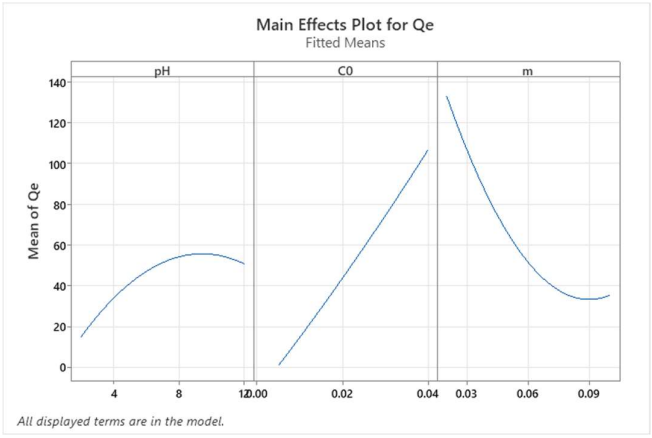


*Figure 52: effects of factors in the adsorption capacity*

For the removal efficacy R, the most influential factor is the initial MB concentration, since its coefficient is the highest, followed by the mass of FEN and the pH factor, which has the lowest coefficient in modulus. They all have positive coefficients, but all negative coefficients for the squared terms, which means they will all cause the removal efficacy to increase until they reach a maximum, which is the maximum value, then decrease, which results in a decrease in removal efficacy.

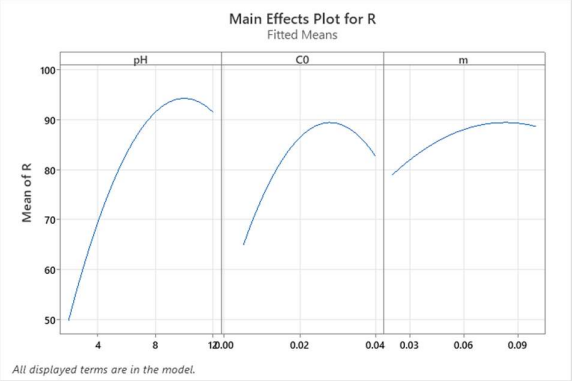


*Figure 53:effects of factors in the removal efficacy*

The interaction profile presented in Figure 54 shows the effect of each factor on the high and low levels of another factor.

In the Qe, the interaction between pH and mass of FEN are not that noticeable and between pH and the initial concentration isn't significant at all, while the interaction between the mass and the initial concentration is significant.

In the R, all the interactions between the factors are insignificant.

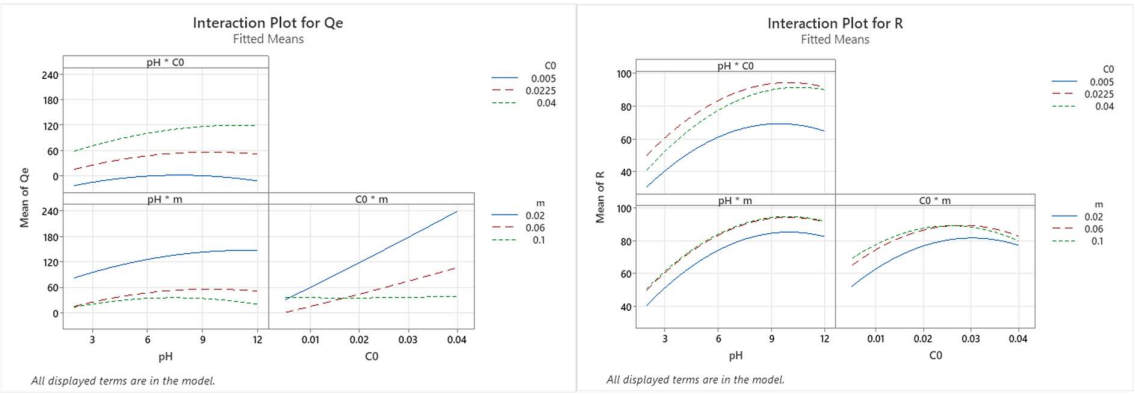


*Figure 54:Effect of Interactions between factors on the adsorption capacity and removal efficacy respectively*

- **Analysis of variance (FISHER's test):**

*Table 24:Analysis of variance for MB adsorption by TH*

| Source | Degree of freedom | Sum of squares | Mean sum of squares | F-value | P-value |
|---|---|---|---|---|---|
| Model | 9 | 61466.7 | 6829.6 | 6.64 | 0.007 |
| Error | 5 | 5143.1 | 1028.6 | | |
| Total | 14 | 66609.8 | | | |

*Table 25:Analysis of variance for MB adsorption by FEN*

| Source | Degree of freedom | Sum of squares | Mean sum of squares | F-value | P-value |
|---|---|---|---|---|---|
| Model | 9 | 6128.2 | 680.91 | 13.22 | 6.34E04 |
| Error | 5 | 257.61 | 51.52 | | |
| Total | 14 | 6385.8 | | | |

In this test, the hypothesis $H_0$ is rejected because $F_{obs}$, which equals 6.64 for respond Qe and 13.22 for the respond R, is greater than $F_{critical}$= 3.4817, which we got from Fisher's table ($F_{obs}>F_{critical}$ and probability (P = 0.007 & 6.34E-04< 0.05), therefore our model is therefore valid.

- **Optimisation and desirability (D):**

  According to Figure 55, the maximum adsorbed quantity is 265.6731 ± 37.9 mg/g. This value corresponds to a desirability of 0.9777, for which the optimum operating conditions are as follows:

  - An initial MB concentration of 0.04 mg/mL;
  - A pH equal to 12;
  - A mass of adsorbent equal to 0.02 g.

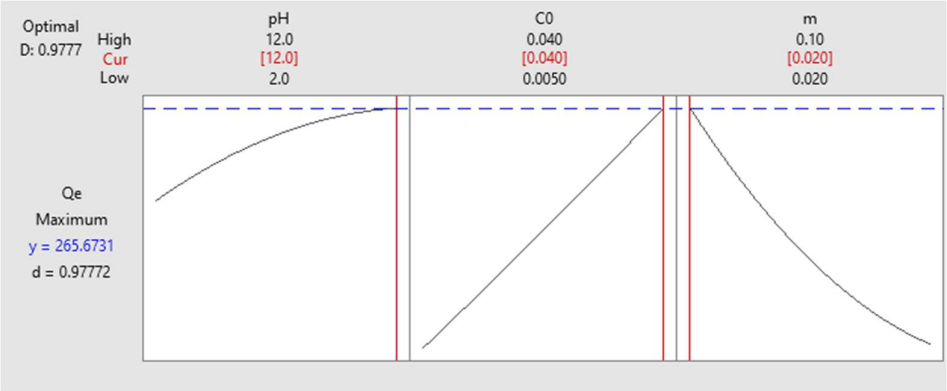


*Figure 55: Prediction profiler and desirability function for Qe*

According to Figure 56, the maximum removal efficacy is 97.08 ± 3.83 %. This value corresponds to a desirability of 1, for which the optimum operating conditions are as follows:

- An initial MB concentration of 0.0287 mg/mL;
- A pH equal to 10.18;
- A mass of adsorbent equal to 0.076 g.

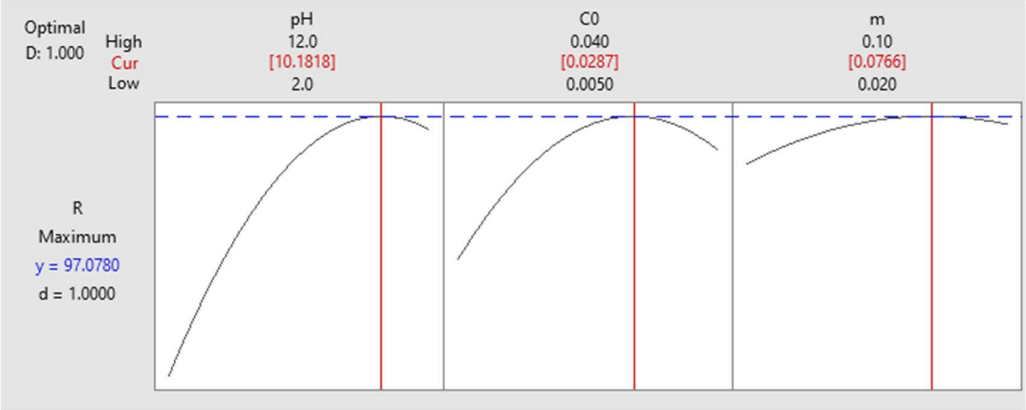


*Figure 56:Prediction profiler and desirability function for R*

According to Figure 57, the optimum operating conditions to maximize Qe and R simultaneously for a, for which Qe = 263.3783 ± 33.6 mg/g and R = 85.77 ± 7.52 % corresponding to a desirability of 0.9230, are:

- An initial phenol concentration of 0.04 mg/mL;
- A pH equal to 10.99;
- A mass of adsorbent equal to 0.02g.

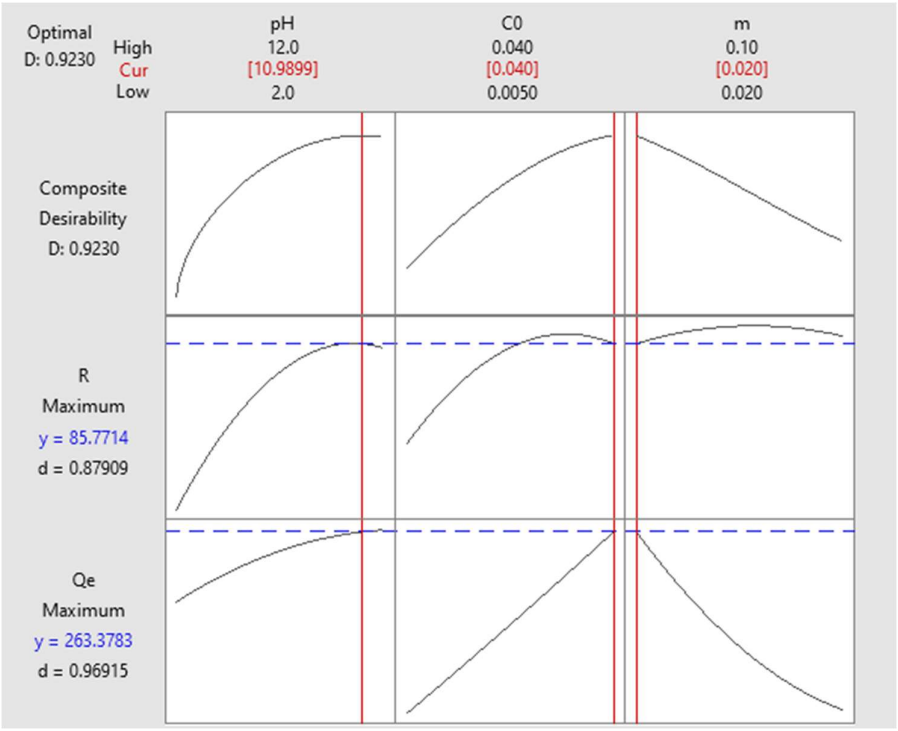


*Figure 57:Prediction profiler and desirability function for both Qe and R*

A spatial representation (3D) of the response was produced using Minitab software to help visualize the results obtained.

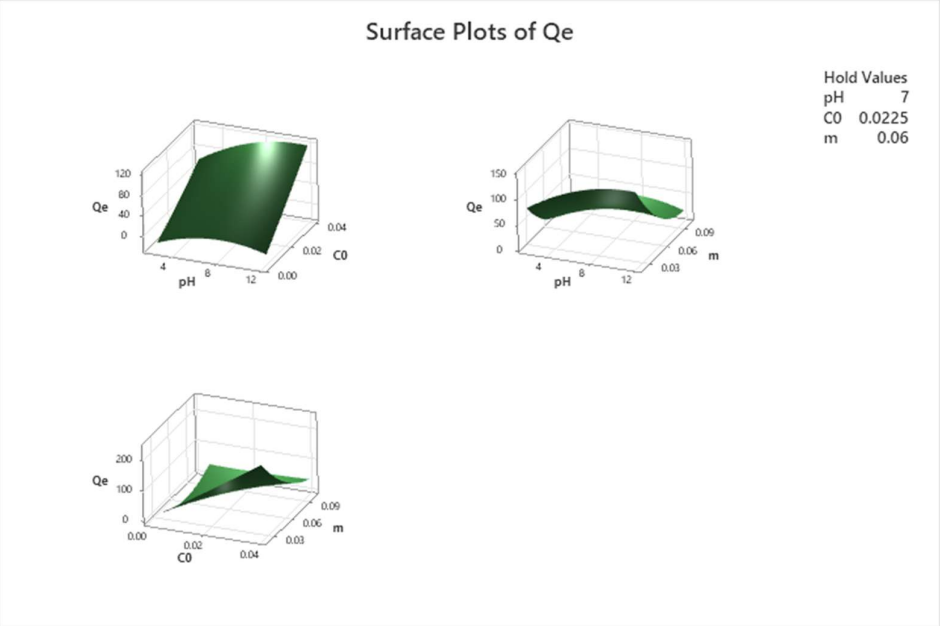


*Figure 58:Spatial representation of the quantity of MB adsorbed BY FBIO as a function of pH, C and m.*

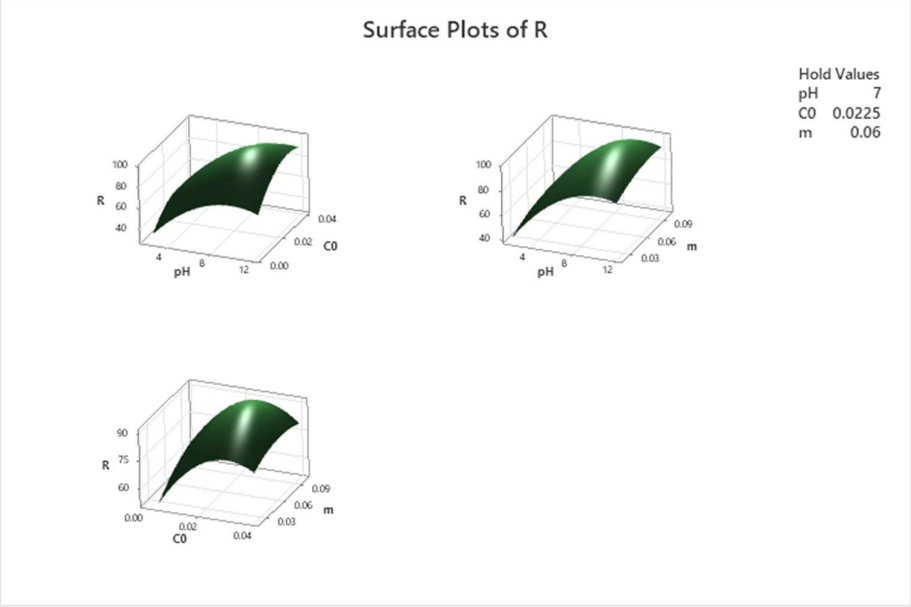


*Figure 59:Spatial representation of the quantity of MB removed BY FBIO as a function of pH, C and m*

## V.3. Modelling of adsorption equilibriums and kinetics using Dragonfly Algorithm (DA):

The problem that engineers face when regressing data is the starting point, or initial point. Choosing the right starting point allows the data to be fitted as closely as possible to the chosen model. To solve this problem, the Dragonfly algorithm was chosen to select the best position with the lowest possible error. The best position contains the starting point of the regression model. The regression was carried using the function “Nlinfit” from MATLAB.

The algorithm shown in Figure 60 was followed with: max iteration chosen was 300 and the number of search agents is 30.

The results of the regression of 32 isothermal models of MB adsorption by FEN, FBIO, and TH are presented in Appendix 3. The results of the regression of 15 kinetic models of CTC-HCl adsorption by FEN, FBIO, and TH are presented in Appendix 3.

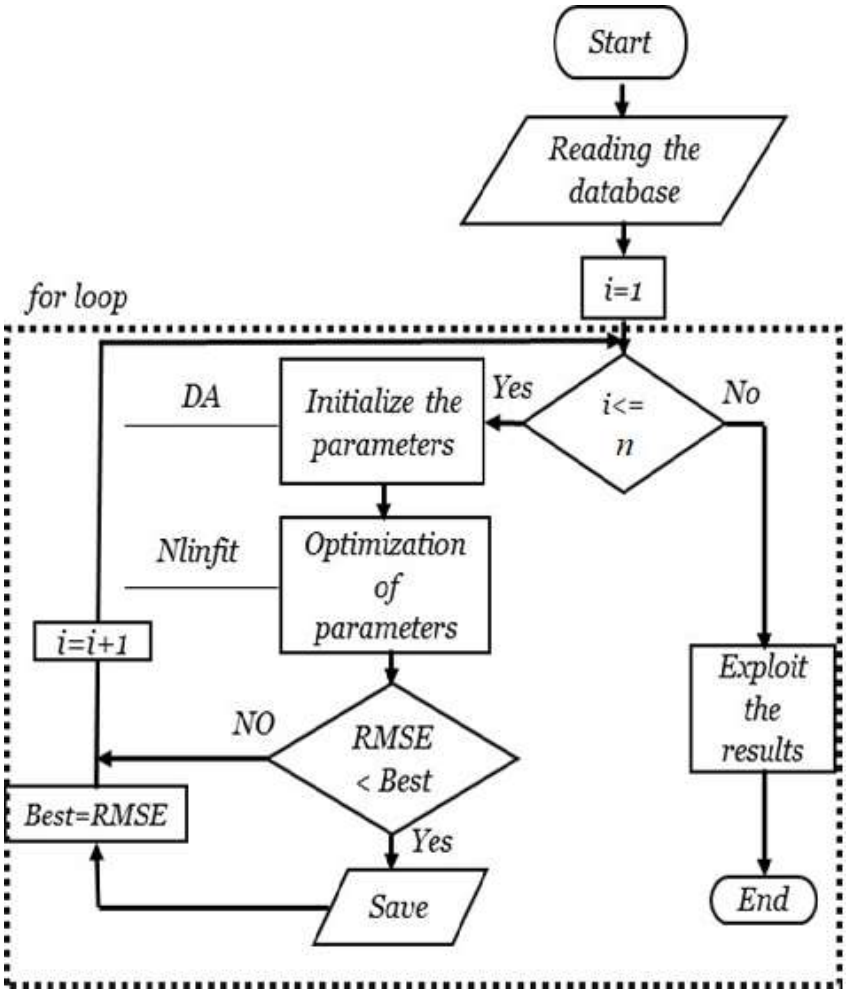


*Figure 60: DA-Nlinfit algorithm used in the modelling*

## V.3.1. Modelling of adsorption equilibriums:

For this, three isotherm models for BM adsorption by the three were taken with high $R^2$ and Adjusted $R^2$ resulted from the algorithm that contains the DA and the function "lsqcurvefit" from MATLAB which used with constraints with the same initial point that was found by DA on the selected base model.

- **MB adsorption by FEN:** For this we picked 3 of empirical models with best fitness and compared with the most three famous isotherm model: Langmuir, Temkin and Freundlich. Then we will compare the empirical models to see which one is the best fit.

According to the results showing on Appendice 7 and to the Table 26, all empirical models with best fit and isotherms that are based on Langmuir isotherm have the same correlations with Langmuir after applicating constraints on them while the modelling which means Langmuir is the best then them, that means the adsorption is monolayer with heterogeneous surface of the bioadsorbent and favourable ($n_F$<1).

But after the comparison that's shown in Table 26, Brouers-Sotolongo isotherm model is the best fit model with $R^2$=0.99371 and adj$R^2$= 0.98426.
According to Figure 61, the isotherm is a type I isotherm which is favorable.
The model expression is shown as follows:

$$Qe = 179.39(1 - 0.0559e^{1.22C_e}) \qquad \textit{(Eq LIX)}$$

*Table 26: Comparison of the result of modelling of the isotherm models for BM adsorption by FEN*

| Model | Empirical model parameters | | Validation | | parameters | | Validation | |
|---|---|---|---|---|---|---|---|---|
| Baudu | $Q_{max}$ | 24.1258 | $R^2$ | 0.99634 | $Q_{max}$ | 262.5585 | $R^2$ | 0.99033 |
| | $K_B$ | 0.07125 | adj$R^2$ | 0.98169 | $K_B$ | 0.054297 | adj$R^2$ | 0.95163 |
| | x | 5.6236 | Chi | 36.524 | x | -8.94E-10 | Chi | 96.495 |
| | y | 0.2455 | RMSE | 3.4892 | y | -1.17E-09 | RMSE | 5.6714 |
| Fritz-Shluender 4 para | C | 1.7204 | $R^2$ | 0.99634 | C | 14.2561 | $R^2$ | 0.99033 |
| | $\alpha_{FS}$ | 7.1671 | adj$R^2$ | 0.98169 | $\alpha_{FS}$ | 1 | adj$R^2$ | 0.95163 |
| | D | 0.0713 | Chi | 36.524 | D | 0.0543 | Chi | 96.495 |
| | $\beta_{FS}$ | 6.6216 | RMSE | 3.4892 | $\beta_{FS}$ | 1 | RMSE | 5.6714 |
| Brouers-Sotolongo | $Q_{max}$ | 179.3873 | $R^2$ | 0.99371 | | | | |
| | K | 0.0559 | adj$R^2$ | 0.98426 | | | | |
| | $\alpha_{BS}$ | 1.2194 | Chi | 41.856 | | | | |
| | | | RMSE | 4.5747 | | | | |
| Langmuir | $Q_{max}$ | 262.5586 | $R^2$ | 0.99033 | | | | |
| | | | adj$R^2$ | 0.95163 | | | | |
| | $K_L$ | 0.0543 | Chi | 96.495 | | | | |
| | | | RMSE | 5.6714 | | | | |
| Temkin | B | 50.8014 | $R^2$ | 0.97697 | | | | |
| | | | adj$R^2$ | 0.96162 | | | | |
| | $K_T$ | 0.8355 | Chi | 114.86 | | | | |
| | | | RMSE | 8.7505 | | | | |
| Freundlich | $K_F$ | 18.3148 | $R^2$ | 0.97588 | | | | |
| | | | adj$R^2$ | 0.9598 | | | | |
| | $n_F$ | 0.6233 | Chi | 120.28 | | | | |
| | | | RMSE | 8.9548 | | | | |

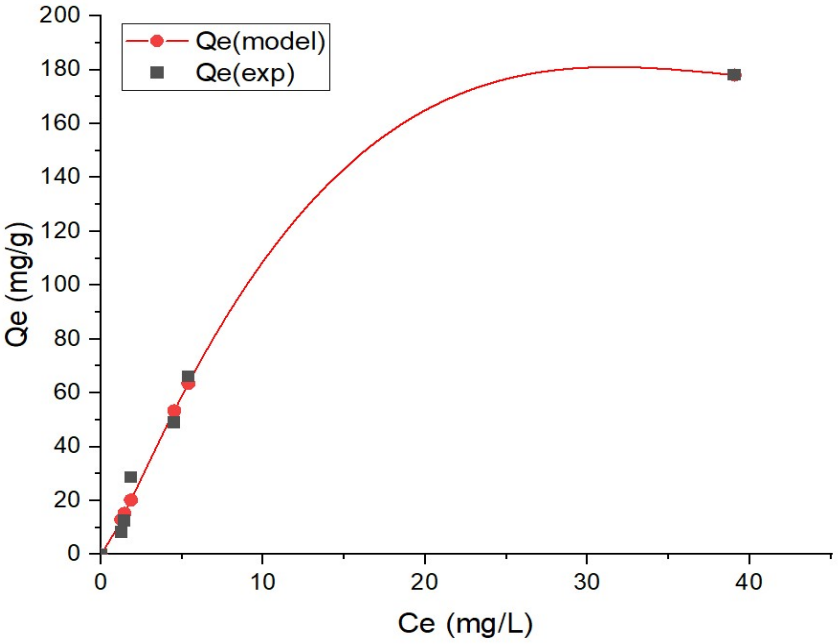


*Figure 61: BM adsorption by FEN isotherm (Brouers-Sotolongo isotherm)*

- **MB adsorption by FBIO:**

  For this we picked 3 of those isotherm models and compared with the most three famous isotherm model: Langmuir, Temkin and Freundlich. Then we will compare the empirical models to see which one is the best fit.

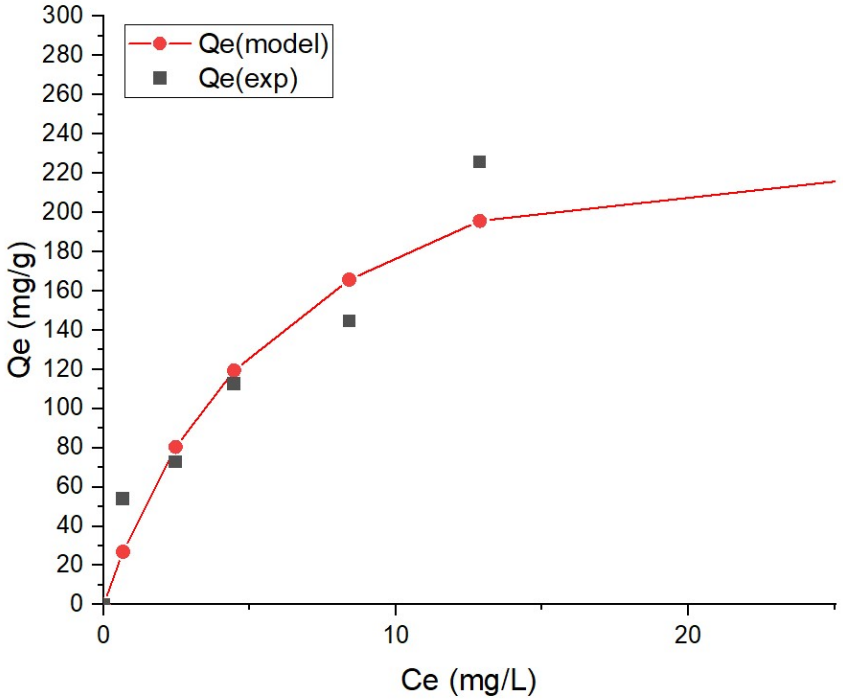


*Figure 62: BM adsorption by FBIO isotherm (Langmuir isotherm)*

*Table 27: Comparison of the result of modelling of the isotherm models for BM adsorption by FBIO*

| Model | Empirical model parameters | | Validation | | parameters | | Validation | |
|---|---|---|---|---|---|---|---|---|
| Baudu | $Q_{max}$ | 6.31E+08 | $R^2$ | 0.97213 | $Q_{max}$ | 1327.8 | $R^2$ | 0.94779 |
| | $b_0$ | 7.14E-05 | adj$R^2$ | 0.86066 | $b_0$ | 36.9057 | adj$R^2$ | 0.73897 |
| | x | 3.1133 | Chi | 471.063 | X | -1.638E-08 | Chi | 882.49 |
| | y | -3.5059 | RMSE | 12.5308 | Y | -0.3041 | RMSE | 17.151 |
| Fritz-Shluender 4 para | $C_{FS}$ | 45.1370 | $R^2$ | 0.97249 | $C_{FS}$ | 49.0158 | $R^2$ | 0.94779 |
| | $\alpha_{FS}$ | 0.6061 | adj$R^2$ | 0.86243 | $\alpha_{FS}$ | 0.6956 | adj$R^2$ | 0.73897 |
| | $D_{FS}$ | 1.234E-13 | Chi | 465.11 | $D_{FS}$ | 0.0369 | Chi | 882.49 |
| | $\beta_{FS}$ | 7.4326 | RMSE | 12.451 | $\beta_{FS}$ | 1 | RMSE | 17.151 |
| Vieth-Sladek | $Q_{max}$ | 512.3732 | $R^2$ | 0.94357 | $Q_{max}$ | 296.4331 | $R^2$ | 0.93446 |
| | $K_{VS}$ | -2.7431 | adj$R^2$ | 0.85894 | $K_{VS}$ | 2.77E-08 | adj$R^2$ | 0.83615 |
| | $\beta_{VS}$ | 0.0714 | Chi | 635.88 | $\beta_{VS}$ | 0.1509 | Chi | 738.61 |
| | | | RMSE | 17.831 | | | RMSE | 19.217 |
| Langmuir | $Q_{max}$ | 296.4331 | $R^2$ | 0.93446 | | | | |
| | | | adj$R^2$ | 0.89076 | | | | |
| | $K_L$ | 0.1509 | Chi | 553.96 | | | | |
| | | | RMSE | 19.217 | | | | |
| BET | $Q_{max}$ | 13213 | $R^2$ | 0.57541 | | | | |
| | $C_{BET}$ | 0.0085 | adj$R^2$ | -0.06147 | | | | |
| | $C_{sat}$ | 154.9525 | Chi | 4784.9 | | | | |
| | | | RMSE | 48.913 | | | | |
| Temkin | $B_T$ | 47.7346 | $R^2$ | 0.89589 | | | | |
| | | | adj$R^2$ | 0.82649 | | | | |
| | $K_T$ | 2.7399 | Chi | 879.93 | | | | |
| | | | RMSE | 24.22 | | | | |
| Freundlich | $K_F$ | 72.7461 | $R^2$ | 0.87654 | | | | |
| | | | adj$R^2$ | 0.79424 | | | | |
| | $n_F$ | 0.3335 | Chi | 1043.5 | | | | |
| | | | RMSE | 26.375 | | | | |

After the comparison that's showing in Table 26, Langmuir isotherm model is the best fit model with $R^2$=0.93446 and adj$R^2$= 0.89076. that means the adsorption is monolayer with heterogeneous surface of the bioadsorbent and favourable ($n_F$<1). Then the model expression is shown as follows:

$$Qe = \frac{44.732C_e}{1 + 0.1509C_e} \qquad \textit{(Eq LX)}$$

According to Figure 62, the isotherm is a type I isotherm which is favorable.

- **MB adsorption by TH:**

For this we picked 4 of those isotherm models and compared with the most 4 famous isotherm model: Langmuir, Temkin, Freundlich. Then we will compare the empirical models to see which one is the best fit.

*Table 28: Comparison of the result of modelling of the isotherm models for BM adsorption by TH*

| Model | Empirical model parameters | | Validation | | parameters | | Validation | |
|---|---|---|---|---|---|---|---|---|
| Khan | $Q_{max}$ | 40373 | $R^2$ | 0.975 | $Q_{max}$ | 1.4473 | $R^2$ | 0.55591 |
| | $b_{KH}$ | 1.048E-05 | $adjR^2$ | 0.9375 | $b_{KH}$ | 16.5526 | $adjR^2$ | -0.1102 |
| | $\alpha_{KH}$ | -61799 | Chi | 446.22 | $\alpha_{KH}$ | 6.837E-09 | Chi | 7926.2 |
| | | | RMSE | 14.937 | | | RMSE | 62.953 |
| Koble-Corrigan | $a_{KC}$ | 5.1906 | $R^2$ | 0.99712 | $a_{KC}$ | 0.01222 | $R^2$ | 0.9624 |
| | | | $adjR^2$ | 0.9928 | | | $adjR^2$ | 0.90605 |
| | $b_{KC}$ | -0.4650 | Chi | 51.417 | $b_{KC}$ | 2.3384E-14 | Chi | 670.71 |
| | $n_{KC}$ | 0.3730 | RMSE | 5.07 | $n_{KC}$ | 5.1532 | RMSE | 18.313 |
| Oswin modified | $A'_{OS}$ | 3.324E12 | $R^2$ | 0.96250 | $A'_{OS}$ | 930 | $R^2$ | 0.69723 |
| | $B'_{OS}$ | 8.51E10 | $adjR^2$ | 0.9063 | $B'_{OS}$ | 1000.5 | $adjR^2$ | 0.24307 |
| | $n'_{OS}$ | 5.1198 | Chi | 669.214 | $n'_{OS}$ | 0.0015 | Chi | 5403.9 |
| | | | RMSE | 18.292 | | | RMSE | 51.98 |
| Langmuir | $Q_{max}$ | 40480 | $R^2$ | 0.55481 | | | | |
| | | | $adjR^2$ | 0.25802 | | | | |
| | $K_L$ | 5.898E-04 | Chi | 5959.3 | | | | |
| | | | RMSE | 63.031 | | | | |
| BET | $Q_{max}$ | 27.1547 | $R^2$ | 0.99766 | | | | |
| | $C_{BET}$ | 2.4678 | $adjR^2$ | 0.99415 | | | | |
| | $C_{sat}$ | 7.7378 | Chi | 41.794 | | | | |
| | | | RMSE | 4.5713 | | | | |
| Temkin | $B_T$ | 19.0199 | $R^2$ | 0.54413 | | | | |
| | | | $adjR^2$ | 0.24021 | | | | |
| | $K_T$ | 0.5147 | Chi | 6012.3 | | | | |
| | | | RMSE | 63.782 | | | | |
| Freundlich | $K_F$ | 0.0122 | $R^2$ | 0.9624 | | | | |
| | | | $adjR^2$ | 0.9374 | | | | |
| | $n_F$ | 5.1530 | Chi | 503.03 | | | | |
| | | | RMSE | 18.313 | | | | |

According to Appendice 7 and Table 26, BET isotherm model and all based isotherms on BET are the best fit isotherms but due to the nature of isotherm (liquid-solid adsorption) and due to the poor prediction of results, Freundlich isotherm model is the best fit model with $R^2$=0.9624 and $adjR^2$= 0.9374. that means the adsorption is monolayer and unfavourable ($n_F$>1).

According to Figure 63, the isotherm is a type V isotherm which is unfavourable.

Then the model expression is shown as follows:

$$Qe = 0.0122{C_e}^{5.1530} \qquad \textit{(Eq LXI)}$$

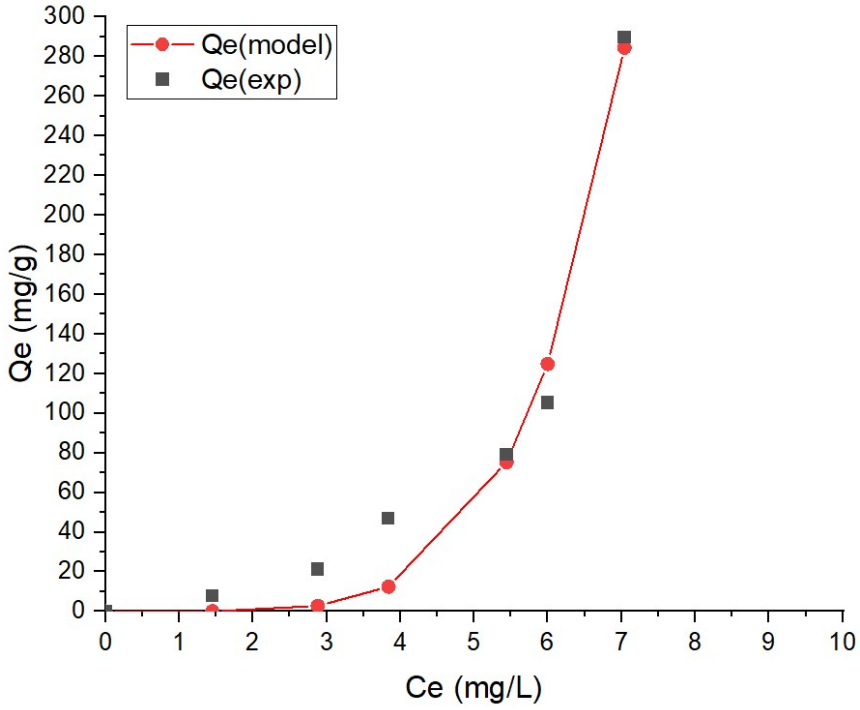


*Figure 63: BM adsorption by TH isotherm (Freundlich isotherm)*

## V.3.2. Modelling of adsorption kinetics:

The data from kinetics studies of CTC-HCl adsorption were used to fit 15 models chosen from the known models (Appendice 8), three kinetic models for each bioadsorbent were taken according to their high $R^2$ and Adjusted $R^2$ resulted from the DA and the function "lsqcurvefit" from MATLAB. The following table shows the result of the regression nonlinear using "lsqcurvefit" with the initial point which is calculated from DA.

All the results of fitting 15 models are shown in the appendice 8.

According to Appendice 8 and Table 29, the best fitting model for the three adsorption kinetics is Pseudo-first order model.

*Table 29: Result of modelling adsorption kinetics using DA optimization*

| **CTC-HCl adsorption by FEN** | | | | | | | | | |
|---|---|---|---|---|---|---|---|---|---|
| **Pseudo-first order model** | | | **Avrami's model** | | | | **Pseudo-second order** | | |
| Qe | k1 | $R^2$ | Qe | kav | nav | $R^2$ | Qe | k2 | $R^2$ |
| | | 0.9965 | | | | 0.9965 | | | 0.9954 |
| 288.9976 | 0.0068 | $AdjR^2$ | 288.9976 | 0.017 | 0.398 | $AdjR^2$ | 447.0092 | 1.03E-05 | $AdjR^2$ |
| | | 0.9953 | | | | 0.9944 | | | 0.9934 |
| **CTC-HCl adsorption by FBIO** | | | | | | | | | |
| **Pseudo-first order model** | | | **Exponential form** | | | | **Pseudo-second order** | | |
| Qe | k1 | $R^2$ | Qe | ke | $R^2$ | | Qe | k2 | $R^2$ |
| | | 0.7888 | | | 0.7742 | | | | 0.7692 |
| 87.5832 | 0.0123 | $AdjR^2$ | 96.1717 | 0.071 | $AdjR^2$ | | 124.411 | 7.41E-05 | $AdjR^2$ |
| | | 0.7184 | | | 0.6989 | | | | 0.6923 |
| **CTC-HCl adsorption by TH** | | | | | | | | | |
| **Pseudo-first order model** | | | **Modification pseudo-second-order model** | | | | **Pseudo-second order** | | |
| Qe | k1 | $R^2$ | Qe | kflso | a | $R^2$ | Qe | k2 | $R^2$ |
| | | 0.9916 | | | | 0.9896 | | | 0.9889 |
| 29.9401 | 0.011 | $AdjR^2$ | 37.2085 | 0.0002 | 1.1292 | $AdjR^2$ | 41.7526 | 2.00E-04 | $AdjR^2$ |
| | | 0.9888 | | | | 0.9833 | | | 0.9852 |

The fitting data of the CTC-HCl adsorption on the models wasn't good or convincing because of the point (t=120min, Qt=106.28 mg/g), which did not fit to any of the models. After repeating the regression without that point, the results were convenient with $R^2$ = 0.9543 and AdjR2 = 0.9359 but there weren't any big changes in the coefficients (Qe=87.7471 mg/g and k1=0.0095 $min^{-1}$).

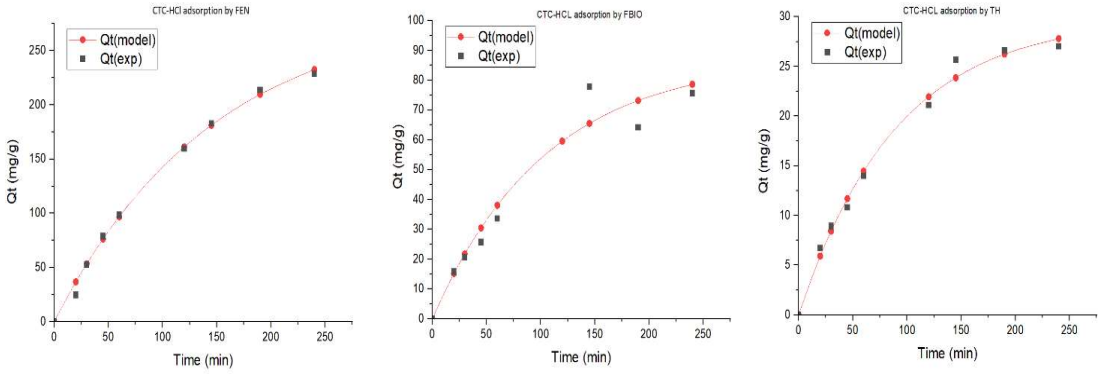


*Figure 64: CTC-HCl adsorption kinetic model for FEN, FBIO and TH (PFO model)*

## V.4. Comparison between modelling using linear and nonlinear regression:

Linear and nonlinear regressions are powerful methods for exploring relationships or fitting a set of variables to a model. Linear models tend to be simple and easy to interpret, but they're limited to linear relationships or equations, while nonlinear regressions are more appropriate for fitting data on nonlinear equations or for curve-fitting data to discover the relationships between variables [106].

To compare between them, one model from the results of modelling from each adsorption equilibrium and kinetics was taken and got compared with the results of linear regression of the linear form of the models.

- **Linear regression of BM adsorption by FEN-Langmuir model:**

  Using the data from the BM adsorption by FEN equilibrium study, the data were fitted in the linear form of Langmuir model and the linearized equation is as follows:

$$\frac{Ce}{Q_e} = \frac{Ce}{Q_{max}} + \frac{1}{Q_{max}K_L} \qquad \textit{(Eq LXII)}$$

  The linear regression was done by the software "OriginLab", the results are shown in the figure bellow:

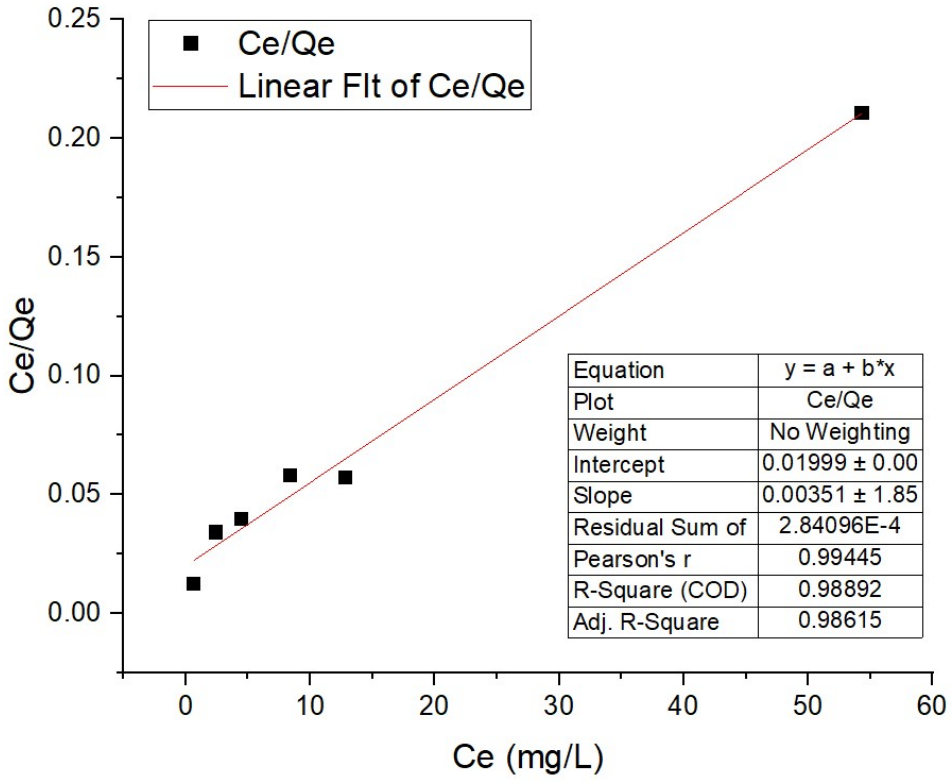


*Figure 65: Linear fit of the Langmuir isotherm of BM adsorption by FEN*

Where: $Q_{max} = 284.9\ mg/g$ and $K_L = 0.17559\ L/mg$, and after evaluation the model with these parameters, the model has: $R^2$=0.9301 and Adj$R^2$=0.8841.

- **Linear regression of CTC-HCl adsorption by FEN-PFO model:**

Using the data from the CTC-HCl adsorption by FEN kinetic study, the data were fitted in the linear form of PFO model by supposing Qe=240 mg/g from the graph in Figure 34 and the linearized equation is as follows:

$$ln(q_e - q_t) = lnq_e - k_1 t \qquad \textit{(Eq LXIII)}$$

The linear regression was done by the software "OriginLab", the results are shown in the figure bellow:

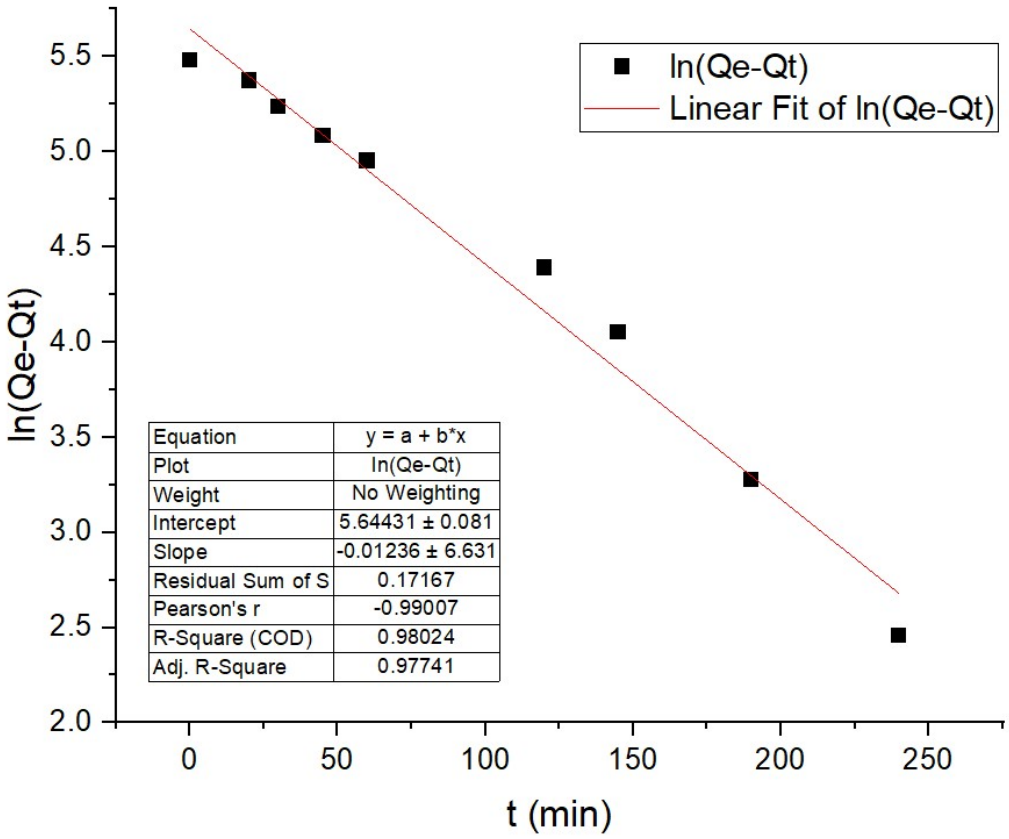


*Figure 66: Linear fit of the PFO kinetic of CTC-HCl adsorption by FEN*

Where: $Q_e = 282.6784\ mg/g$ and $k_1 = 0.01236\ min^{-1}$, and after evaluation the model with these parameters the model has: $R^2$=0.7052 and Adj$R^2$=0.6069 which is so low compared to the evaluation to the linear form as result of the choice of Qe value from the graph which it was supposed to be around 240 min but it appears that Qe=282.67 which is far from the supposed value.

- **Comparison of the results between linear and nonlinear regression:**

*Table 30:Comparison of results between linear and nonlinear regression*

| | nonlinear regression | | | | Linear regression | | | |
|---|---|---|---|---|---|---|---|---|
| Langmuir model | $Q_{max}$ | 262.5586 | $R^2$ | 0.9903 | $Q_{max}$ | 284.9 | $R^2$ | 0.9301 |
| | $K_L$ | 0.0543 | Adj$R^2$ | 0.9516 | $K_L$ | 0.17559 | Adj$R^2$ | 0.8841 |
| PFO model | Qe | 288.9976 | $R^2$ | 0.9965 | Qe | 282.6784 | $R^2$ | 0.7052 |
| | k1 | 0.0068 | Adj$R^2$ | 0.9953 | k1 | 0.01236 | Adj$R^2$ | 0.6069 |

According to Table 30, nonlinear regression was better in term of fitting the data into a model with high precisions (high $R^2$ and Adj$R^2$) that thanks to the flexibility in curve-fitting functionality ,but in the other hand, it can take considerable effort to choose the nonlinear function that creates the best fit for the particular shape of the curve which is the same thing that happened to the BET model in BM adsorption by FEN which it can't predict accurate results after the maximum value in the data, and difficulty of choosing a starting point which can greatly affect the outcome .

In the other side, linear regression was simpler and more performed incredibly on linear forms of Langmuir and PFO models (high $R^2$ and Adj$R^2$) but failed to fit the complex data like in the PFO model case (big difference between $R^2$ and Adj$R^2$ from linear and nonlinear form) because it only assumed the linear relationship between variables.

## V.5. Conclusion:

In this study, DOE were used to model and optimize the factors influencing adsorption capacity Qe and elimination rate %R which indicates that the most optimum conditions to maximize the elimination and the adsorption capacity of CTC-HCl are:

- pH=9.56, $C_0$=0.034 mg/mL and 0.02g of mass for FEN (Qe = 122.89 ± 9.87 mg/g and R = 74.66 ± 2.14 % with desirability = 1);
- pH=8.36, $C_0$=0.034 mg/mL and 0.025g of mass for FBIO (Qe = 254.25 ± 34.4 mg/g and R = 89.20 ± 4.01 % with desirability = 0.8434);
- pH=10.99, $C_0$=0.04 mg/mL and 0.02g of mass for TH (Qe = 263.3783 ± 33.6 mg/g and R = 85.77 ± 7.52 % with desirability = 0.9230).

as TH and FBIO were the most performable adsorbents for eliminating CTC-HCl.

DA were used to optimize the search of the best starting point to model CTC-HCl adsorption kinetics and BM adsorption equilibriums based on 32 equilibrium model and 15 kinetic model using nonlinear regression MATLAB functions "nlinfit" and "lsqcruvefit". The results indicates that:

- BM adsorption by FEN: was a Brouers-Sotolongo isotherm model ($R^2$=0.99371), a Langmuir isotherm model ($R^2$=0.93446) by FBIO and a Freundlich isotherm model ($R^2$=0.9624) by TH.
- CTC-HCl adsorption kinetic by FEN, FBIO and TH is PFO kinetic model with $R^2$ equals to 0.9965, 0.7888 and 0.9916, respectively.

After comparing the results of linear and nonlinear regression for modelling BM and CTC-HCl adsorption kinetic and equilibrium, nonlinear regression was more precise and accurate than the linear regression of the linear form of PFO (kinetic) and Langmuir (equilibrium) model.

# *General conclusion*

# General conclusion

The aim of this thesis work was to develop and prepare a bio-adsorbent with interesting properties at a lower cost for industrial applications using plant waste, capable of considerably reducing the organic pollutants in effluents. The effectiveness of these materials in depollution processes has met with great success, but their use remains limited in the recovery of these materials in the form of powder.

In this study, Fennel seeds and Sweet Thapsia roots were used as biosorbents to eliminate two model organic pollutants: MB and CTC-HCl. The various materials produced will be used as adsorbents in the batch adsorption process.

These biosorbents, prepared in powder form with particle sizes of 350 µm, were characterized using various physicochemical analysis techniques to determine their properties. The characteristics examined were zero-charge pH, bulk density, and Fourier transform infrared spectroscopy (FTIR).

A study of the influence of a number of factors (pollutant concentration, adsorbent mass, and pH) on the adsorption capacity of MB on FEN, FBIO, and TH led to the following conclusions:

- Adsorption capacity increases with increasing concentrations of MB.
- Increasing the dosage of the adsorbent had a negative influence on the adsorption capacity but a positive influence on the removal rate.
- The highest adsorption capacities and elimination rates were observed at pH 10–11.
- FEN demonstrated the highest removal efficacy for CTC-HCl at 180 minutes, with %R = 64.12%, compared to FBIO ($t_{opt}$ = 120 min and %R = 32.79%) and TH ($t_{opt}$ = 120 min and %R = 6.40%).

Applying the Box Behnken design to the adsorption of CTC-HCl allowed us to determine and to model the effects of the factors considered on the response as well as any interactions between them which allowed us to optimize the system's response.

Adsorption tests on CTC-HCl, carried out in batch mode, showed that the adsorption capacity is influenced by these parameters. The optimum conditions are:

- $pH_{opt}$ between 8.36 and 10.99;
- CTC-HCl concentration $C_{0opt}$ between 0.03 and 0.04 mg/mL;
- an adsorbent mass $m_{opt}$ of 0.02 to 0.025 g.

Modelling of the adsorption kinetics on FEN, FBIO, and TH by applying 15 kinetic models using nonlinear regression coupled by DA led to the conclusion that in the tree studied cases, the experimental curves are generally well described by a pseudo-First-order equation (FEN: Qe = 288.99 mg/g, k1 = 0.0068; FBIO: Qe = 88.58, k1 = 0.0123; and TH: Qe = 29.94, k1 = 0.011.

Modelling of the adsorption isotherm using 32 kinetic models using nonlinear regression coupled by DA led to the conclusion that the Brourers-Sotolongo, Langmuir, and Freundlich models better describe the phenomenon of MB adsorption on FEN, FBIO, and TH, respectively.

The comparison between linear and nonlinear regression for modelling BM and CTC-HCl adsorption kinetics and equilibrium allowed us to prove that nonlinear regression is more precise and accurate than linear regression.

The comparison of the experimental study and the modelling and optimisation study revealed that in, MB adsorption, a maximum adsorption capacity of 296.43 mg/g and 179.39 mg/g and, in CTC-HCl adsorption, an optimal contact time of 120 min and 180 min for fennel seed-based organic fibres (FBIO) and fennel seeds (FEN) respectively, which express the efficacity of using biological treatment in bioadsorbents developments.

Through the work carried out, the feasibility of a process based on the use of biomaterials for the elimination of organic compounds was approved. However, certain aspects need to be taken into account to validate these materials and their use in water treatment. In order to propose a mechanism for the future, it would be interesting to complete the study with more in-depth characterization:

- ✓ Use these materials for the elimination of other pollutants, both organic and inorganic, such as pharmaceuticals;
- ✓ Physico-chemical surface analyses, such as Nuclear magnetic resonance (NMR), electron photon spectroscopy (XPS), electron microscopy (SEM), and measurement of specific surface area (BET).
- ✓ Carrying out studies in binary or ternary systems;
- ✓ Carrying out studies in continuous and semi-continuous systems;
- ✓ Studying the regeneration process of these bioadsorbents;
- ✓ A technoeconomic study of the manufacture of this bio-adsorbent

# *Bibliographic references*

# Bibliographic references


[1] N. Gertsen and L. Sønderby, Eds., *Water purification*. in Air, water and soil pollution science and technology series. New York: Nova Science Publishers, 2009.

[2] R. M. Harrison, Ed., *Pollution: causes, effects, and control*, 4th ed. Cambridge: Royal Society of Chemistry, 2001.

[3] H. Qadri, R. A. Bhat, M. A. Mehmood, and G. H. Dar, Eds., *Fresh Water Pollution Dynamics and Remediation*. Singapore: Springer Singapore, 2020. doi: 10.1007/978-981-13-8277-2.

[4] K. M. Vigil, *Clean water: an introduction to water quality and pollution control*, 2nd ed. Corvallis: Oregon State University Press, 2003.

[5] C. Gadipelly *et al.*, "Pharmaceutical Industry Wastewater: Review of the Technologies for Water Treatment and Reuse," *Ind. Eng. Chem. Res.*, vol. 53, no. 29, pp. 11571–11592, Jul. 2014, doi: 10.1021/ie501210j.

[6] A. Sonune and R. Ghate, "Developments in wastewater treatment methods," *Desalination*, vol. 167, pp. 55–63, Aug. 2004, doi: 10.1016/j.desal.2004.06.113.

[7] G. Crini and E. Lichtfouse, "Advantages and disadvantages of techniques used for wastewater treatment," *Environ. Chem. Lett.*, vol. 17, no. 1, pp. 145–155, Mar. 2019, doi: 10.1007/s10311-018-0785-9.

[8] A. Bhatnagar, W. Hogland, M. Marques, and M. Sillanpää, "An overview of the modification methods of activated carbon for its water treatment applications," *Chem. Eng. J.*, vol. 219, pp. 499–511, Mar. 2013, doi: 10.1016/j.cej.2012.12.038.

[9] Y. A. B. Neolaka *et al.*, "Potential of activated carbon from various sources as a low-cost adsorbent to remove heavy metals and synthetic dyes," *Results Chem.*, vol. 5, p. 100711, Jan. 2023, doi: 10.1016/j.rechem.2022.100711.

[10] R. M. Harrison, Ed., *Pollution: causes, effects, and control*, 4th ed. Cambridge: Royal Society of Chemistry, 2001.

[11] R. Fuller *et al.*, "Pollution and health: a progress update," *Lancet Planet. Health*, vol. 6, no. 6, pp. e535–e547, Jun. 2022, doi: 10.1016/S2542-5196(22)00090-0.

[12] L. Lin, H. Yang, and X. Xu, "Effects of Water Pollution on Human Health and Disease Heterogeneity: A Review," *Front. Environ. Sci.*, vol. 10, p. 880246, Jun. 2022, doi: 10.3389/fenvs.2022.880246.

[13] J. J. Peirce, R. F. Weiner, P. A. Vesilind, and P. A. Vesilind, *Environmental pollution and control*, 4th ed. Boston: Butterworth-Heinemann, 1998.

[14] M. Shigei, A. Assayed, A. Hazaymeh, and S. S. Dalahmeh, "Pharmaceutical and Antibiotic Pollutant Levels in Wastewater and the Waters of the Zarqa River, Jordan," *Appl. Sci.*, vol. 11, no. 18, p. 8638, Sep. 2021, doi: 10.3390/app11188638.

[15] S. Dalhatou, “Application des techniques d’oxydation avancée pour la dépollution des effluents organiques dans les eaux de rejets industriels: cas des savonneries”.

[16] H. B. Mansour, O. Boughzala, D. Dridi, D. Barillier, L. Chekir-Ghedira, and R. Mosrati, “Les colorants textiles sources de contamination de l’eau : CRIBLAGE de la toxicité et des méthodes de traitement,” *Rev. Sci. L’eau*, vol. 24, no. 3, pp. 209–238, Nov. 2011, doi: 10.7202/1006453ar.

[17] S. Hammami, “Étude de dégradation des colorants de textile par les procédés d’oxydation avancée. Application à la dépollution des rejets industriels”.

[18] F. Zaviska, P. Drogui, G. Mercier, and J.-F. Blais, “Procédés d’oxydation avancée dans le traitement des eaux et des effluents industriels: Application à la dégradation des polluants réfractaires,” *Rev. Sci. Eau*, vol. 22, no. 4, pp. 535–564, Oct. 2009, doi: 10.7202/038330ar.

[19] E. E. Baruth, American Society of Civil Engineers, and American Water Works Association, Eds., *Water treatment plant design*, 4th ed. in McGraw-Hill handbooks. New York: McGraw-Hill, 2005.

[20] A. Singh, M. Agrawal, and S. B. Agrawal, Eds., *Water Pollution and Management Practices*. Singapore: Springer Singapore, 2021. doi: 10.1007/978-981-15-8358-2.

[21] E. Worch, *Adsorption technology in water treatment: fundamentals, processes, and modeling*. Berlin ; Boston: De Gruyter, 2012.

[22] C. Tien, *Introduction to Adsorption*. Cambridge: Elsevier, 2019. doi: 10.1016/B978-0-12-816446-4.09991-7.

[23] W. J. Thomas and B. D. Crittenden, *Adsorption technology and design*. Oxford ; Boston: Butterworth-Heinemann, 1998.

[24] L. Zhou, Ed., *Adsorption: progress in fundamental and application research: selected reports at the 4th Pacific Basin Conference on Adsorption Science and Technology: Tianjin, China, 22-26 May 2006*. Singapore ; Hackensack, NJ: World Scientific, 2007.

[25] F. Rouquerol, J. Rouquerol, and K. S. W. Sing, *Adsorption by powders and porous solids: principles, methodology, and applications*. San Diego: Academic Press, 1999.

[26] J. S. Piccin, T. R. S. Cadaval, L. A. A. De Pinto, and G. L. Dotto, “Adsorption Isotherms in Liquid Phase: Experimental, Modeling, and Interpretations,” in *Adsorption Processes for Water Treatment and Purification*, A. Bonilla-Petriciolet, D. I. Mendoza-Castillo, and H. E. Reynel-Ávila, Eds., Cham: Springer International Publishing, 2017, pp. 19–51. doi: 10.1007/978-3-319-58136-1_2.

[27] R. Gourdon, “Etude de l’adsorption-désorption de polluants organiques dans les sols. Approche méthodologique et application au pentachlorophénol et aux hydrocarbures aromatiques polycycliques.”

[28] M. Mozaffari Majd, V. Kordzadeh-Kermani, V. Ghalandari, A. Askari, and M. Sillanpää, “Adsorption isotherm models: A comprehensive and systematic review (2010−2020),”

*Sci. Total Environ.*, vol. 812, p. 151334, Mar. 2022, doi: 10.1016/j.scitotenv.2021.151334.

[29] M. A. Al-Ghouti and D. A. Da'ana, "Guidelines for the use and interpretation of adsorption isotherm models: A review," *J. Hazard. Mater.*, vol. 393, p. 122383, Jul. 2020, doi: 10.1016/j.jhazmat.2020.122383.

[30] N. Ayawei, A. N. Ebelegi, and D. Wankasi, "Modelling and Interpretation of Adsorption Isotherms," *J. Chem.*, vol. 2017, pp. 1–11, 2017, doi: 10.1155/2017/3039817.

[31] P. Ehiomogue, I. I. Ahuchaogu, and I. E. Ahaneku, "REVIEW OF ADSORPTION ISOTHERMS MODELS".

[32] R. Saadi, Z. Saadi, R. Fazaeli, and N. E. Fard, "Monolayer and multilayer adsorption isotherm models for sorption from aqueous media," *Korean J. Chem. Eng.*, vol. 32, no. 5, pp. 787–799, May 2015, doi: 10.1007/s11814-015-0053-7.

[33] M. Haerifar and S. Azizian, "Mixed Surface Reaction and Diffusion-Controlled Kinetic Model for Adsorption at the Solid/Solution Interface," *J. Phys. Chem. C*, vol. 117, no. 16, pp. 8310–8317, Apr. 2013, doi: 10.1021/jp401571m.

[34] J. Wang and X. Guo, "Adsorption kinetic models: Physical meanings, applications, and solving methods," *J. Hazard. Mater.*, vol. 390, p. 122156, May 2020, doi: 10.1016/j.jhazmat.2020.122156.

[35] R. K. Gautam and M. C. Chattopadhyaya, "Chapter 5 - Kinetics and Equilibrium Isotherm Modeling: Graphene-Based Nanomaterials for the Removal of Heavy Metals From Water," pp. 79–109, 2016, doi: http://dx.doi.org/10.1016/B978-0-12-804609-8.00005-4.

[36] H. Qiu, L. Lv, B. Pan, Q. Zhang, W. Zhang, and Q. Zhang, "Critical review in adsorption kinetic models," *J. Zhejiang Univ.-Sci. A*, vol. 10, no. 5, pp. 716–724, May 2009, doi: 10.1631/jzus.A0820524.

[37] A. A. Inyinbor, F. A. Adekola, and G. A. Olatunji, "Kinetics, isotherms and thermodynamic modeling of liquid phase adsorption of Rhodamine B dye onto Raphia hookerie fruit epicarp," *Water Resour. Ind.*, vol. 15, pp. 14–27, Sep. 2016, doi: 10.1016/j.wri.2016.06.001.

[38] Md. Ahmaruzzaman, "Adsorption of phenolic compounds on low-cost adsorbents: A review," *Adv. Colloid Interface Sci.*, vol. 143, no. 1–2, pp. 48–67, Nov. 2008, doi: 10.1016/j.cis.2008.07.002.

[39] Z. Du *et al.*, "Adsorption behavior and mechanism of perfluorinated compounds on various adsorbents—A review," *J. Hazard. Mater.*, vol. 274, pp. 443–454, Jun. 2014, doi: 10.1016/j.jhazmat.2014.04.038.

[40] E. I. Ugwu *et al.*, "Adsorption mechanisms for heavy metal removal using low cost adsorbents: A review," *IOP Conf. Ser. Earth Environ. Sci.*, vol. 614, no. 1, p. 012166, Dec. 2020, doi: 10.1088/1755-1315/614/1/012166.

[41] A. Witek-Krowiak, K. Chojnacka, D. Podstawczyk, A. Dawiec, and K. Pokomeda, "Application of response surface methodology and artificial neural network methods in modelling and optimization of biosorption process," *Bioresour. Technol.*, vol. 160, pp. 150–160, May 2014, doi: 10.1016/j.biortech.2014.01.021.

[42] N. R. Draper and F. Pukelsheim, "An overview of design of experiments," *Stat. Pap.*, vol. 37, no. 1, pp. 1–32, Mar. 1996, doi: 10.1007/BF02926157.

[43] A. K. Das and S. Dewanjee, "Optimization of Extraction Using Mathematical Models and Computation," in *Computational Phytochemistry*, Elsevier, 2018, pp. 75–106. doi: 10.1016/B978-0-12-812364-5.00003-1.

[44] J. Goupy, *Introduction aux plans d'expériences: avec applications*, 5e éd. in Technique et ingénierie. Paris: "l'Usine nouvelle" Dunod, 2013.

[45] W. Tinson, *Plans d'expérience: constructions et analyses statistiques*, vol. 67. in Mathématiques et Applications, vol. 67. Berlin, Heidelberg: Springer Berlin Heidelberg, 2010. doi: 10.1007/978-3-642-11472-4.

[46] L. Vera Candioti, M. M. De Zan, M. S. Cámara, and H. C. Goicoechea, "Experimental design and multiple response optimization. Using the desirability function in analytical methods development," *Talanta*, vol. 124, pp. 123–138, Jun. 2014, doi: 10.1016/j.talanta.2014.01.034.

[47] S. Mirjalili, "Dragonfly algorithm: a new meta-heuristic optimization technique for solving single-objective, discrete, and multi-objective problems," *Neural Comput. Appl.*, vol. 27, no. 4, pp. 1053–1073, May 2016, doi: 10.1007/s00521-015-1920-1.

[48] C. M. Rahman and T. A. Rashid, "Dragonfly Algorithm and Its Applications in Applied Science Survey," *Comput. Intell. Neurosci.*, vol. 2019, pp. 1–21, Dec. 2019, doi: 10.1155/2019/9293617.

[49] E. Lodhi *et al.*, "A Dragonfly Optimization Algorithm for Extracting Maximum Power of Grid-Interfaced PV Systems," *Sustainability*, vol. 13, no. 19, p. 10778, Sep. 2021, doi: 10.3390/su131910778.

[50] M. Hentabli, A. E. Belhadj, and F. Dahmoune, "Dragonfly Support Vector Machine Modelling of the Adsorption Phenomenon of Certain Phenols by Activated Carbon Fibres," *Kem. U Ind.*, no. 9–10, Aug. 2021, doi: 10.15255/KUI.2020.073.

[51] T. Chai and R. R. Draxler, "Root mean square error (RMSE) or mean absolute error (MAE)? – Arguments against avoiding RMSE in the literature," *Geosci. Model Dev.*, vol. 7, no. 3, pp. 1247–1250, Jun. 2014, doi: 10.5194/gmd-7-1247-2014.

[52] D. Chicco, M. J. Warrens, and G. Jurman, "The coefficient of determination R-squared is more informative than SMAPE, MAE, MAPE, MSE and RMSE in regression analysis evaluation," *PeerJ Comput. Sci.*, vol. 7, p. e623, Jul. 2021, doi: 10.7717/peerj-cs.623.

[53] V. Plevris, G. Solorzano, N. Bakas, and M. Ben Seghier, "Investigation of performance metrics in regression analysis and machine learning-based prediction models," in *8th European Congress on Computational Methods in Applied Sciences and Engineering*, CIMNE, 2022. doi: 10.23967/eccomas.2022.155.

[54] J. Karch, "Improving on Adjusted R-Squared," *Collabra Psychol.*, vol. 6, no. 1, p. 45, Jan. 2020, doi: 10.1525/collabra.343.

[55] G. D. Ruxton, "The unequal variance t-test is an underused alternative to Student's t-test and the Mann–Whitney U test," *Behav. Ecol.*, vol. 17, no. 4, pp. 688–690, Jul. 2006, doi: 10.1093/beheco/ark016.

[56] A. C. Leon, "Descriptive and Inferential Statistics," in *Comprehensive Clinical Psychology*, Elsevier, 1998, pp. 243–285. doi: 10.1016/B0080-4270(73)00264-9.

[57] P. Mishra, U. Singh, C. Pandey, P. Mishra, and G. Pandey, "Application of student's t-test, analysis of variance, and covariance," *Ann. Card. Anaesth.*, vol. 22, no. 4, p. 407, 2019, doi: 10.4103/aca.ACA_94_19.

[58] P. R. Bevington and D. K. Robinson, *Data reduction and error analysis for the physical sciences*, 3rd ed. Boston: McGraw-Hill, 2003. [Online]. Available: http://experimentationlab.berkeley.edu/sites/default/files/pdfs/Bevington.pdf

[59] S. T. Nihan, "Karl Pearsons chi-square tests," *Educ. Res. Rev.*, vol. 15, no. 9, pp. 575–580, Sep. 2020, doi: 10.5897/ERR2019.3817.

[60] S. De Gisi, G. Lofrano, M. Grassi, and M. Notarnicola, "Characteristics and adsorption capacities of low-cost sorbents for wastewater treatment: A review," *Sustain. Mater. Technol.*, vol. 9, pp. 10–40, Sep. 2016, doi: 10.1016/j.susmat.2016.06.002.

[61] A. Halimi, *النباتات الطبية في الجزائر [Medicinal plants of Algeria]*. 2004 ,منشورة برتي. [Online]. Available: https://books.google.dz/books?id=du3oXwAACAAJ

[62] "*Thapsia garganica*," *Wikipédia*. May 12, 2022. Accessed: Jun. 17, 2023. [Online]. Available: https://fr.wikipedia.org/w/index.php?title=Thapsia_garganica&oldid=193630919

[63] "Thapsia garganica L." https://www.gbif.org/species/6026849 (accessed Jun. 17, 2023).

[64] N. P. Makunga, A. K. Jäger, and J. Van Staden, "Micropropagation of Thapsia garganica—a medicinal plant," *Plant Cell Rep.*, vol. 21, no. 10, pp. 967–973, Jun. 2003, doi: 10.1007/s00299-003-0623-8.

[65] PubChem, "Thapsigargin." https://pubchem.ncbi.nlm.nih.gov/compound/446378 (accessed Jun. 17, 2023).

[66] T. B. Andersen *et al.*, "Localization and in-Vivo Characterization of *Thapsia garganica* CYP76AE2 Indicates a Role in Thapsigargin Biosynthesis," *Plant Physiol.*, vol. 174, no. 1, pp. 56–72, May 2017, doi: 10.1104/pp.16.00055.

[67] N. García-Jiménez, M. J. Péerez-Alonso, and A. Velasco-Negueruela, "Chemical Composition of Fennel Oil, *Foeniculum vulgare* Miller, from Spain," *J. Essent. Oil Res.*, vol. 12, no. 2, pp. 159–162, Mar. 2000, doi: 10.1080/10412905.2000.9699487.

[68] A. Gholami Zali, P. Ehsanzadeh, A. Szumny, and A. Matkowski, "Genotype-specific response of Foeniculum vulgare grain yield and essential oil composition to proline

treatment under different irrigation conditions," *Ind. Crops Prod.*, vol. 124, pp. 177–185, Nov. 2018, doi: 10.1016/j.indcrop.2018.07.067.

[69] W.-R. Diao, Q.-P. Hu, H. Zhang, and J.-G. Xu, "Chemical composition, antibacterial activity and mechanism of action of essential oil from seeds of fennel (Foeniculum vulgare Mill.)," *Food Control*, vol. 35, no. 1, pp. 109–116, Jan. 2014, doi: 10.1016/j.foodcont.2013.06.056.

[70] G. Parmoon, A. Ebadi, M. Hashemi, B. Hawrylak-Nowak, C. Baskin, and S. Jahanbakhsh, "Plant Growth Regulators Improve Grain Production and Water Use Efficiency of Foeniculum vulgare Mill. under Water Stress," *Plants*, vol. 11, no. 13, p. 1718, Jun. 2022, doi: 10.3390/plants11131718.

[71] P. Alam, M. S. Abdel-Kader, M. H. Alqarni, H. H. Zaatout, S. R. Ahamad, and F. Shakeel, "Chemical composition of fennel seed extract and determination of fenchone in commercial formulations by GC–MS method," *J. Food Sci. Technol.*, vol. 56, no. 5, pp. 2395–2403, May 2019, doi: 10.1007/s13197-019-03695-9.

[72] S. Ben Abdesslem *et al.*, "Chemical composition and biological activities of fennel ( *Foeniculum vulgare* Mill.) essential oils and ethanolic extracts of conventional and organic seeds," *J. Food Process. Preserv.*, vol. 45, no. 1, Jan. 2021, doi: 10.1111/jfpp.15034.

[73] L. Barros, A. M. Carvalho, and I. C. F. R. Ferreira, "The nutritional composition of fennel (Foeniculum vulgare): Shoots, leaves, stems and inflorescences," *LWT - Food Sci. Technol.*, vol. 43, no. 5, pp. 814–818, Jun. 2010, doi: 10.1016/j.lwt.2010.01.010.

[74] M. A. Madani, "Adsorption d'un colorant basique (bleu de méthylène) sur différents adsorbants (charbon actif en poudre, charbon en grain et la bitonite)," Université Mohamed Khaider-Biskra, Biskra, 2014.

[75] PubChem, "Methylene Blue." https://pubchem.ncbi.nlm.nih.gov/compound/6099 (accessed Jun. 17, 2023).

[76] N. Alaounia, "Dégradation photocatalytique de polluants organiques (Méthyle orange, Pentachlorophénol et Acide benzoïque) en présence du dioxyde de titane nanocristallin élaboré par la méthode sol-gel," BADJI MOKHTAR-ANNABA UNIVERSITY, Annaba, 2009.

[77] A. Boukhira, "Intoxications aigues-profil épidemiologique-prise en charge - pronostic".

[78] United States Pharmacopeia, "SAFETY DATA SHEET-Methylene Blue." Dec. 04, 2019. https://static.usp.org/pdf/EN/referenceStandards/msds/1428008.pdf

[79] L. P. Nguyen and N. S. Gerstein, "Cardiovascular Pharmacology in Noncardiac Surgery," in *Essentials of Cardiac Anesthesia for Noncardiac Surgery*, Elsevier, 2019, pp. 247–288. doi: 10.1016/B978-0-323-56716-9.00011-4.

[80] G. Schwartzman, L. Wayland, T. Alexander, K. Furnkranz, and G. Selzer, "Chlortetracycline Hydrochloride," in *Analytical Profiles of Drug Substances*, K. Florey, Ed., Academic Press, 1979, pp. 101–137. doi: 10.1016/S0099-5428(08)60115-X.

[81] PubChem, “Chlortetracycline HCl.” https://pubchem.ncbi.nlm.nih.gov/compound/54684459 (accessed Jun. 18, 2023).

[82] Santa Cruz Biotechnology, “Chlortetracycline hydrochloride | CAS 64-72-2.” https://www.scbt.com/fr/p/chlortetracycline-hydrochloride-64-72-2 (accessed Jun. 18, 2023).

[83] P. Wurmbach and K. H. Nierhaus, “Codon-anticodon interaction at the ribosomal P (peptidyl-tRNA) site,” *Proc. Natl. Acad. Sci.*, vol. 76, no. 5, pp. 2143–2147, May 1979, doi: 10.1073/pnas.76.5.2143.

[84] M. Liu, D. Zou, T. Ma, Z. Liu, and Y. Li, “Simultaneous efficient adsorption and accelerated photocatalytic degradation of chlortetracycline hydrochloride over novel Fe-based MOGs under visible light irradiation assisted by hydrogen peroxide,” *Inorg. Chem. Front.*, vol. 6, no. 6, pp. 1388–1397, 2019, doi: 10.1039/C9QI00046A.

[85] B. He, Y. Yang, B. Liu, Z. Zhao, J. Shang, and X. Cheng, “Degradation of Chlortetracycline Hydrochloride by Peroxymonosulfate Activation on Natural Manganese Sand Through Response Surface Methodology,” In Review, preprint, Jan. 2022. doi: 10.21203/rs.3.rs-770720/v1.

[86] F. Ahmad, D. Zhu, and J. Sun, “Environmental fate of tetracycline antibiotics: degradation pathway mechanisms, challenges, and perspectives,” *Environ. Sci. Eur.*, vol. 33, no. 1, p. 64, Dec. 2021, doi: 10.1186/s12302-021-00505-y.

[87] R. Daghrir, P. Drogui, and M. A. El Khakani, “Photoelectrocatalytic oxidation of chlortetracycline using Ti/TiO2 photo-anode with simultaneous H2O2 production,” *Electrochimica Acta*, vol. 87, pp. 18–31, Jan. 2013, doi: 10.1016/j.electacta.2012.09.020.

[88] C. J. Alteri and H. L. Mobley, “Escherichia coli physiology and metabolism dictates adaptation to diverse host microenvironments,” *Curr. Opin. Microbiol.*, vol. 15, no. 1, pp. 3–9, Feb. 2012, doi: 10.1016/j.mib.2011.12.004.

[89] M. Basavaraju and B. S. Gunashree, “*Escherichia coli* : An Overview of Main Characteristics,” in *Escherichia coli - Old and New Insights*, M. Starčič Erjavec, Ed., IntechOpen, 2023. doi: 10.5772/intechopen.105508.

[90] A. N. Ebelegi, E. I. Toneth, and M. A. Bokizibe, “Determination of Physiochemical Properties of Biosorbents Synthesized from Water Melon Rind Using Microwave Assisted Irradiation Procedure,” *Open J. Phys. Chem.*, vol. 12, no. 02, pp. 19–30, 2022, doi: 10.4236/ojpc.2022.122002.

[91] E. A. Al-Maliky, H. A. Gzar, and M. G. Al-Azawy, “Determination of Point of Zero Charge (PZC) of Concrete Particles Adsorbents,” *IOP Conf. Ser. Mater. Sci. Eng.*, vol. 1184, no. 1, p. 012004, Sep. 2021, doi: 10.1088/1757-899X/1184/1/012004.

[92] T. Kawther and N. Jasim, “REMOVAL OF CRYSTAL VIOLET AND METHYLENE BLUE FROM SYNTHETIC INDUSTRIAL WASTEWATER USING FENNEL SEED AS AN ADSORBENT,” vol. 14, pp. 2947–2963, Oct. 2019.

[93] N. Mabungela *et al.*, "Multi-application of fennel (Foeniculum vulgaris) seed composites for the adsorption and photo-degradation of methylene blue in water," *South Afr. J. Chem. Eng.*, vol. 44, pp. 283–296, Apr. 2023, doi: 10.1016/j.sajce.2023.03.001.

[94] A. Machrouhi, M. Farnane, A. Elhalil, M. Abdennouri, H. Tounsadi, and N. Barka, "Heavy metals biosorption by Thapsia transtagana stems powder: Kinetics, equilibrium and thermodynamics," 2019.

[95] "Infrared spectroscopy correlation table," *Wikipedia*. Jun. 28, 2023. Accessed: Jun. 29, 2023.[Online]. Available: https://en.wikipedia.org/w/index.php?title=Infrared_spectroscopy_correlation_table&oldid=1162282390

[96] Merck, "Table de correspondance des spectres IR." https://www.sigmaaldrich.com/DZ/fr/technical-documents/technical-article/analytical-chemistry/photometry-and-reflectometry/ir-spectrum-table (accessed Jun. 29, 2023).

[97] Lachimie , "Table Infra-rouge : interprétation des spectres IR." https://www.lachimie.fr/analytique/infrarouge/table-infra-rouge.php (accessed Jun. 29, 2023).

[98] Q. Chen, Z. Guo, J. Zhao, and Q. Ouyang, "Comparisons of different regressions tools in measurement of antioxidant activity in green tea using near infrared spectroscopy," *J. Pharm. Biomed. Anal.*, vol. 60, pp. 92–97, Feb. 2012, doi: 10.1016/j.jpba.2011.10.020.

[99] C. A. Stanford, M. Khraisheh, F. Al Momani, A. B. Albadarin, G. M. Walker, and M. A. Al Ghouti, "Use of nanoadvanced activated carbon, alumina and ferric adsorbents for humics removal from water: isotherm study," *Emergent Mater.*, vol. 3, no. 6, pp. 841–856, Dec. 2020, doi: 10.1007/s42247-020-00083-4.

[100] D. W. Underhill, "Correlation of the Specific Surface Area and Bulk Density of Commercial Charcoals with Their Adsorption Capacity for Radioactive Krypton and Xenon," *Nucl. Sci. Eng.*, vol. 79, no. 1, pp. 19–25, Sep. 1981, doi: 10.13182/NSE81-A19039.

[101] I. M. B and M. M. B, "Dynamic Adsorption Studies for the Removal of Cd (II) and Ni (II) from Aqueous Solutions using Mahogany Leaves," *Chem. Soc. Niger. Kano Chapter*, p. 12, Jun. 2017, doi: http://dx.doi.org/10.4314/csj.v8i1.1.

[102] N. S. Maurya and A. K. Mittal, "Biosorptive uptake of cationic dyes from aqueous phase using immobilised dead macro fungal biomass," *Int. J. Environ. Technol. Manag.*, vol. 14, no. 1/2/3/4, p. 282, 2011, doi: 10.1504/IJETM.2011.039275.

[103] S. J. Kim, J. H. Chung, T. Y. Kim, and S. Y. Cho, "Biosorption of heavy metals and cyanide complexes on biomass," in *Studies in Surface Science and Catalysis*, Elsevier, 2006, pp. 141–144. doi: 10.1016/S0167-2991(06)81553-3.

[104] S. Bouchareb, "Optimisation et modélisation de la biosorption du phénol sur des biomatériaux innovants composites en modes batch et continu," PhD thesis, National Polytechnic School Algiers, Algiers, 2023. [Online]. Available: http://repository.enp.edu.dz/jspui/handle/123456789/10717

[105] S. Kumar, Y. Rizvi, and R. Kumar, “A REVIEW OF MODELLING AND OPTIMIZATION TECHNIQUES IN TURNING PROCESSES”.

[106] R. E. Kass, U. T. Eden, and E. N. Brown, “Generalized Linear and Nonlinear Regression,” in *Analysis of Neural Data*, in Springer Series in Statistics. New York, NY: Springer New York, 2014, pp. 391–412. doi: 10.1007/978-1-4614-9602-1_14.

# *Appendix*

# Appendix

**Appendice 1:** Technologies available for pollutant removal

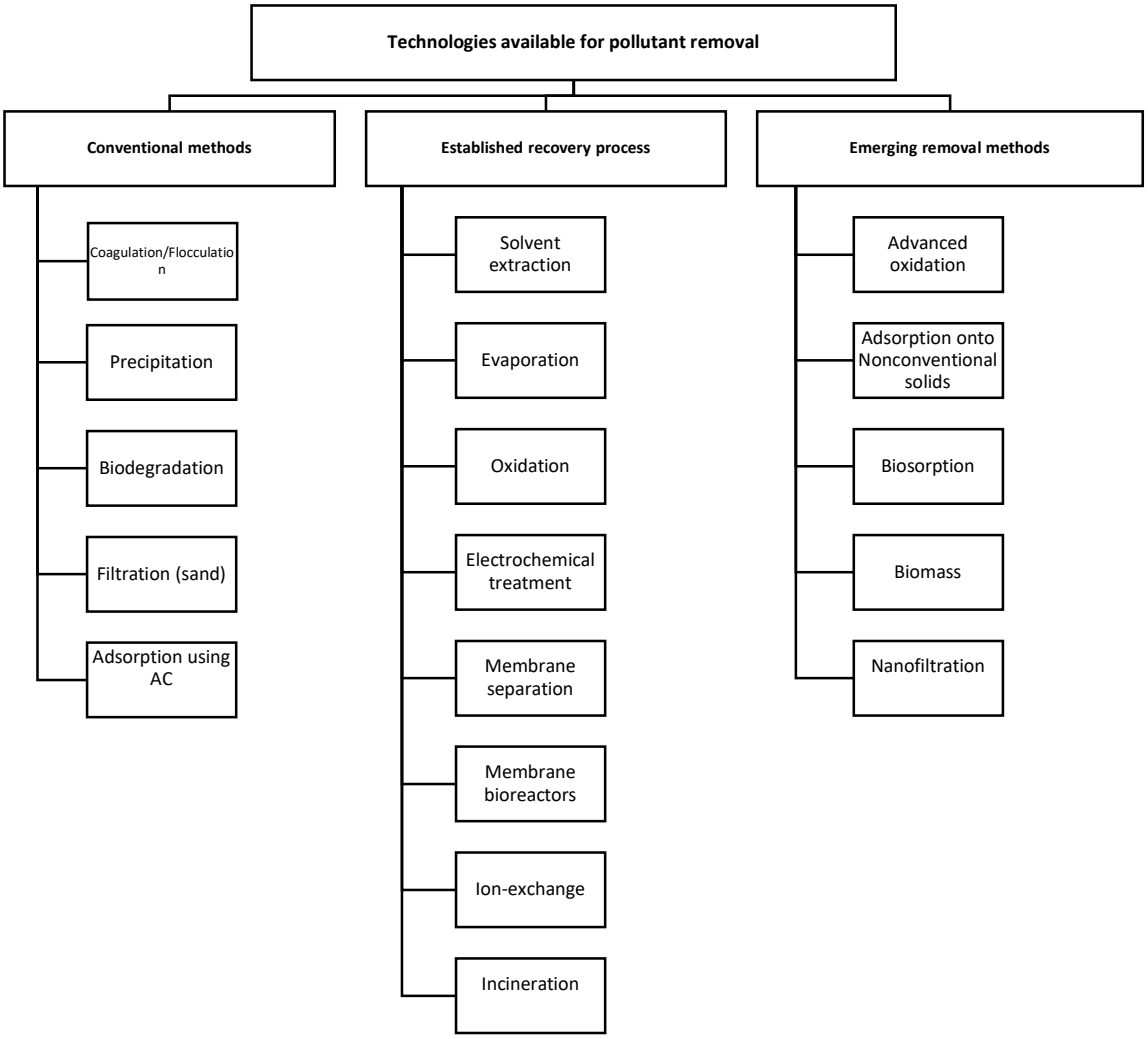


*Fig a: Technologies available for pollutant removal [7]*

**Appendice 2:** Respond surface methodology

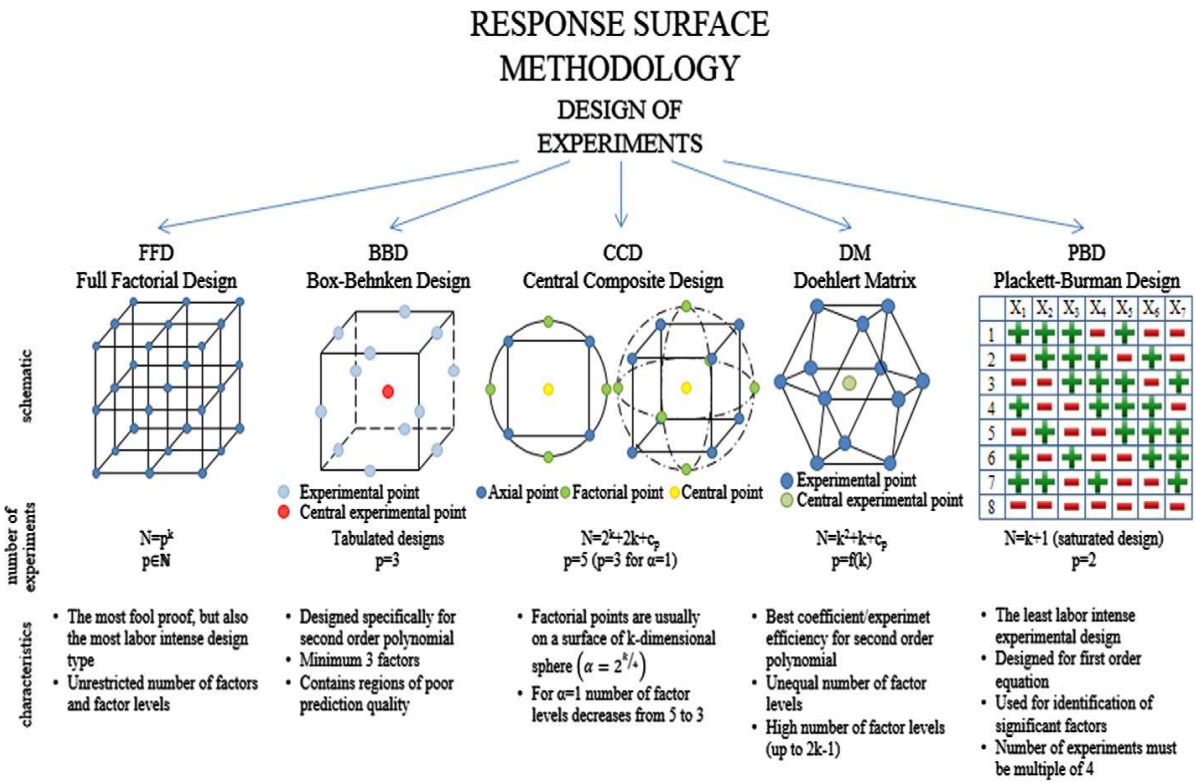


*Fig b: Respond surface methodology*

**Appendice 3:** MB and CTC-HCL calibration curve

A stock solution of methylene blue and chlortetracycline hydroxide was prepared in a 100 ml flask using distilled water. The calibration curve was established for a concentration range from 0 to 0.07 mg/ml of methylene blue, and the table and calibration line giving concentration as a function of absorbance are also provided at $\lambda_{max}(MB) = 659$ and $\lambda_{max}(CTC - HCl) = 373$.

The experimental data reported below indicate a linear relationship between absorbance and concentration with a correlation coefficient R2 =1.

The methylene blue and chlortetracycline hydroxide concentrations determined from the equation of the following regression line.

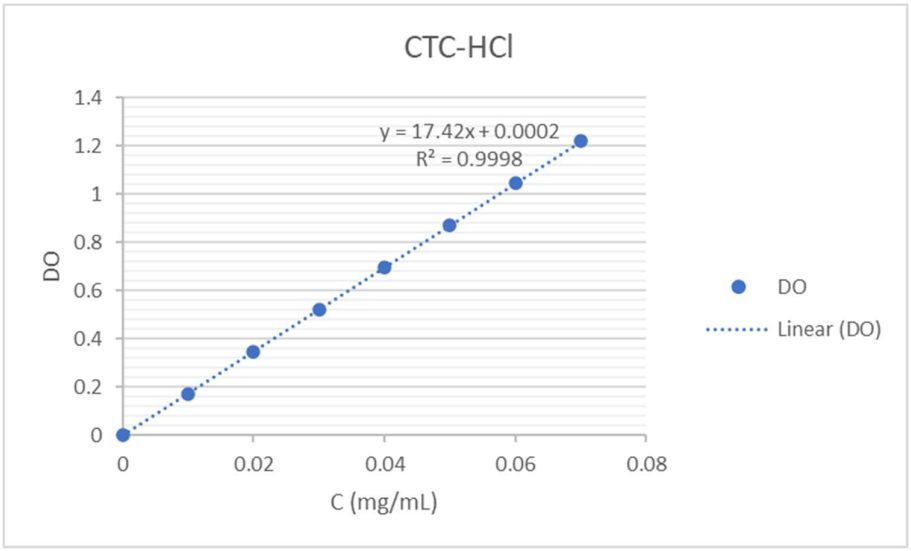


*Fig c: CTC-HCL calibration curve*

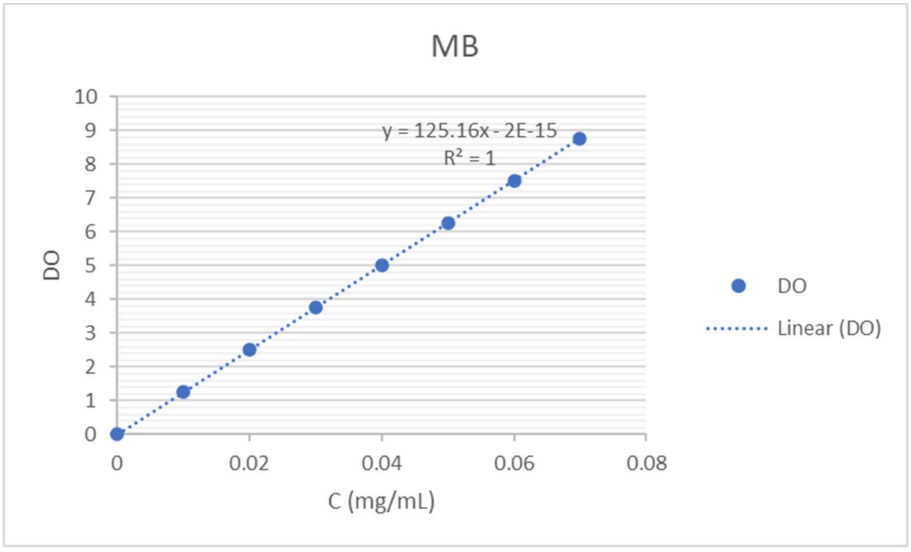


*Fig d: MB calibration curve*

**Appendice 4:** Student's t-test table

*Table A. 1: Student's t-test table*

Numbers in each row of the table are values on a *t*-distribution with (*df*) degrees of freedom for selected right-tail (greater-than) probabilities (*p*).

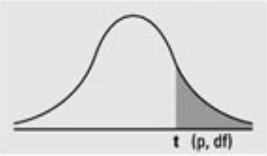


| df/p | 0.40 | 0.25 | 0.10 | 0.05 | 0.025 | 0.01 | 0.005 | 0.0005 |
|---|---|---|---|---|---|---|---|---|
| 1 | 0.324920 | 1.000000 | 3.077684 | 6.313752 | 12.70620 | 31.82052 | 63.65674 | 636.6192 |
| 2 | 0.288675 | 0.816497 | 1.885618 | 2.919986 | 4.30265 | 6.96456 | 9.92484 | 31.5991 |
| 3 | 0.276671 | 0.764892 | 1.637744 | 2.353363 | 3.18245 | 4.54070 | 5.84091 | 12.9240 |
| 4 | 0.270722 | 0.740697 | 1.533206 | 2.131847 | 2.77645 | 3.74695 | 4.60409 | 8.6103 |
| 5 | 0.267181 | 0.726687 | 1.475884 | 2.015048 | 2.57058 | 3.36493 | 4.03214 | 6.8688 |
| 6 | 0.264835 | 0.717558 | 1.439756 | 1.943180 | 2.44691 | 3.14267 | 3.70743 | 5.9588 |
| 7 | 0.263167 | 0.711142 | 1.414924 | 1.894579 | 2.36462 | 2.99795 | 3.49948 | 5.4079 |
| 8 | 0.261921 | 0.706387 | 1.396815 | 1.859548 | 2.30600 | 2.89646 | 3.35539 | 5.0413 |
| 9 | 0.260955 | 0.702722 | 1.383029 | 1.833113 | 2.26216 | 2.82144 | 3.24984 | 4.7809 |
| 10 | 0.260185 | 0.699812 | 1.372184 | 1.812461 | 2.22814 | 2.76377 | 3.16927 | 4.5869 |
| 11 | 0.259556 | 0.697445 | 1.363430 | 1.795885 | 2.20099 | 2.71808 | 3.10581 | 4.4370 |
| 12 | 0.259033 | 0.695483 | 1.356217 | 1.782288 | 2.17881 | 2.68100 | 3.05454 | 43178 |
| 13 | 0.258591 | 0.693829 | 1.350171 | 1.770933 | 2.16037 | 2.65031 | 3.01228 | 4.2208 |
| 14 | 0.258213 | 0.692417 | 1.345030 | 1.761310 | 2.14479 | 2.62449 | 2.97684 | 4.1405 |
| 15 | 0.257885 | 0.691197 | 1.340606 | 1.753050 | 2.13145 | 2.60248 | 2.94671 | 4.0728 |
| 16 | 0.257599 | 0.690132 | 1.336757 | 1.745884 | 2.11991 | 2.58349 | 2.92078 | 4.0150 |
| 17 | 0.257347 | 0.689195 | 1.333379 | 1.739607 | 2.10982 | 2.56693 | 2.89823 | 3.9651 |
| 18 | 0.257123 | 0.688364 | 1.330391 | 1.734064 | 2.10092 | 2.55238 | 2.87844 | 3.9216 |
| 19 | 0.256923 | 0.687621 | 1.327728 | 1.729133 | 2.09302 | 2.53948 | 2.86093 | 3.8834 |
| 20 | 0.256743 | 0.686954 | 1.325341 | 1.724718 | 2.08596 | 2.52798 | 2.84534 | 3.8495 |
| 21 | 0.256580 | 0.686352 | 1.323188 | 1.720743 | 2.07961 | 2.51765 | 2.83136 | 3.8193 |
| 22 | 0.256432 | 0.685805 | 1.321237 | 1.717144 | 2.07387 | 2.50832 | 2.81876 | 3.7921 |
| 23 | 0.256297 | 0.685306 | 1.319460 | 1.713872 | 2.06866 | 2.49987 | 2.80734 | 3.7676 |
| 24 | 0.256173 | 0.684850 | 1.317836 | 1.710882 | 2.06390 | 2.49216 | 2.79694 | 3.7454 |
| 25 | 0.256060 | 0.684430 | 1.316345 | 1.708141 | 2.05954 | 2.48511 | 2.78744 | 3.7251 |
| 26 | 0.255955 | 0.684043 | 1.314972 | 1.705618 | 2.05553 | 2.47863 | 2.77871 | 3.7066 |
| 27 | 0.255858 | 0.683685 | 1.313703 | 1.703288 | 2.05183 | 2.47266 | 2.77068 | 3.6896 |
| 28 | 0.255768 | 0.683353 | 1.312527 | 1.701131 | 2.04841 | 2.46714 | 2.76326 | 3.6739 |
| 29 | 0.255684 | 0.683044 | 1.311434 | 1.699127 | 2.04523 | 2.46202 | 2.75639 | 3.6594 |
| 30 | 0.255605 | 0.682756 | 1.310415 | 1.697261 | 2.04227 | 2.45726 | 2.75000 | 3.6460 |
| *z* | 0.253347 | 0.674490 | 1.281552 | 1.644854 | 1.95996 | 2.32635 | 2.57583 | 3.2905 |
| CI | ——— | ——— | 80% | 90% | 95% | 98% | 99% | 99.9% |

**Appendice 5:** Fisher's test table

*Table A. 2: Fisher's test table*

| $v_2$ \ $v_1$ | 1 | 2 | 3 | 4 | 5 | 6 | 7 | 8 | 9 | 10 | 11 | 12 | 13 | 14 | 15 | 16 | 17 | 18 |
|---|---|---|---|---|---|---|---|---|---|---|---|---|---|---|---|---|---|---|
| 1 | 161 | 200 | 216 | 225 | 230 | 234 | 237 | 239 | 241 | 242 | 243 | 244 | 245 | 245 | 246 | 246 | 247 | 247 |
| 2 | 18.5 | 19.0 | 19.2 | 19.2 | 19.3 | 19.3 | 19.4 | 19.4 | 19.4 | 19.4 | 19.4 | 19.4 | 19.4 | 19.4 | 19.4 | 19.4 | 19.4 | 19.4 |
| 3 | 10.1 | 9.55 | 9.28 | 9.12 | 9.01 | 8.94 | 8.89 | 8.85 | 8.81 | 8.79 | 8.76 | 8.74 | 8.73 | 8.71 | 8.70 | 8.69 | 8.68 | 8.67 |
| 4 | 7.71 | 6.94 | 6.59 | 6.39 | 6.26 | 6.16 | 6.09 | 6.04 | 6.00 | 5.96 | 5.94 | 5.91 | 5.89 | 5.87 | 5.86 | 5.84 | 5.83 | 5.82 |
| 5 | 6.61 | 5.79 | 5.41 | 5.19 | 5.05 | 4.95 | 4.88 | 4.82 | 4.77 | 4.74 | 4.70 | 4.68 | 4.66 | 4.64 | 4.62 | 4.60 | 4.59 | 4.58 |
| 6 | 5.99 | 5.14 | 4.76 | 4.53 | 4.39 | 4.28 | 4.21 | 4.15 | 4.10 | 4.06 | 4.03 | 4.00 | 3.98 | 3.96 | 3.94 | 3.92 | 3.91 | 3.90 |
| 7 | 5.59 | 4.74 | 4.35 | 4.12 | 3.97 | 3.87 | 3.79 | 3.73 | 3.68 | 3.64 | 3.60 | 3.57 | 3.55 | 3.53 | 3.51 | 3.49 | 3.48 | 3.47 |
| 8 | 5.32 | 4.46 | 4.07 | 3.84 | 3.69 | 3.58 | 3.50 | 3.44 | 3.39 | 3.35 | 3.31 | 3.28 | 3.26 | 3.24 | 3.22 | 3.20 | 3.19 | 3.17 |
| 9 | 5.12 | 4.26 | 3.86 | 3.63 | 3.48 | 3.37 | 3.29 | 3.23 | 3.18 | 3.14 | 3.10 | 3.07 | 3.05 | 3.03 | 3.01 | 2.99 | 2.97 | 2.96 |
| 10 | 4.90 | 4.10 | 3.71 | 3.48 | 3.33 | 3.22 | 3.14 | 3.07 | 3.02 | 2.98 | 2.94 | 2.91 | 2.89 | 2.86 | 2.85 | 2.83 | 2.81 | 2.80 |
| 11 | 4.84 | 3.98 | 3.59 | 3.36 | 3.20 | 3.09 | 3.01 | 2.95 | 2.90 | 2.85 | 2.82 | 2.79 | 2.76 | 2.74 | 2.72 | 2.70 | 2.69 | 2.67 |
| 12 | 4.75 | 3.89 | 3.49 | 3.26 | 3.11 | 3.00 | 2.91 | 2.85 | 2.80 | 2.75 | 2.72 | 2.69 | 2.66 | 2.64 | 2.62 | 2.60 | 2.58 | 2.57 |
| 13 | 4.67 | 3.81 | 3.41 | 3.18 | 3.03 | 2.92 | 2.83 | 2.77 | 2.71 | 2.67 | 2.63 | 2.60 | 2.58 | 2.55 | 2.53 | 2.51 | 2.50 | 2.48 |
| 14 | 4.60 | 3.74 | 3.34 | 3.11 | 2.96 | 2.85 | 2.76 | 2.70 | 2.65 | 2.60 | 2.57 | 2.53 | 2.51 | 2.48 | 2.46 | 2.44 | 2.43 | 2.41 |
| 15 | 4.54 | 3.68 | 3.29 | 3.06 | 2.90 | 2.79 | 2.71 | 2.64 | 2.59 | 2.54 | 2.51 | 2.48 | 2.45 | 2.42 | 2.40 | 2.38 | 2.37 | 2.35 |
| 16 | 4.49 | 3.63 | 3.24 | 3.01 | 2.85 | 2.74 | 2.66 | 2.59 | 2.54 | 2.49 | 2.46 | 2.42 | 2.40 | 2.37 | 2.35 | 2.33 | 2.32 | 2.30 |
| 17 | 4.45 | 3.59 | 3.20 | 2.96 | 2.81 | 2.70 | 2.61 | 2.55 | 2.49 | 2.45 | 2.41 | 2.38 | 2.35 | 2.33 | 2.31 | 2.29 | 2.27 | 2.26 |
| 18 | 4.41 | 3.55 | 3.16 | 2.93 | 2.77 | 2.66 | 2.58 | 2.51 | 2.46 | 2.41 | 2.37 | 2.34 | 2.31 | 2.29 | 2.27 | 2.25 | 2.23 | 2.22 |
| 19 | 4.38 | 3.52 | 3.13 | 2.90 | 2.74 | 2.63 | 2.54 | 2.48 | 2.42 | 2.38 | 2.34 | 2.31 | 2.28 | 2.26 | 2.23 | 2.21 | 2.20 | 2.18 |
| 20 | 4.35 | 3.49 | 3.10 | 2.87 | 2.71 | 2.60 | 2.51 | 2.45 | 2.39 | 2.35 | 2.31 | 2.28 | 2.25 | 2.22 | 2.20 | 2.18 | 2.17 | 2.15 |
| 21 | 4.32 | 3.47 | 3.07 | 2.84 | 2.68 | 2.57 | 2.49 | 2.42 | 2.37 | 2.32 | 2.28 | 2.25 | 2.22 | 2.20 | 2.18 | 2.16 | 2.14 | 2.12 |
| 22 | 4.30 | 3.44 | 3.05 | 2.82 | 2.66 | 2.55 | 2.46 | 2.40 | 2.34 | 2.30 | 2.26 | 2.23 | 2.20 | 2.17 | 2.15 | 2.13 | 2.11 | 2.10 |
| 23 | 4.28 | 3.42 | 3.03 | 2.80 | 2.64 | 2.53 | 2.44 | 2.37 | 2.32 | 2.27 | 2.23 | 2.20 | 2.18 | 2.15 | 2.13 | 2.11 | 2.09 | 2.07 |
| 24 | 4.26 | 3.40 | 3.01 | 2.78 | 2.62 | 2.51 | 2.42 | 2.36 | 2.30 | 2.25 | 2.21 | 2.18 | 2.15 | 2.13 | 2.11 | 2.09 | 2.07 | 2.05 |
| 25 | 4.24 | 3.39 | 2.99 | 2.76 | 2.60 | 2.49 | 2.40 | 2.34 | 2.28 | 2.24 | 2.20 | 2.16 | 2.14 | 2.11 | 2.09 | 2.07 | 2.05 | 2.04 |
| 26 | 4.23 | 3.37 | 2.98 | 2.74 | 2.59 | 2.47 | 2.39 | 2.32 | 2.27 | 2.22 | 2.18 | 2.15 | 2.12 | 2.09 | 2.07 | 2.05 | 2.03 | 2.02 |
| 27 | 4.21 | 3.35 | 2.96 | 2.73 | 2.57 | 2.46 | 2.37 | 2.31 | 2.25 | 2.20 | 2.17 | 2.13 | 2.10 | 2.08 | 2.06 | 2.04 | 2.02 | 2.00 |
| 28 | 4.20 | 3.34 | 2.95 | 2.71 | 2.56 | 2.45 | 2.36 | 2.29 | 2.24 | 2.19 | 2.15 | 2.12 | 2.09 | 2.06 | 2.04 | 2.02 | 2.00 | 1.99 |
| 29 | 4.18 | 3.33 | 2.93 | 2.70 | 2.55 | 2.43 | 2.35 | 2.28 | 2.22 | 2.18 | 2.14 | 2.10 | 2.08 | 2.05 | 2.03 | 2.01 | 1.99 | 1.97 |
| 30 | 4.17 | 3.32 | 2.92 | 2.69 | 2.53 | 2.42 | 2.33 | 2.27 | 2.21 | 2.16 | 2.13 | 2.09 | 2.06 | 2.04 | 2.01 | 1.99 | 1.98 | 1.96 |
| 32 | 4.15 | 3.29 | 2.90 | 2.67 | 2.51 | 2.40 | 2.31 | 2.24 | 2.19 | 2.14 | 2.10 | 2.07 | 2.04 | 2.01 | 1.99 | 1.97 | 1.95 | 1.94 |
| 34 | 4.13 | 3.28 | 2.88 | 2.65 | 2.49 | 2.38 | 2.29 | 2.23 | 2.17 | 2.12 | 2.08 | 2.05 | 2.02 | 1.99 | 1.97 | 1.95 | 1.93 | 1.92 |
| 36 | 4.11 | 3.26 | 2.87 | 2.63 | 2.48 | 2.36 | 2.28 | 2.21 | 2.15 | 2.11 | 2.07 | 2.03 | 2.00 | 1.98 | 1.95 | 1.93 | 1.92 | 1.90 |
| 38 | 4.10 | 3.24 | 2.85 | 2.62 | 2.46 | 2.35 | 2.26 | 2.19 | 2.14 | 2.09 | 2.05 | 2.02 | 1.99 | 1.96 | 1.94 | 1.92 | 1.90 | 1.88 |
| 40 | 4.08 | 3.23 | 2.84 | 2.61 | 2.45 | 2.34 | 2.25 | 2.18 | 2.12 | 2.08 | 2.04 | 2.00 | 1.97 | 1.95 | 1.92 | 1.90 | 1.89 | 1.87 |
| 42 | 4.07 | 3.22 | 2.83 | 2.59 | 2.44 | 2.32 | 2.24 | 2.17 | 2.11 | 2.06 | 2.03 | 1.99 | 1.96 | 1.93 | 1.91 | 1.89 | 1.87 | 1.86 |
| 44 | 4.06 | 3.21 | 2.82 | 2.58 | 2.43 | 2.31 | 2.23 | 2.16 | 2.10 | 2.05 | 2.01 | 1.98 | 1.95 | 1.92 | 1.90 | 1.88 | 1.86 | 1.84 |
| 46 | 4.05 | 3.20 | 2.81 | 2.57 | 2.42 | 2.30 | 2.22 | 2.15 | 2.09 | 2.04 | 2.00 | 1.97 | 1.94 | 1.91 | 1.89 | 1.87 | 1.85 | 1.83 |
| 48 | 4.04 | 3.19 | 2.80 | 2.57 | 2.41 | 2.29 | 2.21 | 2.14 | 2.08 | 2.03 | 1.99 | 1.96 | 1.93 | 1.90 | 1.88 | 1.86 | 1.84 | 1.82 |
| 50 | 4.03 | 3.18 | 2.79 | 2.56 | 2.40 | 2.29 | 2.20 | 2.13 | 2.07 | 2.03 | 1.99 | 1.95 | 1.92 | 1.89 | 1.87 | 1.85 | 1.83 | 1.81 |
| 55 | 4.02 | 3.16 | 2.77 | 2.54 | 2.38 | 2.27 | 2.18 | 2.11 | 2.06 | 2.01 | 1.97 | 1.93 | 1.90 | 1.88 | 1.85 | 1.83 | 1.81 | 1.79 |
| 60 | 4.00 | 3.15 | 2.76 | 2.53 | 2.37 | 2.25 | 2.17 | 2.10 | 2.04 | 1.99 | 1.95 | 1.92 | 1.89 | 1.86 | 1.84 | 1.82 | 1.80 | 1.78 |
| 65 | 3.99 | 3.14 | 2.75 | 2.51 | 2.36 | 2.24 | 2.15 | 2.08 | 2.03 | 1.98 | 1.94 | 1.90 | 1.87 | 1.85 | 1.82 | 1.80 | 1.78 | 1.76 |
| 70 | 3.98 | 3.13 | 2.74 | 2.50 | 2.35 | 2.23 | 2.14 | 2.07 | 2.02 | 1.97 | 1.93 | 1.89 | 1.86 | 1.84 | 1.81 | 1.79 | 1.77 | 1.75 |
| 80 | 3.96 | 3.11 | 2.72 | 2.49 | 2.33 | 2.21 | 2.13 | 2.06 | 2.00 | 1.95 | 1.91 | 1.88 | 1.84 | 1.82 | 1.79 | 1.77 | 1.75 | 1.73 |
| 90 | 3.95 | 3.10 | 2.71 | 2.47 | 2.32 | 2.20 | 2.11 | 2.04 | 1.99 | 1.94 | 1.90 | 1.86 | 1.83 | 1.80 | 1.78 | 1.76 | 1.74 | 1.72 |
| 100 | 3.94 | 3.09 | 2.70 | 2.46 | 2.31 | 2.19 | 2.10 | 2.03 | 1.97 | 1.93 | 1.89 | 1.85 | 1.82 | 1.79 | 1.77 | 1.75 | 1.73 | 1.71 |
| 125 | 3.92 | 3.07 | 2.68 | 2.44 | 2.29 | 2.17 | 2.08 | 2.01 | 1.96 | 1.91 | 1.87 | 1.83 | 1.80 | 1.77 | 1.75 | 1.72 | 1.70 | 1.69 |
| 150 | 3.90 | 3.06 | 2.66 | 2.43 | 2.27 | 2.16 | 2.07 | 2.00 | 1.94 | 1.89 | 1.85 | 1.82 | 1.79 | 1.76 | 1.73 | 1.71 | 1.69 | 1.67 |
| 200 | 3.89 | 3.04 | 2.65 | 2.42 | 2.26 | 2.14 | 2.06 | 1.98 | 1.93 | 1.88 | 1.84 | 1.80 | 1.77 | 1.74 | 1.72 | 1.69 | 1.67 | 1.66 |
| 300 | 3.87 | 3.03 | 2.63 | 2.40 | 2.24 | 2.13 | 2.04 | 1.97 | 1.91 | 1.86 | 1.82 | 1.78 | 1.75 | 1.72 | 1.70 | 1.68 | 1.66 | 1.64 |
| 500 | 3.86 | 3.01 | 2.62 | 2.39 | 2.23 | 2.12 | 2.03 | 1.96 | 1.90 | 1.85 | 1.81 | 1.77 | 1.74 | 1.71 | 1.69 | 1.66 | 1.64 | 1.62 |
| 1000 | 3.85 | 3.00 | 2.61 | 2.38 | 2.22 | 2.11 | 2.02 | 1.95 | 1.89 | 1.84 | 1.80 | 1.76 | 1.73 | 1.70 | 1.68 | 1.65 | 1.63 | 1.61 |
| ∞ | 3.84 | 3.00 | 2.60 | 2.37 | 2.21 | 2.10 | 2.01 | 1.94 | 1.88 | 1.83 | 1.79 | 1.75 | 1.72 | 1.69 | 1.67 | 1.64 | 1.62 | 1.60 |

**Appendice 6:** Chi square test table

*Table A. 3: Chi square test table*

| Degrees of freedom (*df*) | Significance level (α) | | | | | | | |
|---|---|---|---|---|---|---|---|---|
| | .99 | .975 | .95 | .9 | .1 | .05 | .025 | .01 |
| 1 | ------- | 0.001 | 0.004 | 0.016 | 2.706 | 3.841 | 5.024 | 6.635 |
| 2 | 0.020 | 0.051 | 0.103 | 0.211 | 4.605 | 5.991 | 7.378 | 9.210 |
| 3 | 0.115 | 0.216 | 0.352 | 0.584 | 6.251 | 7.815 | 9.348 | 11.345 |
| 4 | 0.297 | 0.484 | 0.711 | 1.064 | 7.779 | 9.488 | 11.143 | 13.277 |
| 5 | 0.554 | 0.831 | 1.145 | 1.610 | 9.236 | 11.070 | 12.833 | 15.086 |
| 6 | 0.872 | 1.237 | 1.635 | 2.204 | 10.645 | 12.592 | 14.449 | 16.812 |
| 7 | 1.239 | 1.690 | 2.167 | 2.833 | 12.017 | 14.067 | 16.013 | 18.475 |
| 8 | 1.646 | 2.180 | 2.733 | 3.490 | 13.362 | 15.507 | 17.535 | 20.090 |
| 9 | 2.088 | 2.700 | 3.325 | 4.168 | 14.684 | 16.919 | 19.023 | 21.666 |
| 10 | 2.558 | 3.247 | 3.940 | 4.865 | 15.987 | 18.307 | 20.483 | 23.209 |
| 11 | 3.053 | 3.816 | 4.575 | 5.578 | 17.275 | 19.675 | 21.920 | 24.725 |
| 12 | 3.571 | 4.404 | 5.226 | 6.304 | 18.549 | 21.026 | 23.337 | 26.217 |
| 13 | 4.107 | 5.009 | 5.892 | 7.042 | 19.812 | 22.362 | 24.736 | 27.688 |
| 14 | 4.660 | 5.629 | 6.571 | 7.790 | 21.064 | 23.685 | 26.119 | 29.141 |
| 15 | 5.229 | 6.262 | 7.261 | 8.547 | 22.307 | 24.996 | 27.488 | 30.578 |
| 16 | 5.812 | 6.908 | 7.962 | 9.312 | 23.542 | 26.296 | 28.845 | 32.000 |
| 17 | 6.408 | 7.564 | 8.672 | 10.085 | 24.769 | 27.587 | 30.191 | 33.409 |
| 18 | 7.015 | 8.231 | 9.390 | 10.865 | 25.989 | 28.869 | 31.526 | 34.805 |
| 19 | 7.633 | 8.907 | 10.117 | 11.651 | 27.204 | 30.144 | 32.852 | 36.191 |
| 20 | 8.260 | 9.591 | 10.851 | 12.443 | 28.412 | 31.410 | 34.170 | 37.566 |
| 21 | 8.897 | 10.283 | 11.591 | 13.240 | 29.615 | 32.671 | 35.479 | 38.932 |
| 22 | 9.542 | 10.982 | 12.338 | 14.041 | 30.813 | 33.924 | 36.781 | 40.289 |
| 23 | 10.196 | 11.689 | 13.091 | 14.848 | 32.007 | 35.172 | 38.076 | 41.638 |
| 24 | 10.856 | 12.401 | 13.848 | 15.659 | 33.196 | 36.415 | 39.364 | 42.980 |
| 25 | 11.524 | 13.120 | 14.611 | 16.473 | 34.382 | 37.652 | 40.646 | 44.314 |
| 26 | 12.198 | 13.844 | 15.379 | 17.292 | 35.563 | 38.885 | 41.923 | 45.642 |
| 27 | 12.879 | 14.573 | 16.151 | 18.114 | 36.741 | 40.113 | 43.195 | 46.963 |
| 28 | 13.565 | 15.308 | 16.928 | 18.939 | 37.916 | 41.337 | 44.461 | 48.278 |
| 29 | 14.256 | 16.047 | 17.708 | 19.768 | 39.087 | 42.557 | 45.722 | 49.588 |
| 30 | 14.953 | 16.791 | 18.493 | 20.599 | 40.256 | 43.773 | 46.979 | 50.892 |
| 40 | 22.164 | 24.433 | 26.509 | 29.051 | 51.805 | 55.758 | 59.342 | 63.691 |
| 50 | 29.707 | 32.357 | 34.764 | 37.689 | 63.167 | 67.505 | 71.420 | 76.154 |
| 60 | 37.485 | 40.482 | 43.188 | 46.459 | 74.397 | 79.082 | 83.298 | 88.379 |
| 70 | 45.442 | 48.758 | 51.739 | 55.329 | 85.527 | 90.531 | 95.023 | 100.425 |
| 80 | 53.540 | 57.153 | 60.391 | 64.278 | 96.578 | 101.879 | 106.629 | 112.329 |
| 100 | 61.754 | 65.647 | 69.126 | 73.291 | 107.565 | 113.145 | 118.136 | 124.116 |
| 1000 | 70.065 | 74.222 | 77.929 | 82.358 | 118.498 | 124.342 | 129.561 | 135.807 |

**Appendice 7:** Results of MB adosption equilibriums modelling

*Table A. 4: Results of MB adosption by FEN isotherm modelling*

| Rank | model | RMSE | CHI | R^2 | R2ADJ | MAE | MSE | T_STAT | MAPE |
|---|---|---|---|---|---|---|---|---|---|
| 1 | 'Baudu' | 3.48923 | 59.5861444 | 0.996338 | 0.981691 | 2.596106 | 12.174703 | 0.000383 | 8.708304 |
| 2 | 'Fritz-Shluender 4 para' | 3.48923 | 36.5241076 | 0.996338 | 0.981691 | 2.596129 | 12.174703 | 0.000382 | 8.70777 |
| 3 | 'Fritz-Shluender 5 para' | 3.48923 | 74.9200335 | 0.996338 | #NAME? | 2.596183 | 12.174704 | 0.000378 | 8.70638 |
| 4 | 'Marczewski-Jaroniec ( Ce mg/g)' | 4.44195 | 41.8563093 | 0.994065 | 0.970327 | 3.770783 | 19.73094 | 0.00312 | 18.07577 |
| 5 | 'Brouers-Sotolongo' | 4.57473 | 19755.357 | 0.993705 | 0.984263 | 3.800476 | 20.928155 | 3.65E-03 | 19.97305 |
| 6 | 'Hills' | 4.57477 | 9877.6785 | 0.993705 | 0.984263 | 3.838275 | 20.928554 | 0.004053 | 19.76804 |
| 7 | 'Koble-Corrigan' | 4.57477 | 120.283389 | 0.993705 | 0.984263 | 3.838275 | 20.928554 | 0.004053 | 19.76804 |
| 8 | 'Sips' | 4.57477 | 45.0852334 | 0.993705 | 0.984263 | 3.838275 | 20.928554 | 0.004053 | 19.76804 |
| 9 | 'Redlich-Peterson' | 4.74397 | 36.5241079 | 0.993231 | 0.983077 | 4.163551 | 22.505295 | 0.113475 | 25.04621 |
| 10 | 'Toth' | 4.74398 | 73.0482229 | 0.993231 | 0.983077 | 4.16356 | 22.505366 | 0.113473 | 25.04623 |
| 11 | 'Fritz-Shluender 3 para' | 4.74791 | 96.4947298 | 0.99322 | 0.983049 | 4.169343 | 22.542617 | 0.114461 | 25.07927 |
| 12 | 'Radke-Prausnitz' | 4.74791 | 135.731906 | 0.99322 | 0.983049 | 4.169343 | 22.542617 | 0.114461 | 25.07927 |
| 13 | 'Modified Guggenheim-Andersen-de Boer(GAB)' | 4.75626 | 120.283389 | 0.993196 | #NAME? | 3.330699 | 22.621984 | 5.05E-07 | 21.25347 |
| 14 | 'Vieth-Sladek' | 5.00751 | 121.769371 | 0.992458 | 0.981145 | 4.458199 | 25.075205 | 0.208025 | 27.63396 |
| 15 | 'Khan' | 5.19472 | 6649.50586 | 0.991884 | 0.979709 | 4.623121 | 26.985164 | 0.246081 | 28.99988 |
| 16 | 'Aranovich' | 5.4583 | 574.160114 | 0.991039 | 0.977598 | 4.82515 | 29.793072 | 0.268639 | 30.58433 |
| 17 | 'Langmuir' | 5.67141 | 41.8571084 | 0.990326 | 0.983876 | 4.971869 | 32.164866 | 0.266592 | 31.65902 |
| 18 | 'Guggenheim-Andersen-de Boer(GAB)' | 5.67141 | 9877.6785 | 0.990326 | 0.951628 | 4.97187 | 32.16491 | 0.26659 | 31.65903 |
| 19 | 'Brunauer- Emmet-Teller(BET)' | 6.12046 | 53.9703278 | 0.988733 | 0.971832 | 5.111922 | 37.460017 | 0.040364 | 33.74111 |
| 20 | 'Temkin' | 8.75051 | 41.8571084 | 0.976969 | 0.961616 | 7.747066 | 76.571366 | 4.93E-18 | 26.69919 |
| 21 | 'Halsey' | 8.95483 | 48.2472988 | 0.975881 | 0.959802 | 7.138694 | 80.188926 | 0.117992 | 45.47261 |
| 22 | 'Freundlich' | 8.95483 | 5520.34372 | 0.975881 | 0.959802 | 7.138687 | 80.188926 | 0.117994 | 45.47264 |
| 23 | 'Henderson' | 9.00997 | 59.1928193 | 0.975583 | 0.959305 | 7.180741 | 81.179581 | 0.117094 | 45.71262 |
| 24 | 'Oswin modefid ce mg/ml' | 9.06497 | 123.260423 | 0.975284 | 0.938211 | 7.222595 | 82.173615 | 0.116195 | 45.9515 |
| 25 | 'Oswin ce mg/ml' | 9.06497 | 164.34723 | 0.975284 | 0.958807 | 7.222594 | 82.173615 | 0.116195 | 45.9515 |
| 26 | 'Smith ce( mg/ml)' | 13.9832 | 45.0852335 | 0.94119 | 0.852974 | 11.51198 | 195.52959 | 2.51E-22 | 63.33943 |
| 27 | 'Henry' | 21.8739 | 45.0105904 | 0.85609 | 0.820112 | 17.43012 | 478.46676 | 3.57472 | 43.43926 |
| 28 | 'MacMillan-Teller (MET)' | 52.5373 | 41.8571084 | 0.169811 | -1.07547 | 40.93112 | 2760.1719 | 0.037223 | 190.8413 |
| 29 | 'Henderson modefid' | 57.6607 | 391.059189 | -1.17E-07 | -1.5 | 43.32568 | 3324.7529 | 4.66E-11 | 190.2817 |
| 30 | 'Dubinin-Astakhov (DA)' | 81.1487 | 114.85705 | -0.98063 | -8.90317 | 57.09962 | 6585.119 | 4.903172 | 100 |
| 31 | 'Dubinin-Radushkevich(DR)' | 81.1487 | 45.010733 | -0.98063 | -2.30106 | 57.09962 | 6585.119 | 4.903172 | 100 |
| 32 | 'Jovanovich' | 81.1487 | 50.150409 | -0.98063 | -2.30106 | 57.09962 | 6585.119 | 4.903172 | 100 |

*Table A. 5: Results of MB adosption by FBIO isotherm modelling*

| Rank | model | RMSE | CHI | R^2 | R2ADJ | MAE | MSE | T_STAT | MAPE |
|---|---|---|---|---|---|---|---|---|---|
| 1 | 'Brunauer- Emmet-Teller(BET)' | 11.4302 | 261.2977 | 0.976814 | 0.942034 | 9.340804 | 130.64883 | 0.030961 | 11.48794 |
| 2 | 'Fritz-Shluender 4 para' | 12.4514 | 465.1107 | 0.972485 | 0.862427 | 9.574325 | 155.03689 | 0.060235 | 10.31781 |
| 3 | 'Baudu' | 12.5308 | 471.0654 | 0.972133 | 0.860665 | 9.629688 | 157.0218 | 0.060613 | 10.357 |
| 4 | 'Vieth-Sladek' | 17.8309 | 635.8828 | 0.943574 | 0.858936 | 12.77062 | 317.94139 | 0.333844 | 14.78428 |
| 5 | 'Aranovich' | 18.0623 | 652.4898 | 0.942101 | 0.855252 | 13.01592 | 326.24489 | 0.273946 | 14.47336 |
| 6 | 'Khan' | 18.0666 | 652.8066 | 0.942073 | 0.855182 | 13.08705 | 326.40332 | 0.345783 | 15.08926 |
| 7 | 'Redlich-Peterson' | 18.543 | 687.6888 | 0.938977 | 0.847444 | 13.57821 | 343.84441 | 0.285185 | 14.98873 |
| 8 | 'Fritz-Shluender 3 para' | 18.543 | 687.6888 | 0.938977 | 0.847444 | 13.57823 | 343.84441 | 0.285175 | 14.98867 |
| 9 | 'Sips' | 19.1113 | 730.4805 | 0.93518 | 0.837951 | 16.78461 | 365.24024 | 0.041701 | 15.8434 |
| 10 | 'Koble-Corrigan' | 19.1113 | 730.4805 | 0.93518 | 0.837951 | 16.78461 | 365.24024 | 0.041701 | 15.8434 |
| 11 | 'Hills' | 19.1113 | 730.4805 | 0.93518 | 0.837951 | 16.78462 | 365.24024 | 0.0417 | 15.8434 |
| 12 | 'Toth' | 19.1275 | 731.7228 | 0.93507 | 0.837675 | 15.49554 | 365.8614 | 0.160721 | 15.76247 |
| 13 | 'Langmuir' | 19.2174 | 553.9608 | 0.934458 | 0.890764 | 16.48689 | 369.30723 | 0.085811 | 16.14649 |
| 14 | 'Guggenheim-Andersen-de Boer(GAB)' | 19.2174 | 1107.925 | 0.934458 | 0.672292 | 16.48572 | 369.30819 | 0.086003 | 16.14539 |
| 15 | 'Temkin' | 24.2202 | 879.9272 | 0.895892 | 0.826487 | 21.20774 | 586.6181 | 1.87E-16 | 20.87892 |
| 16 | 'Fritz-Shluender 5 para' | 26.0066 | 4058.057 | 0.879968 | #NAME? | 18.83306 | 676.34278 | 0.006727 | 13.54463 |
| 17 | 'Freundlich' | 26.3752 | 1043.476 | 0.876542 | 0.794236 | 19.7927 | 695.65076 | 0.014259 | 15.51052 |
| 18 | 'Halsey' | 26.3752 | 1043.476 | 0.876542 | 0.794236 | 19.79269 | 695.65076 | 0.014259 | 15.5105 |
| 19 | 'Henderson' | 26.5494 | 1057.307 | 0.874905 | 0.791509 | 19.92178 | 704.87156 | 0.014379 | 15.67614 |
| 20 | 'Oswin modefid ce mg/ml' | 26.7234 | 1428.281 | 0.87326 | 0.683151 | 20.04985 | 714.1404 | 0.014489 | 15.84088 |
| 21 | 'Oswin ce mg/ml' | 26.7234 | 1071.211 | 0.87326 | 0.788767 | 20.04985 | 714.1404 | 0.014489 | 15.84089 |
| 22 | 'Radke-Prausnitz' | 36.9039 | 2723.794 | 0.758302 | 0.395755 | 28.20342 | 1361.897 | 2.02419 | 19.16017 |
| 23 | 'Smith ce( mg/ml)' | 43.6013 | 3802.147 | 0.662614 | 0.156534 | 34.4418 | 1901.0737 | 2.24E-22 | 32.41596 |
| 24 | 'Marczewski-Jaroniec ( Ce mg/g)' | 49.9952 | 7498.556 | 0.556407 | -1.21797 | 42.6866 | 2499.5187 | 1.08499 | 45.1241 |
| 25 | 'MacMillan-Teller (MET)' | 61.6323 | 7597.091 | 0.325866 | -0.68533 | 55.42152 | 3798.5455 | 0.04001 | 55.00163 |
| 26 | 'Brouers-Sotolongo' | 63.204 | 7989.493 | 0.291046 | -0.77238 | 52.7242 | 3994.7465 | 3.41E-22 | 40.95627 |
| 27 | 'Henry' | 90.1082 | 9743.387 | -0.44098 | -0.80122 | 83.50077 | 8119.4895 | 4.862678 | 67.61107 |
| 28 | 'Henderson modefid' | 96.29 | 18543.52 | -6.45E-01 | -3.11368 | 84.90055 | 9271.7586 | 3.23E+00 | 102.4568 |
| 29 | 'Modified Guggenheim-Andersen-de Boer(GAB)' | 106.962 | 68645.43 | -1.03044 | #NAME? | 54.66365 | 11440.905 | 0.967768 | 28.7287 |
| 30 | 'Dubinin-Astakhov (DA)' | 162.89 | 79599.4 | -3.70888 | -22.5444 | 144.5629 | 26533.135 | 18.54438 | 100 |
| 31 | 'Dubinin-Radushkevich(DR)' | 162.89 | 39799.7 | -3.70888 | -6.84813 | 144.5629 | 26533.135 | 18.54438 | 100 |
| 32 | 'Jovanovich' | 162.89 | 39799.7 | -3.70888 | -6.84813 | 144.5629 | 26533.135 | 18.54438 | 100 |

*Table A. 6: Results of MB adosption by TH isotherm modelling*

| Rank | model | RMSE | CHI | R^2 | R2ADJ | MAE | MSE | T_STAT | MAPE |
|---|---|---|---|---|---|---|---|---|---|
| 1 | 'Modified Guggenheim-Andersen-de Boer(GAB)' | 2.72336 | 44.50022 | 0.999169 | #NAME? | 2.182758 | 7.4167039 | 1.70E-01 | 13.56723 |
| 2 | 'Aranovich' | 3.82999 | 29.33766 | 0.998356 | 0.995891 | 2.757802 | 14.668832 | 0.192799 | 15.55427 |
| 3 | 'Guggenheim-Andersen-de Boer(GAB)' | 4.57132 | 62.69082 | 0.997658 | 0.988292 | 3.601777 | 20.896942 | 0.016194 | 16.42867 |
| 4 | 'Koble-Corrigan' | 5.07035 | 51.41688 | 0.997119 | 0.992798 | 3.970614 | 25.708439 | 0.002236 | 17.83097 |
| 5 | 'Brunauer- Emmet-Teller(BET)' | 6.4045 | 82.03533 | 0.995404 | 0.988509 | 5.219112 | 41.017664 | 0.050389 | 28.75543 |
| 6 | 'Khan' | 14.9368 | 446.2168 | 0.974999 | 0.937498 | 11.97267 | 223.10839 | 0.919895 | 37.00093 |
| 7 | 'Oswin modefid ce mg/ml' | 18.2923 | 669.214 | 0.962505 | 0.906262 | 14.90828 | 334.60698 | 1.370891 | 47.31689 |
| 8 | 'Henderson' | 18.3025 | 502.4712 | 0.962463 | 0.937438 | 14.91687 | 334.98082 | 1.372482 | 47.34043 |
| 9 | 'Freundlich' | 18.3127 | 503.0327 | 0.962421 | 0.937368 | 14.92546 | 335.35515 | 1.374108 | 47.36403 |
| 10 | 'Baudu' | 18.3127 | 1006.065 | 0.962421 | 0.812105 | 14.92546 | 335.35515 | 1.374112 | 47.36404 |
| 11 | 'Halsey' | 18.3127 | 503.0327 | 0.962421 | 0.937368 | 14.92546 | 335.35515 | 1.374095 | 47.364 |
| 12 | 'Fritz-Shluender 5 para' | 18.3127 | 2012.131 | 0.962421 | #NAME? | 14.92606 | 335.35516 | 1.374569 | 47.36423 |
| 13 | 'Fritz-Shluender 4 para' | 18.3127 | 1006.066 | 0.962421 | 0.812105 | 14.92738 | 335.35521 | 1.375568 | 47.36464 |
| 14 | 'Hills' | 18.3127 | 670.7104 | 0.962421 | 0.906053 | 14.92546 | 335.35521 | 1.37411 | 47.36404 |
| 15 | 'Redlich-Peterson' | 18.3127 | 670.7104 | 0.962421 | 0.906053 | 14.92546 | 335.35521 | 1.374108 | 47.36403 |
| 16 | 'Brouers-Sotolongo' | 18.3163 | 670.974 | 0.962406 | 0.906016 | 14.92885 | 335.48698 | 1.37E+00 | 47.37054 |
| 17 | 'Sips' | 18.3186 | 671.1446 | 0.962397 | 0.905992 | 14.93109 | 335.57229 | 1.374213 | 47.37435 |
| 18 | 'Oswin ce mg/ml' | 18.5603 | 516.7249 | 0.961398 | 0.935664 | 15.46013 | 344.48325 | 0.788087 | 46.12936 |
| 19 | 'Marczewski-Jaroniec ( Ce mg/g)' | 38.6736 | 4486.943 | 0.832402 | 0.16201 | 25.86133 | 1495.6477 | 4.044369 | 66.66667 |
| 20 | 'Fritz-Shluender 3 para' | 42.4107 | 3597.331 | 0.798447 | 0.496117 | 34.00758 | 1798.6654 | 0.28386 | 41.01615 |
| 21 | 'Radke-Prausnitz' | 42.4876 | 3610.387 | 0.797715 | 0.494288 | 34.10955 | 1805.1934 | 0.286834 | 41.34954 |
| 22 | 'Smith ce( mg/ml)' | 51.116 | 5225.689 | 0.707212 | 0.268031 | 43.44547 | 2612.8445 | 4.39E-23 | 122.1292 |
| 23 | 'Vieth-Sladek' | 52.8444 | 5585.053 | 0.687078 | 0.217694 | 43.6734 | 2792.5265 | 0.017992 | 84.85652 |
| 24 | 'Henry' | 62.9531 | 4755.713 | 0.555907 | 0.444884 | 54.9564 | 3963.0943 | 0.280215 | 134.1627 |
| 25 | 'Toth' | 62.9531 | 7926.19 | 0.555907 | -0.11023 | 54.95762 | 3963.0949 | 0.280321 | 134.1676 |
| 26 | 'Langmuir' | 62.9535 | 5944.715 | 0.555902 | 0.259836 | 54.95659 | 3963.143 | 0.280203 | 134.1636 |
| 27 | 'Temkin' | 63.7825 | 6102.309 | 0.544129 | 0.240215 | 56.05144 | 4068.2061 | 2.16E-21 | 161.7881 |
| 28 | 'MacMillan-Teller (MET)' | 92.2922 | 17035.7 | 0.045515 | -1.38621 | 69.36618 | 8517.8494 | 0.002699 | 260.3607 |
| 29 | 'Henderson modefid' | 94.4671 | 17848.05 | 1.81E-08 | -1.5 | 70.54568 | 8924.0237 | 5.05E-11 | 266.271 |
| 30 | 'Dubinin-Astakhov (DA)' | 131.655 | 51999.48 | -0.9423 | -8.71152 | 91.70133 | 17333.158 | 4.711515 | 100 |
| 31 | 'Dubinin-Radushkevich(DR)' | 131.655 | 25999.74 | -0.9423 | -2.23717 | 91.70133 | 17333.158 | 4.711515 | 100 |
| 32 | 'Jovanovich' | 131.655 | 25999.74 | -0.9423 | -2.23717 | 91.70133 | 17333.158 | 4.711515 | 100 |

## **Appendice 8:** Results of CTC-HCl adosption kinetics modelling

*Table A. 7: Results of CTC-HCl adosption by FEN kinetic modelling*

| Rank | model | RMSE | CHI | R^2 | R2ADJ | MAE | MSE | T_STAT |
|---|---|---|---|---|---|---|---|---|
| 1 | 'pseudo-first-order model' | 4.65497849 | 27.8599175 | 0.9965169 | 0.99535586 | 3.18756064 | 21.6688247 | 2.56E-01 |
| 2 | 'Avramis model' | 4.65497849 | 32.5032371 | 0.9965169 | 0.99442704 | 3.18756064 | 21.6688247 | 2.56E-01 |
| 3 | 'pseudo-second-order' | 5.37106972 | 37.0907871 | 0.99536284 | 0.99381711 | 3.75163173 | 28.8483899 | 0.253556 |
| 4 | 'Bangham model' | 9.89860125 | 125.977251 | 0.98425007 | 0.97900009 | 7.93355632 | 97.9823067 | 0.09266002 |
| 5 | 'intraparticle diffusion model' | 13.5938257 | 237.589838 | 0.97029604 | 0.96039472 | 10.9505425 | 184.792096 | 3.82E-22 |
| 6 | 'power model' | 18.5479131 | 442.31796 | 0.94470052 | 0.92626736 | 14.7239141 | 344.02508 | 0.96000526 |
| 7 | 'Ritchie second-order' | 43.2616361 | 2406.3032 | 0.69915913 | 0.59887884 | 37.8705486 | 1871.56916 | 0.11688368 |
| 8 | 'Boyds model' | 46.7991287 | 2815.91801 | 0.64794826 | 0.53059768 | 42.434265 | 2190.15845 | 0.55316442 |
| 9 | 'Marczewski mode' | 67.5153401 | 6837.48172 | 0.26728366 | -0.17234614 | 58.8506667 | 4558.32114 | 4.34E-20 |
| 10 | 'exponential form' | 67.5153401 | 5860.69861 | 0.26728366 | 0.02304488 | 58.8506667 | 4558.32114 | 1.48E-19 |
| 11 | 'modification pseudo-first-order model' | 67.5153401 | 6837.48172 | 0.26728366 | -0.17234614 | 58.8506667 | 4558.32114 | 2.47E-21 |
| 12 | 'Haerifar and Azizian 2013' | 67.5153401 | 6837.48172 | 0.26728366 | -0.17234614 | 58.8506667 | 4558.32114 | 3.93E-21 |
| 13 | 'modification pseudo-second-order model' | Nan | Nan | Nan | Nan | Nan | Nan | Nan |
| 14 | 'modification mixed 1, 2-order model' | 67.5153401 | 8204.97806 | 0.26728366 | -0.46543267 | 58.8506667 | 4558.32114 | 9.17E-16 |
| 15 | 'Lagergren' | 78.712103 | 7965.7652 | 0.004104 | -0.32786133 | 71.567037 | 6195.59516 | 1.30E-19 |

*Table A. 8: Results of CTC-HCl adosption by FBIO kinetic modelling*

| Rank | model | RMSE | CHI | R^2 | R2ADJ | MAE | MSE | T_STAT |
|---|---|---|---|---|---|---|---|---|
| 1 | 'pseudo-first-order model' | 15.3984047 | 304.856829 | 0.78876471 | 0.71835294 | 11.0260335 | 237.110867 | 5.46E-02 |
| 2 | 'exponential form' | 15.9213725 | 325.915847 | 0.77417291 | 0.69889722 | 11.5278234 | 253.490104 | 4.37E-02 |
| 3 | 'pseudo-second-order' | 16.0958824 | 333.099553 | 0.76919532 | 0.69226043 | 11.5707843 | 259.07743 | 0.02947873 |
| 4 | 'Bangham model' | 17.7016246 | 402.875373 | 0.72084766 | 0.62779688 | 13.0014023 | 313.347512 | 0.01332472 |
| 5 | 'power model' | 17.7808737 | 406.490747 | 0.71834257 | 0.62445675 | 13.452586 | 316.15947 | 3.86E-02 |
| 6 | 'intraparticle diffusion model' | 17.7808737 | 406.490747 | 0.71834256 | 0.62445675 | 13.4525838 | 316.15947 | 0.03862073 |
| 7 | 'modification pseudo-second-order model' | 29.1669244 | 1276.06421 | 0.24212724 | -0.21259641 | 25.3812385 | 850.709476 | 5.6108E-12 |
| 8 | 'Avramis model' | 29.1676815 | 1276.13046 | 0.2420879 | -0.21265937 | 25.382 | 850.753642 | 2.8787E-19 |
| 9 | 'Marczewski mode' | 16.8768715 | 427.243187 | 0.74625417 | 0.59400667 | 12.4579697 | 284.828792 | 5.26E+00 |
| 10 | 'Haerifar and Azizian 2013' | 29.1676815 | 1276.13046 | 0.2420879 | -0.21265937 | 25.382 | 850.753642 | 8.63E-16 |
| 11 | 'modification pseudo-first-order model' | 29.1676815 | 1276.13046 | 0.2420879 | -0.21265937 | 25.382 | 850.753642 | 5.58E-21 |
| 12 | 'modification mixed 1, 2-order model' | 29.1676815 | 1531.35656 | 0.2420879 | -0.51582421 | 25.382 | 850.753642 | 3.13E-15 |
| 13 | 'Boyds model' | 29.947652 | 1153.10811 | 0.2010114 | -0.06531813 | 27.6239968 | 896.861862 | 0.01660496 |
| 14 | 'Lagergren' | 33.3501721 | 1430.01511 | 0.00914254 | -0.32114328 | 30.4638519 | 1112.23398 | 5.93E-24 |
| 15 | 'Ritchie second-order' | 33.5036781 | 1443.20972 | -1.6825E-10 | -0.33333333 | 30.562617 | 1122.49645 | 6.05E-14 |

*Table A. 9: Results of CTC-HCl adosption by TH kinetic modelling*

| Rank | model | RMSE | CHI | R^2 | R2ADJ | MAE | MSE | T_STAT |
|---|---|---|---|---|---|---|---|---|
| 1 | 'pseudo-first-order model' | 0.85017489 | 0.92931087 | 0.99161201 | 0.98881601 | 0.71487769 | 0.72279735 | 8.88E-03 |
| 2 | 'modification pseudo-second-order model' | 0.94760332 | 1.34692807 | 0.98957935 | 0.98332696 | 0.78784446 | 0.89795204 | 8.21E-03 |
| 3 | 'pseudo-second-order' | 0.97762212 | 1.22881502 | 0.98890867 | 0.98521156 | 0.72430259 | 0.95574502 | 0.00096771 |
| 4 | 'Bangham model' | 1.49259791 | 2.86437668 | 0.97414603 | 0.96552804 | 1.08871063 | 2.22784853 | 0.019123 |
| 5 | 'power model' | 1.57949201 | 3.20759359 | 0.97104814 | 0.96139753 | 1.30426772 | 2.49479501 | 1.93E-01 |
| 6 | 'intraparticle diffusion model' | 1.57949203 | 3.20759365 | 0.97104814 | 0.96139752 | 1.30426776 | 2.49479506 | 0.19325866 |
| 7 | 'Avramis model' | 7.45494068 | 83.3642107 | 0.35504425 | -0.03192921 | 6.6634278 | 55.5761405 | 1.1049E-17 |
| 8 | 'Marczewski mode' | 7.45494068 | 83.3642107 | 0.35504425 | -0.03192921 | 6.6634278 | 55.5761405 | 1.8123E-16 |
| 9 | 'exponential form' | 7.45494068 | 71.4550378 | 0.35504425 | 0.14005899 | 6.6634278 | 55.5761405 | 4.42E-19 |
| 10 | 'Haerifar and Azizian 2013' | 7.45494068 | 83.3642107 | 0.35504425 | -0.03192921 | 6.6634278 | 55.5761405 | 4.92E-16 |
| 11 | 'modification pseudo-first-order model' | 7.45494068 | 83.3642107 | 0.35504425 | -0.03192921 | 6.6634278 | 55.5761405 | 3.38E-17 |
| 12 | 'modification mixed 1, 2-order model' | 7.45494068 | 100.037053 | 0.35504425 | -0.28991151 | 6.6634278 | 55.5761405 | 5.61E-31 |
| 13 | 'Boyds model' | 7.79533595 | 78.1293375 | 0.29480177 | 0.0597357 | 7.41570246 | 60.7672625 | 0.02762954 |
| 14 | 'Lagergren' | 8.96369838 | 103.304428 | 0.06757049 | -0.24323934 | 8.11080481 | 80.3478887 | 1.30E-03 |
| 15 | 'Ritchie second-order' | 9.28280507 | 110.790604 | -1.3977E-10 | -0.33333333 | 8.40172058 | 86.17047 | 9.76E-14 |